

FILE COPY

2

DOT/FAA/DS-89/18

Criteria For Polymer Concrete on Airport Pavements

Advanced System Design Service
Washington, D.C. 20591

AD-A219 168

Advanced System Design Service
Federal Aviation Administration
Washington, D.C. 20591

July 1989

Final Report

This document is available to the public
through the National Technical Information
Service, Springfield, Virginia 22161.



US Department
of Transportation
Federal Aviation
Administration

DTIC
ELECTE
MAR 13 1990
S B D

90 03 12 103

1. Report No. DOT/FAA/DS-89/18	2. Government Accession No.	3. Recipient's Catalog No.
4. Title and Subtitle CRITERIA FOR POLYMER CONCRETE ON AIRPORT PAVEMENTS		5. Report Date July 27, 1989
6. Author's Dr. Krish Pandalai		7. Performing Organization Report No. FAARPTF
8. Performing Organization Name and Address Pandalai Coatings Company 837, 6th Avenue Brackenridge, PA 15014		9. Work Unit No. TR-15
10. Sponsoring Agency Name and Address Federal Aviation Administration, DOT Washington, D.C.		11. Contract or Grant No. DTFA-01-86-Y-01015
12. Supplementary Notes		13. Title of Report and Period Covered Final Report
		14. Sponsoring Agency Code ADS-240

16. Abstract

> The subject of polymer concrete (PC) has generated a lot of interest among researchers during the past decade. This is due to the many advantages that polymer concrete pavement offers compared to regular portland cement concrete. The advantages of polymer concrete, when compared to portland cement concrete include, quick curing and setting, reduced moisture sensitivity and permeability and improved mechanical properties resulting in reduced pavement thickness to support the same load. These advantages will lead to attractive life cycle cost benefits. Material properties and mix designs for PC with epoxy, methylemethacrylate (MMA) and Polyester as the binder material have been investigated and presented in part I of this report. Part II contains pavement thickness design charts, developed for various aircraft, quality control methods, construction procedures and cost analysis. It has been shown in this study that increased material cost of PC can be offset by the reduced thickness of the pavement. In order to develop life cycle cost information, it is necessary to obtain field performance data of PC pavement, especially in the composite design mode. K-110

17. Key Words

Polymer concrete, epoxy, MMA, polyester, compressive stress, modulus of elasticity

18. Distribution Statement

This document is available to the public through the National Technical Information Service. Springfield, VA 22161

19. Security Classification of this report

Unclassified

20. Security Classification of this page

Unclassified

21. Number of Pages

174

METRIC CONVERSION FACTORS

APPROXIMATE CONVERSIONS FROM METRIC MEASURES

APPROXIMATE CONVERSIONS FROM METRIC MEASURES

SYMBOL WHEN YOU KNOW MULTIPLY BY TO FIND SYMBOL

SYMBOL WHEN YOU KNOW MULTIPLY BY TO FIND SYMBOL

LENGTH

mm	millimeters	0.04	inches	in
cm	centimeters	0.4	inches	in
m	meters	3.3	feet	ft
km	kilometers	1.1	yards	yd
		0.6	miles	mi

sq cm	square centimeters	0.16	square inches	sq in
sq m	square meters	1.2	square yards	sq yd
sq km	square kilometers	0.4	square miles	sq mi
ha	hectare (10,000 sq m)	2.5	acres	ac

MASS (weight)

g	grams	0.035	ounces	oz
kg	kilograms	2.2	pounds	lb
t	tonnes (1,000 kg)	1.1	short tons	

VOLUME

ml	milliliters	0.03	fluid ounces	fl oz
l	liters	2.1	pints	pt
		1.06	quarts	qt
		0.26	gallons	gal
cu m	cubic meters	36	cubic feet	cu ft
cu km	cubic kilometers	1.3	cubic yards	cu yd

TEMPERATURE (heat)

°C	Celsius temperature	9/5 (plus add 32)	Fahrenheit temperature	°F
----	---------------------	-------------------	------------------------	----

LENGTH

in	inches	2.5	centimeters	cm
ft	feet	30	centimeters	cm
yd	yards	0.9	meters	m
mi	miles	1.6	kilometers	km

AREA

sq in	square inches	6.5	square centimeters	sq cm
sq ft	square feet	0.09	square meters	sq m
sq yd	square yards	0.6	square meters	sq m
sq mi	square miles	2.6	square kilometers	sq km
acres		0.4	hectares	ha

MASS (weight)

oz	ounces	28	grams	g
lb	pounds	0.45	kilograms	kg
	short tons (2,000 lb)	0.9	tonnes	t

VOLUME

fl oz	fluid ounces	3	milliliters	ml
pt	pints	15	milliliters	ml
qt	quarts	30	milliliters	ml
gal	gallons	0.24	liters	l
cu ft	cubic feet	0.47	liters	l
cu yd	cubic yards	0.95	liters	l
cu m	cubic meters	3.6	liters	l
cu km	cubic kilometers	0.03	cubic meters	cu m
cu mi	cubic miles	0.76	cubic meters	cu m

TEMPERATURE (heat)

°F	Fahrenheit temperature	5/9 (after subtracting 32)	Celsius temperature	°C
----	------------------------	----------------------------	---------------------	----

ACKNOWLEDGMENT

Enclosed is the final report on the a study entitled "Criteria of Polymer Concrete on Airport Pavements", under contract #DTFA 01-86-Y-01015. The author wishes to thank Dr. Aston McLaughlin and Mr. John Rice of the FAA for giving their valuable guidance, and comments during this project period. We also acknowledge with thanks the assistance provided by Resource International in measuring the mechanical properties. The assistance in making thickness calculations provided by Drs. Earnest Barenberg and A.M. Ionnides of the Civil Engineering department of the University of Illinois has been very valuable.



Accession For	
NTIS GRA&I	<input checked="" type="checkbox"/>
DTIC TAB	<input type="checkbox"/>
Unannounced	<input type="checkbox"/>
Justification	
By	
Distribution/	
Availability Codes	
Dist	Avail and/or Special
A-1	

PREFACE

The objective of this project was to investigate the use of polymer as the binder material for airport runway pavement application and to study how these materials will improve the performance of airport pavements in a cost effective manner. The research work described in this report was carried out by Pandalai Coatings Company for the Federal Aviation Administration, under contract # DTFA 01-86-Y-01015. The experimental evaluation of the mechanical properties of polymer concrete was performed by Resource International Inc. of Columbus, Ohio, under a subcontract from Pandalai Coatings Company. The pavement thickness calculations were carried out using the illi-slab finite element method by Drs. Barenberg and Ioannides.

TABLE OF CONTENTS

Part I-Mix Design and Mechanical Properties

Chapter 1.	Introduction	1
Chapter 2.	Literature Study	2
	Meetings and Discussions	19
Chapter 3.	Laboratory Screening Studies & Results	20
	Effect of Gradation on Mechanical Properties	20
	Determination of the Amount of Polymer Required	22
	Epoxy Polymer Concrete	23
	Methyl methacrylate Polymer Concrete	38
	Polyester Polymer Concrete	44
Chapter 4.	Development of Mechanical Properties	51
Chapter 5.	Conclusions and Recommendations	77

Part II-Design Thickness Charts, Quality Control,
Construction Procedures and Cost Analysis

Chapter 1.	Introduction	90
Chapter 2.	Preliminary Pavement Thickness Calculations Based on Polymer Concrete and Comparison with Portland Cement Concrete	92
2.1	FAA Design Methodology	92
2.2	Replacement of PCC with PC	94
2.3	PC Used as an Overlay	96
2.4	PC Used as an Underlay	97
Chapter 3.	PCC Overlay Over PC Underlay	99
Chapter 4.	Quality Control Methods	137
Chapter 5.	Construction Procedures	149
Chapter 6.	Cost Analysis	150
6.1	Estimating Cost for PC	150
6.2	Construction Cost Estimates	152
Chapter 7.	Conclusions and Recommendations	153
References		155
APPENDIX A		
	Finite Element Analysis of Airport Pavements Incorporating Polymer Concrete	158

Part II-Design Thickness Charts, Quality Control,
Construction Procedures, and Cost Analysis

1. Maximum Calculated Responses	94
2. PC Used as an Overlay of 2" Thickness	96
3. PC used as an Underlay of varied Thickness	97
4. PC used as an Underlay of Varied Thickness	97
5. Pavement Data (B-747)	101
6. Pavement Data (B-727)	102
7. Pavement Data (DC-10)	103
8. Pavement Data (L-1011)	104
9a. Physical Porperties of Polymers	138
9b. Physical Porperties of Polymers	139
10a. Physical Porperties of Additives	140
10b. Physical Porperties of Additives	141
11. Cost for PCC at Different Depths	151
12. Cost Data for PCC	151
13. Effect of Young's Modulus on Bending Stress	154

LIST OF TABLES

Part I-Mix Designs and Mechanical Properties

1. Compressive Stress Vs. Curing - Epoxy	26
2. Compressive Stress Vs. Percent Polymer	26
3. Compressive Stress Vs. Moisture content - Epoxy	27
4. Moisture Absorption Vs. Percent Polymer, Epoxy	29
5. Sieve Analysis	30
6. Gradation	31
7. Effect of Moisture - MMA	37
8. Stress Vs. Percent Polymer - MMA	40
9. Stress Vs. Cure Time - MMA	41
10. Stress Vs. Gradation - MMA	42
11. Stress Vs. Percent polymer - Polyester	45
12. Stress Vs. Cure Time - Polyester	46
13. Stress Vs. Gradation - Polyester	47
14. Effect of Moisture - Polyester	48
15. Moisture Absorption - polyester	49
16. Fine Aggregate Gradation	53
17. Coarse aggregate Gradation	53
18. Combined Aggregate Gradation of the Mix	54
19. Modulus of Elasticity Test Results	56
20. Compressive Strength Test Results	57
21. Flexural Strength (FS) Test Results	59
22. Modulus of Resilience Test Results	61
23. Dynamic Modulus of Elasticity	64
24. Fracture Toughness Test Results	67
25. Splitting Tensile Test Results	70
26. Resistance to rapid Freezing and Thawing Test Results	71
27. Creep Compliance Data	73

LIST OF FIGURES

Part I-Mix Designs and Mechanical Properties

1. The Pavement System	7
2. Subgrade Layers	8
3. Dimensionless Cumulative Energy Vs. Dimensionless Depth	9
4. Comparison of Energy Methods Results with Finite Element Solutions	11
5. Load Case 1	13
6. Load Case 2	14
7. Load Case 3	15
8. Load Case 4	16
9. Load Case 5	17
10. Load Case 6	18
11. Aggregate design Curves	32
12. Moisture Content - Epoxy	33
13. Stress Vs. Cure Time - Epoxy	34
14. Stress Vs. Percent Epoxy	35
15. Stress Vs. Water Content - Epoxy	36
16. Cure/Stress/Moisture Chart - MMA	43
17. Cure/Stress/Moisture Chart - Polyester	50
18. Fatigue Failure for Polymer Concrete	72
19. Polymer Concrete Creep Compliance.	76

Part II-Design Thickness Charts, Quality Control,
Construction Procedures, and Cost Analysis

1 - Percent Stress vs Thickness	95
2 - Composite Pavement Slab	99
3 - Chart of B-747 Data	105
4 - Chart of B-747 Data	106
5 - Chart of B-747 Data	107
6 - Chart of B-747 Data	108
7 - Chart of B-747 Data	109
8 - Chart of B-747 Data	111
9 - Chart of B-747 Data	111
10 - Chart of B-747 Data	112
11 - Chart of B-727 Data	113
12 - Chart of B-727 Data	114
13 - Chart of B-727 Data	115
14 - Chart of B-727 Data	116
15 - Chart of B-727 Data	117
16 - Chart of B-727 Data	118
17 - Chart of B-727 Data	119
18 - Chart of B-727 Data	120
19 - Chart of DC-10 Data	121
20 - Chart of DC-10 Data	122
21 - Chart of DC-10 Data	123

List of Figures - cont'd

22 - Chart of DC-10 Data	124
23 - Chart of DC-10 Data	125
24 - Chart of DC-10 Data	126
25 - Chart of DC-10 Data	127
26 - Chart of DC-10 Data	128
27 - Chart of L-1011 Data	129
28 - Chart of L-1011 Data	130
29 - Chart of L-1011 Data	131
30 - Chart of L-1011 Data	132
31 - Chart of L-1011 Data	133
32 - Chart of L-1011 Data	134
33 - Chart of L-1011 Data	135
34 - Chart of L-1011 Data	136
35 - Infrared plot of Epoxy	142
36 - Infrared plot of DMT	143
37 - Infrared plot of CO	144
38 - Infrared plot of MMA	145
39 - Infrared plot of DMA	146
40 - Infrared plot of DETA	147
41 - Infrared plot of Styrene	148

CHAPTER 1

INTRODUCTION

Pandalai Coatings Company was awarded a contract by the Federal Aviation Administration to undertake a study to examine and develop criteria for the use of Polymer Concrete as airport paving material. The material contained in this report has been gathered by Pandalai Coatings Company as a result of the the Phase 1 work performed under contract # DTFA 01-86-Y-01015D. The subject involves the development, use and application of Polymer Concrete for Airport pavement applications. The mix design and selection of candidate formulations were carried out by Pandalai coatings company while the measurement of the mechanical properties were carried out by Resource International Incorporated on a subcontract from Pandalai Coatings. While considerable amount of work has been carried out in the area of polymer concrete for highway application, very little emphasis has been given to this area of research for airport pavement application. As a result of this investigation, many aspects of polymer concrete research and its use for airport runway application have been uncovered. Loads many times greater than what is experienced on interstate highways is applied on airport runway pavements.

Systematic work on the effect of gradation, percent polymer in the mix design, effect of moisture in the aggregates on the mechanical properties have not been carried out in the past. As a result of the present study at Pandalai Coatings Company, data have been presented on the above variables and their effect on mechanical properties. Percent polymer much less than the optimum has been used to examine their usefulness as subgrade material. The results and discussions on mix designs, mechanical properties and other laboratory tests such as freeze/thaw tests are given in the following sections. The results of these tests would be utilized in developing pavement thickness calculations and design charts for various aircraft loads. This task will be carried out during the second phase of this investigation.

The mechanical properties investigated in this study include compressive strength, Flexural strength, Dynamic modulus, Fracture toughness, Fatigue properties and creep compliance. All these properties have been compared with those of Portland Cement Concrete and reported in chapter 4.

CHAPTER 2

LITERATURE STUDY

Research and development work in the area of polymer concrete has been supported by the Federal Highway Administration and the Transportation Research Board for several decades. The results of these efforts are just beginning to pay off in the form of isolated use of polymer concrete on bridge decks. One of the main obstacles in the use of polymer concrete is its exorbitant cost. However a realistic cost analysis will show that the high material cost will be offset by the many advantages polymer concrete has for certain applications. This aspect will be demonstrated in the second phase of this study.

The literature study carried out in this investigation covered the following areas:

1. Development of the polymer concrete formulations and mix designs.
2. Mechanical and structural properties specifically designed to work on airport pavements.
3. Existing methods of analysis to be used in determining characteristic curves of the pavement.

The three American Concrete Institute (ACI) sponsored symposia proceedings on polymer concrete have come out in paper-bound volumes. They are SP-40 (1972 and 1973) (1), SP-58 (1976) (2) containing 22 papers and SP-69 (1981) (3) containing 14 papers. John A. Manson (4) gives an overview of the ongoing research on polymer concrete in the third volume SP-69.

Three principal classes of polymer concrete materials have been described in the literature. They are:

1. Polymer-portland-cement concrete (PPCC)
2. Polymer-impregnated concrete (PIC) and
3. Polymer-concrete (PC).

Only Polymer-Concrete material has been considered in this study because of its unique characteristics of quick setting combined with improved mechanical properties.

PPCC contains a polymer, usually a latex or emulsifiable type, aggregate, cement and water. In the case of PIC, previously-formed portland cement concrete is impregnated with a polymeric material whereas polymer concrete is a mixture of well-graded aggregates and sand, mixed with polymer with no cement added to the mixture.

Research activities in the area of polymer concrete accelerated in the 1970s due to the need to improve materials for highway bridge decks and desalination process equipment and geothermal applications. Work was initiated by the Federal Highway Administration and by the Department of Energy in the field of polymer-concrete. The Department of Defense efforts have been initiated through the Tyndall Air Force Base in Florida and the Army's concrete and structures laboratory at the Waterways Experiment Station in Vicksburg, Mississippi. Monomers that have been recommended are:

1. Polyester-styrene
2. Methyl-Methacrylate
3. Furan derivatives and styrene.

The above monomers are the backbones in the final polymer chain and undergoes polymerization reaction by the addition process in the presence of an initiator such as benzoyl peroxide. The low viscosity of these monomers is the reason for good wetting of the aggregates and the extremely good bond strength. The epoxy resins used appear to be more expensive compared to the polyester-styrene type and efforts are underway to develop less expensive materials and processes that will improve the performance of highway pavement, bridge decks and airport runways. It is also important to select well-graded aggregates to improve wetting and bond strength.

In fact, without a well-graded aggregate in the mix design, it is not possible to compact the polymer concrete mixture well. Without proper compaction, mechanical properties such as compressive strength and the modulus of elasticity will not be optimum. Wide variation in deformation response on application of a load has been found in polymer concrete. This can be attributed to the lack of good gradation and uniformity within the concrete matrix.

Exposure to water seems to reduce the bond strength. In order to solve this problem, monomers that can bond wet aggregates need to be identified. Work along this line is being carried out at the University of Texas and the Brookhaven

National Laboratories. Antonucci (5) is investigating acrylic and other polymers having various functional groups.

According to Virginia Fairweather (6) Degussa Corporation's William Lee contends that polymer concrete overlays are attractive from a bridge deck rehabilitation point of view. The traffic has to be restored very quickly on a bridge where the traffic volume is high and there are no other bridges nearby to cross the river by a detour. The bridge rehabilitation work that is ongoing or just completed are:

1. Three bridges at the Massachusetts turnpike. According to Arthur Dimitz of Transpo Industries, New Rochelle, New York, the polymer concrete is applied at 4 inches thick at a rate of 40 square yards a day. Compressive strength of 4000 psi is achieved in one hour and 6000 psi achieved in 24 hours.
2. I-64 in Virginia where 157 square yards per hour is applied. Work is being done in one lane during night time when traffic is slow.

According to David Whitney of the University of Texas Civil Engineering Department (7) polymer concrete overlays as thin as 3/8" can be applied with quick curing time and early development of mechanical properties. Chadwick Sherrel of Washington State DOT contends that laying down polymer concrete can be done with regular concrete-laying equipment. The estimated cost is \$40.00 per square yard at 1/8" thick. Poly Carb of Cleveland, Ohio, supplied the polymer concrete material to the state of Washington and Washington DOT under the supervision of Mr. Chad Sherrel did the application and laydown work. The bridge had to be down for eight hours only for the rehabilitation work. Two years field evaluation shows that accidents are down and the skid number is good and holding. Two years experience of Sherrel is prompting the state of Washington DOT to start other demonstration projects with the support of the Federal Highway Administration. These demonstration projects are the results of several decades of work in the laboratory in formulation, mix design, testing and evaluation.

While the formulation part of these highway studies are useful for the initial research program for airport runway application, there has to be modification in the strategy and approach for airport pavement design. This is due to the fact that the highway pavement or bridge deck is not exposed to jet blast, high-speed landing and take-off and oil and fuel spills caused during fueling, etc., of the plane as an airport runway, taxiway and hangars. More important than the above reasons are considerably higher loads and much higher shearing forces during turns and braking.

It appears that polyesters have a cost advantage over epoxies and MMAs, but their resistance to oil, grease and aviation fuel

has not been proven in the field. This polymer is being tested in several states such as Virginia, Washington and California. Cady and Weyers (8) think that use of polymer concrete could be a viable alternative to cathodic protection of the bridge deck. In fact tests (6,8) for Pennsylvania Department of Transportation are underway at the present time to rehabilitate bridge decks under the supervision of Professor Cady of Pennsylvania State University.

Fontana and Bartholomew (9) discusses deterioration of concrete bridge decks and the role of the Federal Highway Administration in repairing the deteriorated bridge decks. Under contract from the Federal Highway Administration, the Brookhaven National Laboratory's research efforts produced a polymer concrete patching material that can be premixed while imparting improved properties when compared to portland cement. Engineering News Record estimates (10) the cost of repairing one out of every six bridges in the nation to be in the neighborhood of 25 billion dollars. The high maintenance cost, public inconvenience and safety hazards involved in rehabilitating bridge decks have prompted FHWA to develop rapid curing overlay and patching materials. The same materials can be used for airport runway pavement application and rapid-setting patching materials for railroads to repair or replace track beds in areas where traffic volume is high and traffic delays will be a public inconvenience.

Two methods of application were field tested and they are the dry pack method and the premixed method. In the dry pack method the graded aggregates are placed in the repair area or the section where the overlay has to be placed. The monomers with the appropriate catalyst, promoter, etc., is then sprayed on the surface uniformly. This method requires special care to see that curing takes place uniformly and throughout the horizontal and vertical plane of the aggregate layer. More information can be found in references (11) through (17).

The second method is the usual premixed method. Here special care has to be taken to see that there is sufficient time for mixing and placement before curing reaction starts.

Schrader, E. K., and coworkers (18) and Scanlon, John M., (19) at the Army Engineer Waterways Experiment Station have undertaken work in repairing and rehabilitating stilling basins. Examples of the projects are Dworshak Dam and Libby Dam. Fiber-reinforced epoxy resins have been used which protected the stilling basins against corrosion and erosion due to sand and other abrasive materials carried by the flowing waters. Other examples of the Corps of Engineers work include:

1. Pomona Dam basin slab repair.
2. Upper St. Anthony Falls lock in the Mississippi River near Minneapolis. Further information on the use of polymer

concrete for hydrotechnical application can be found in references (20) through (29).

Robert Perry (30) in a review article describes the use of polymer concrete for electrical insulation application. Bonneville Power Administration has judiciously used polymer concrete for transformer foundation.

Zeldin, Kukacka and Carciello (31) report the use of polymer concrete composites for use in geothermal wells. High temperature resistance of silane polymers is utilized in this case. McNerney (32) describes the use of polymer concrete which has been suggested for the rapid repair of bomb-damaged runways. The rapid runway repair program has the following requirements: Rapid cure; high strength; durability; and rapid placement in all environmental conditions. The use of silane coupling agents and fibrous materials have been found to improve the tensile splitting strength, compressive strength and flexural strength.

Fowler, Meyer and Paul (33) studied the mechanical properties of polymer concrete when the aggregates contained up to 7% moisture. The use of silane coupling agent and fibrous materials have been found to improve the mechanical properties of polymer concrete containing wet aggregates.

The existing literature on special mix designs using different aggregate and polymer mixtures was also studied. The objective here is to obtain an optimum mix design which is cost effective and has improved mechanical properties. One approach that was considered in this study is the use of a polymer blend in the mix design. The advantages of blending two polymers are that the blend will have the properties of both the polymers.

Personal Communications with technical staff at the Army waterways experiment station in Vicksburg (Tony Husbands) shed some light in the use of polymer concrete. One of the probable causes for the lack of widespread use of polymer concrete is the high material cost. Any work toward a low cost mix design with improved mechanical properties and fast curing capability would be a breakthrough in polymer-concrete technology.

Having arrived at a suitable pavement material, it is to provide design curves relating pavement thickness to the load, subgrade stiffness and other mechanical properties. In order to derive these curves, it is necessary to know the shear distribution under the pavement (pavement subgrade interface) and the maximum deflection of the pavement. Of the theories available, the Westergaard analysis is found to be the most suitable. In determining the subgrade stiffness of the multilayered subgrade, the simple energy method proposed by Christano et al. is used because of its simplicity and accuracy.

The design of an airport pavement involves the following

design parameters;

1. load specifications (magnitude, geometry, frequency etc.),
2. pavement and subgrade specifications (geometry, material properties) and
3. allowable stresses and deflections in the system.

It is assumed that all the above parameters except the pavement thickness are known. The following discussion describes how the thickness can be determined as a function of the other variables and constraints.

The purpose of this analysis is to develop a scheme to determine the pavement thickness as a function of load, pavement geometries and material properties. In this design the pavement system is divided into two components, namely subgrade and pavement as shown in Figure 1. The subgrade is made up of the entire soil system except the paving, while the pavement constitutes the crust made up of paving material. The subgrade is modelled as a layered system described by an equivalent stiffness, k , (pressure per unit length) and the pavement is modelled as an elastic plate described by the Young's modulus, E , and Poisson's ratio, ν . The solutions available in the literature are used in this design method.

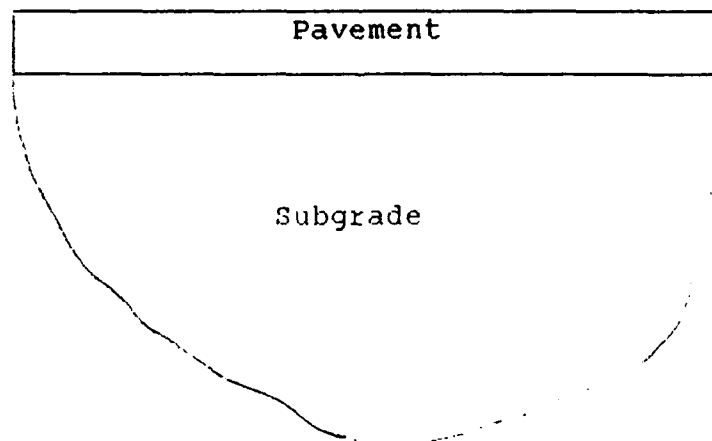


Figure 1. The Pavement System

The subgrade is generally made up of layers. A typical subgrade configuration is shown in Figure 2. Deflections and stresses on the pavement would depend on the subgrade reaction. The exact solutions for stresses and strains in layered elastic systems has been derived by Burmister (1945a, 1945b, 1945c). Burmister's solution, however, requires excessive computations as it involves long, complicated expressions. Although numerical results are available for two and three layered systems (Fox 1948; Acum and Fox, 1951) there are no results available for general multilayered systems. Christiano, Rizzo and Jarecki (1974) have developed a simple method, based on strain energy distribution, to determine the compliance of the subgrade. This method is employed herein because determining the subgrade compliance, treating it as a single layer is inaccurate.

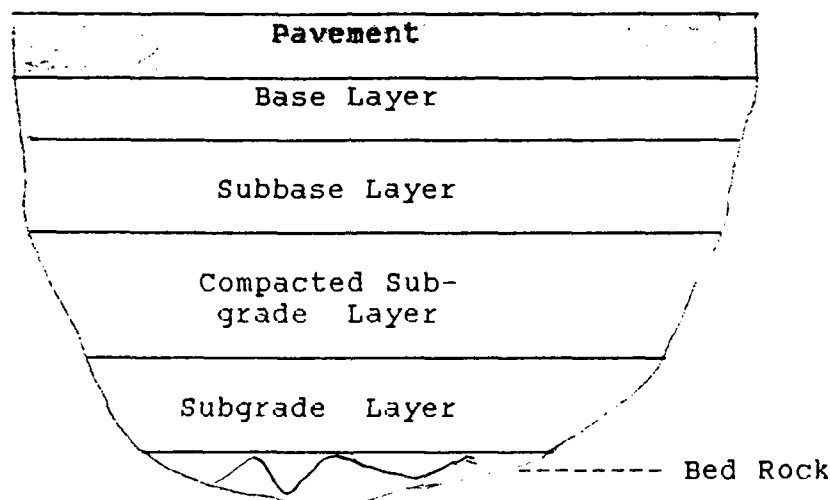


Figure 2. Subgrade Layers

The subgrade is assumed to be made up of n layers. It is assumed that each layer is;

1. homogeneous,
2. linear elastic, and
3. isotropic

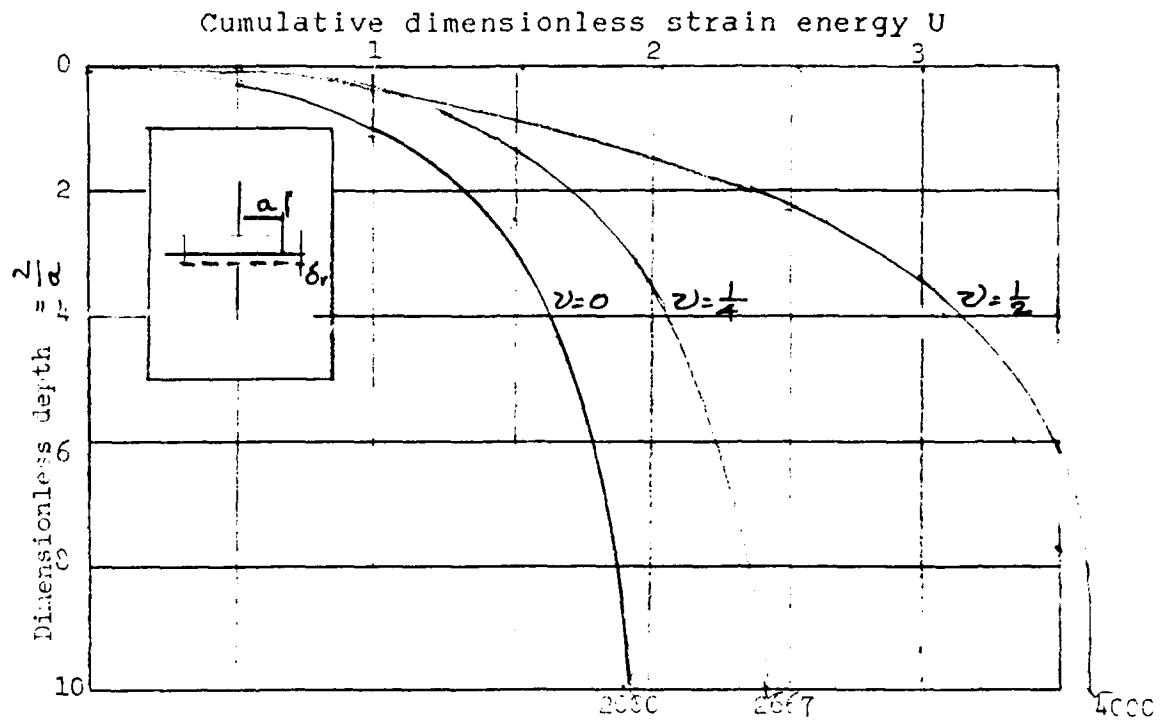


Figure 3. Dimensionless Cumulative Energy Vs. Dimensionless Depth

It is also assumed that the stress distribution in the layered system is the same as that of a homogeneous half-space (Boussinesq solution). This assumption is partly justified by the fact that the stresses in the Boussinesq solution do not depend on the elastic modulus and by the fact that effects of subgrade reaction on pavement performance are minimal (Hornjeff, 1948).

The dimensionless strain energy of each layer, U can be obtained from figure 3. This figure describes the variation of the dimensionless cumulative strain energy with the dimensionless depth. The dimensionless strain energy of the layer is obtained by taking the difference between the cumulative strain energy values at the depths corresponding to top and bottom of the layer.

The compliance of the system, k , is given by,

$$k = \{ U (1-v) / (8au) \}$$

where,

- a = equivalent radius of load area,
- U = dimensionless strain energy in the i -th layer
- u = shear modulus of i -th layer, and
- v = Poissons's ratio.

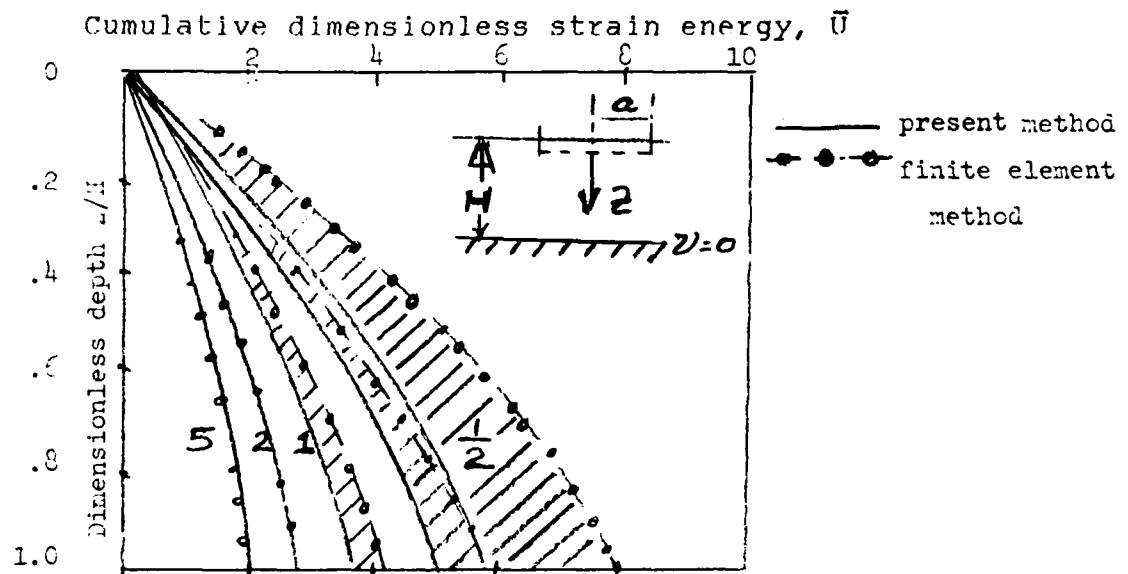


Figure 4. Comparison of Energy Method Results with Finite Element Solutions

Figure 4 shows the results of this method compared to finite element solutions. It is seen from this comparison that the approximation is very good for large depth to load diameter ratio, which indeed is the case for pavement sublayers.

Given the compliance of the subgrade, and pavement material properties, the pavement stresses and deflections can be

calculated using the Westergaard (1948) method. Westergaard makes the following assumptions;

1. slab is linear elastic,
2. slab thickness is a constant,
3. the subgrade effects are modelled by stiffness, and
4. the average length and width of the footprint is greater than the thickness of the slab.

Based on the above mentioned assumptions, Westergaard derived the solutions for plate thickness and stresses for six load cases. These load cases along with the corresponding solutions are given below. These solutions are necessary to calculate the stress distribution and deflections developed at various points of the pavement upon application of the load.

Definition of symbols for equations used for load cases 1 through 6 are as follows.

P = applied stress
h = pavement thickness
 ν = Poisson's ratio
E = Young's modulus
k = subgrade reaction constant
z = deflection
a,b = semiaxes of the ellipse representing the footprint of a tire
x,y = horizontal rectangular coordinates
r, θ = corresponding polar coordinates
l = radius of relative stiffness

Case 1: Load applied in the interior of a panel at a considerable distance away from the edge or joint. The footprint is an ellipse with major and minor axes a and b respectively. (Figure 5)

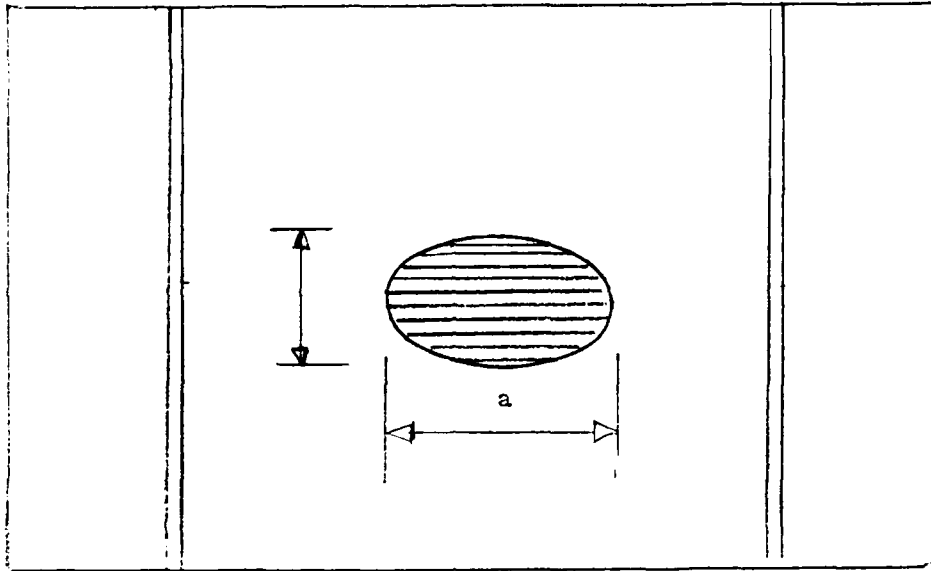


Figure 5. Load Case 1

The stresses in the pavement are given by,

$$x = \frac{P}{h^2} 0.275(1+\mu) \log_{10} \frac{Eh^2}{k \frac{(a+b)}{2}} + 0.239(1-\mu) \frac{(a-b)}{(a+b)} \quad \text{Case 1-1}$$

and the displacement near the loaded area is given by,

$$z = \frac{P}{4} \frac{3(1-\mu^2)}{Eh^3 k} - \frac{0.275(1-\mu^2)P}{Eh^3} \frac{a^2 + b^2}{4} + (x^2 + y^2) \log_{10} \frac{Eh^2}{k \frac{(a+b)}{2}} - \frac{0.239(1-\mu^2)P}{Eh^3} \frac{a^2 + 4ab + b^2}{8} + \frac{a-b}{a+b} \frac{x^2 - y^2}{2}$$

Case 2: Load applied in the interior of a panel at a considerable distance away from the edge or joint. The footprint is an arbitrary symmetric shape with axes of symmetry coinciding with the longitudinal and lateral axes of the pavement. (Figure 6)

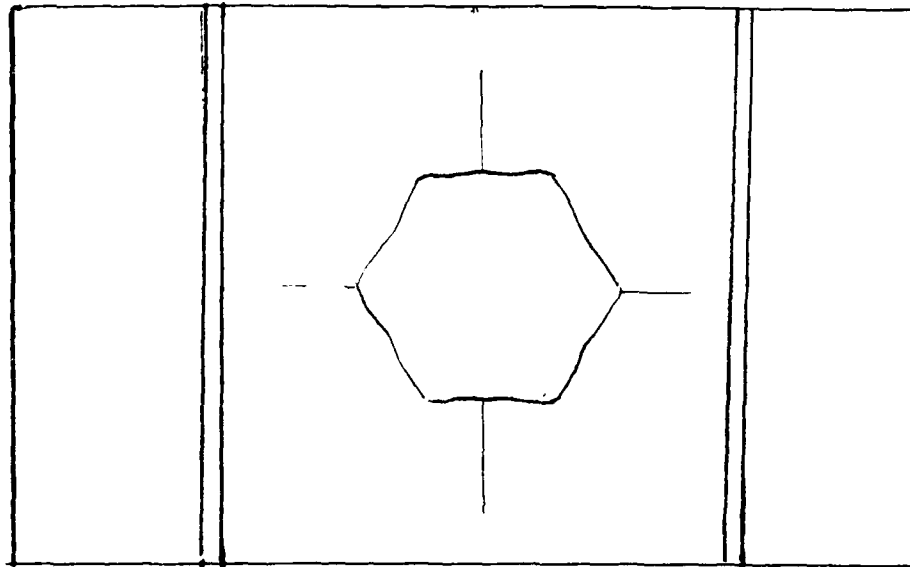


Figure 6. Load Case 2

The stresses in the pavement are given by,

$$\sigma_x = \frac{3P}{2\pi h^2} (1+\mu)(K + 0.1159) + \frac{1-\mu}{2} S$$

$$\sigma_y = \frac{3P}{2\pi h^2} (1+\mu)(K + 0.1159) - \frac{1-\mu}{2} S$$

$$\text{Where, } K = \frac{1}{A} \int dA \log \frac{r}{1} \quad S = - \frac{1}{A} \int dA \cos 2\theta$$

and the displacement near the loaded area is given by,

$$z = \frac{P}{8kl^2} - \frac{P}{8\pi kl^4} \frac{1}{A} \int r^2 dA \log \frac{1}{r} + \frac{1.1159}{A} \int r^2 dA \\ + (K + 0.1159)(x^2 + y^2) + \frac{1}{2} S(x^2 - y^2)$$

Case 3: The load is next to an edge or joint with no capacity for load transmission. Footprint is an ellipse tangential to the edge or joint. (Figure 7)

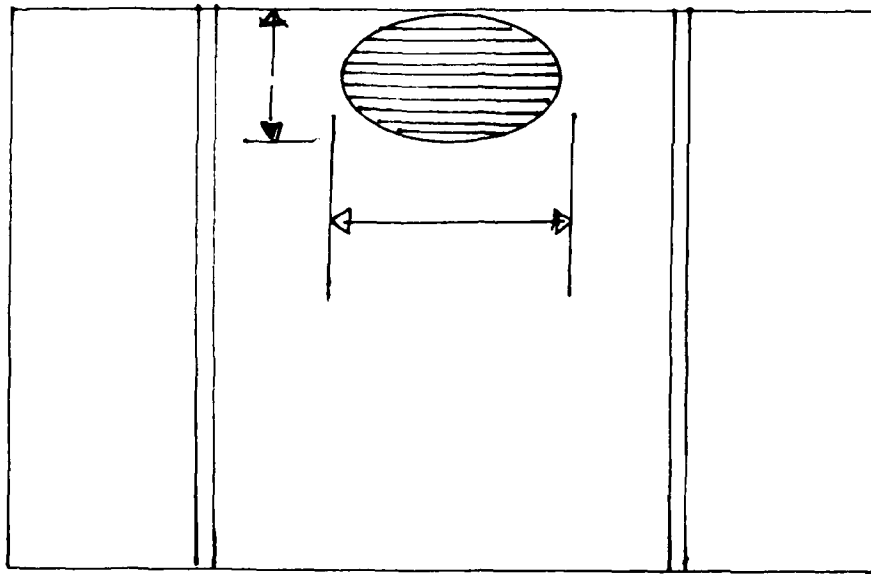


Figure 7. Load Case 3

The stresses in the pavement are given by,

$$\frac{x^2}{a^2} + \frac{(y - b)^2}{b^2} = 1$$

$$\sigma = \frac{2.2(1 + \mu)P}{(3 + \mu)h^2} \left\{ \log_{10} \frac{Eh^3}{100k \frac{(a+b)}{2}} \right. \\ + \frac{3(1 + \mu)P}{\pi(3 + \mu)h^2} \left\{ 1.84 - \frac{4}{3} \mu + (1 + \mu) \frac{a - b}{a + b} \right. \\ \left. \left. + 2(1 - \mu) \frac{ab}{(a + b)^2} + 1.18(1 + 2\mu) \frac{b}{1} \right\} \right\}$$

and the displacement near the loaded area is given by,

$$z = \frac{P\sqrt{2 + 1.2\mu}}{\sqrt{Eh^3 k}} \left\{ 1 - (0.76 + 0.4\mu) \frac{b}{1} \right\} \left\{ 1 - (0.76 + 0.4\mu) \frac{y}{1} \right\}$$

Case 4: The load is next to an edge or joint with no capacity for load transmission. Footprint is a semi ellipse with the major axis on the edge or joint. (Figure 8)

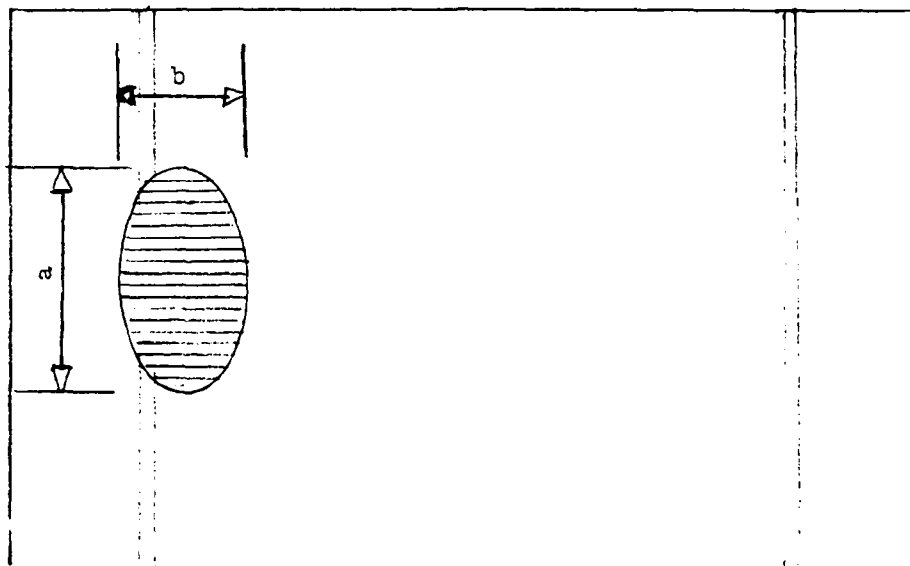


Figure 8. Load Case 4

The stresses in the pavement are given by,

$$\sigma = \frac{2.2(1 + \mu)P}{(3 + \mu)h^2} \log_{10} \frac{Eh^3}{100k(\frac{a+b}{2})^4} + \frac{3(1 + \mu)P}{(3 + \mu)h^2} \left\{ 3.84 - \frac{4}{3}\mu - (1 - \mu) \frac{a - b}{a + b} + .05(1 + 2\mu) \frac{b}{l} \right\}$$

and the displacement near the loaded area is given by,

$$z = \frac{P\sqrt{2 + 1.2\mu}}{\sqrt{Eh^3 k}} \left\{ 1 - (0.323 + 0.17\mu) \frac{b}{l} \right\} \left\{ 1 - (0.76 + 0.4\mu) \frac{y}{l} \right\}$$

Case 5: The hybrid of cases 2 and 4. (Figure 9)

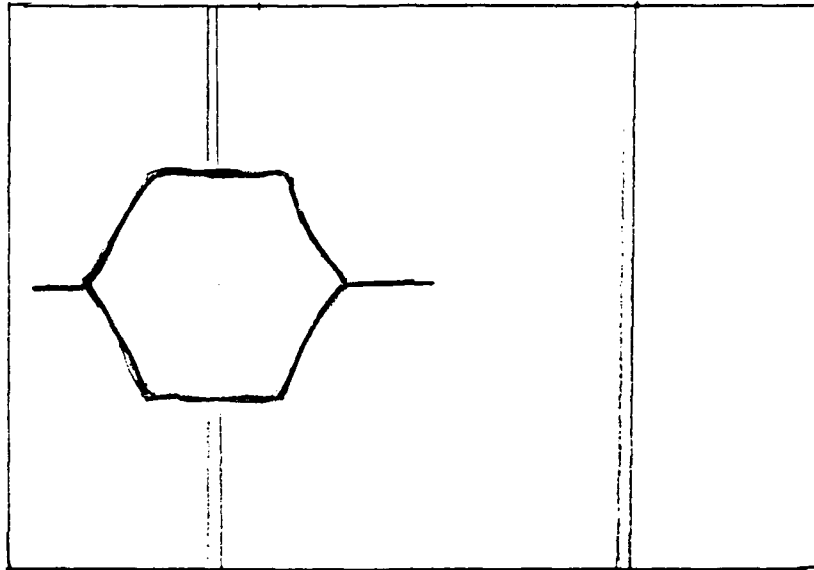


Figure 9. Load Case 5

The stresses in the pavement are given by,

$$\sigma = \frac{3(1 + \mu)P}{(3 + \mu)h^2} \left\{ 4K - 0.28 - \frac{4}{3}\mu - \mu^2 + (1 - \mu)S + 1.18(1 + 2\mu) \frac{Y}{1} \right\}$$

and the displacement near the loaded area is given by,

$$z = \frac{P \sqrt{2 + 1.2\mu}}{\sqrt{Eh^3} k} \left\{ 1 - (0.76 + 0.4\mu) \frac{Y}{1} \right\} \left\{ 1 - (0.76 + 0.4\mu) \frac{Y}{1} \right\}$$

Case 6: This is the case where the load is across a joint of efficiency j . The efficiency is normalized and hence can take values between 0 and 1, including 1. The case $j=0$, is the same as case 5. (Figure 9)

Joint Efficiency j

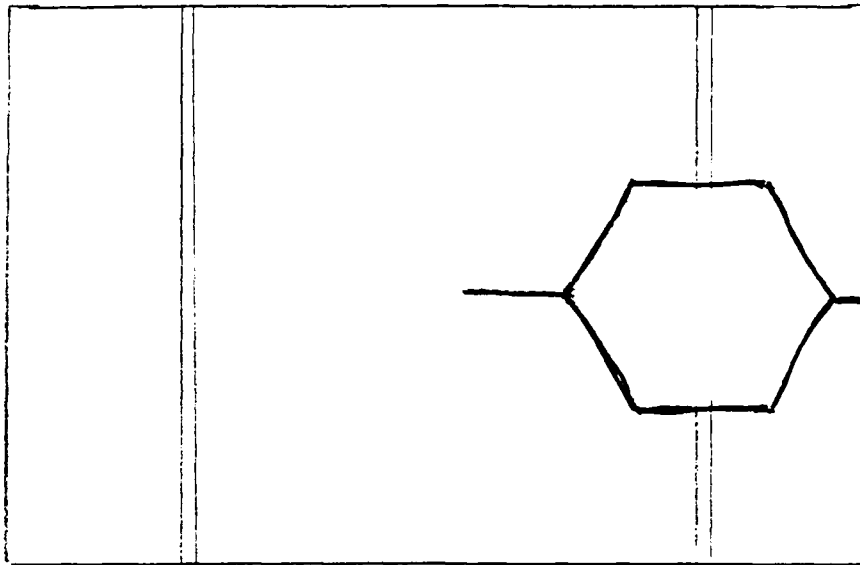


Figure 10. Load Case 6

The stresses in the pavement are given by,

$$z_i - z'_i = (1 - j) - (z_e - z'_e)$$

Where z and z' are the deflections of the adjacent slabs at any point at the joint, while z_e and z'_e are the corresponding deflections that would occur at the same place if the joint had no capacity for load transfer and j is the joint efficiency which is a number between 0 and 1.

$$\begin{aligned} \sigma_i &= (1 - \frac{j}{2})\sigma_e + \frac{j}{2}\sigma'_e \\ \sigma'_i &= \frac{j}{2}\sigma_e + (1 - \frac{j}{2})\sigma'_e \end{aligned}$$

and the displacement near the loaded area is given by,

$$\begin{aligned} z_i &= (1 - \frac{j}{2})z_e + \frac{j}{2}z'_e \\ z'_i &= \frac{j}{2}z_e + (1 - \frac{j}{2})z'_e \end{aligned}$$

Meetings and Discussions

As part of the information gathering task, interviews and discussions were carried out with personnel associated with the Airport Pavement Technology. The following is a summary of these discussions.

- Mr. Tony Husbands, Civil Engineer at the Army Corps of Engineers, Waterways Experiment Station, in Vicksburg, Mississippi. Mr. Husbands worked on the polymer concrete project for the Air Force Runway Pavement Program. About 4000 square feet of the runway surface was paved with a polymer concrete at the McClelland Air Force Base. A medium strength, modified methymethacrylate from Rohm & Haas was the binder material used in the mix design at the McClelland project. After several years of service, Mr. Husbands reports no reflection cracking or other distress at the patched areas, using the methymethacrylate polymer concrete.
- Harry Ulery, Chief of Pavement Technology Division, at the Army Corps of Engineers, Waterways Experiment Station, in Vicksburg, Mississippi. Mr. Ulery's experience with polymer concrete is limited and much information could not be obtained. High cost of polymer concrete is one of the reasons for the lack of wide spread use of concrete for paving application.
- Ms. Pat Suggs at Tyndal Air Force Base. The rapid repair program of bomb damaged runways is underway at Tyndal. An extremely fast curing urethane material is being tried for rapid curing of damaged runways. The objective is to carry out the curing reaction under wet conditions.
- Mr. William Stuenkel at Pittsburgh International Airport. During a meeting with Mr. Stuenkel, possibility of some field testing opportunity using the mix design developed by Pandalai Coatings Company was discussed. This matter will be further taken up as new laboratory mix design developments become available.

CHAPTER 3

LABORATORY SCREENING STUDIES AND RESULTS

Development of Mix Design

The early part of this study involved developing a good mix design, determining the right gradation, and curing schedule for the various polymer systems.

The following methodologies have been used in developing good mix designs and thereby improving the mechanical properties of the polymer concrete. Selection of the type of aggregates and proper gradation is necessary for a good mix design. Using aggregates, having different gradations, 3" x 6" cylindrical specimens were prepared for compressive stress measurements. This test was used as the yardstick in determining whether the polymer concrete cured properly or not. The large aggregates used were the regular Penn Dot specification material. All the aggregates and sand used can be obtained from regular concrete mixing companies. For example the sand and gravel that were used in this study have been obtained from standard supply houses in Pennsylvania and Ohio. A typical aggregate design curve is shown in Figure 11. Curves 1 through 3 represent size distributions of fine and coarse sand. Coarse aggregate sizes No.8 through No.2 are also shown in Figure 11. This figure can be used very conveniently to make modifications in the gradation of a new mix design.

Initially, experiments were carried out to determine the curing mechanism and the variables that affect curing and mechanical properties of the polymer concrete. This included polymer to aggregate ratio(Amount of Polymer), gradation and effect of temperature on the curing reaction, and development of mechanical properties.

Effect of Gradation on Mechanical Properties

Suitable coarse and fine aggregate percentages were derived from void ratio derivations. Dry graded aggregates were used to examine the effect of gradation on mechanical properties. Based upon FAA Advisory Circular 150/5370-10 for class 'A' paving concrete, a trial mix for gravel was designed, based on the recommended 25-75% sand to gravel ratio. By varying the polymer content from 10.4 to 14.2 %, it was determined that a content of less than 12% led to "Honeycombing" of the test cylinder and greater than 14% led to excess polymer "bleeding" out into the surface. However if mechanical properties were satisfactory, some extent of honeycombing would be tolerable.

In order to investigate the effect of the ratio of coarse aggregate to fine aggregate(sand), compressive stress values were determined by making samples containing the same polymer content but different gradation of aggregates. Tables 1 and 2 gives the gradation of the fine and coarse aggregates respectively. It can be seen that the gradations selected fall within the FAA P-501 specifications given in Table 1(page 319) and Table 2(page 320) of the Advisory Circular, AC150/5370-10 dated 10-24-74. Table 3 through 5 shows the effect of increasing the amount of coarse aggregates in the mix design on compressive stress. It can be seen that increasing the amount of coarse aggregate increases the compressive stress when the polymer content is kept constant, for epoxy, MMA and polyester polymer concretes.

Several 3"diameter by 6"long polymer concrete samples were prepared using different polymeric materials and were subjected to various tests to evaluate the following parameters.

1. Compressive stress of material Vs. Curing time
2. Compressive Stress of material Vs. variation in gradation
3. Compressive stress of material Vs. polymer content
4. Compressive stress of material Vs. Aggregate moisture content
5. Effect of temperature on curing rate

Several samples were prepared for the evaluation of the effect of curing time on the strength of polymer concrete. In order to accomplish this, the following procedure was adopted. The samples prepared, were stored in the laboratory in a constant temperature chamber and compressive stress was measured after 4, 24, 48, 72 and 96 hours.

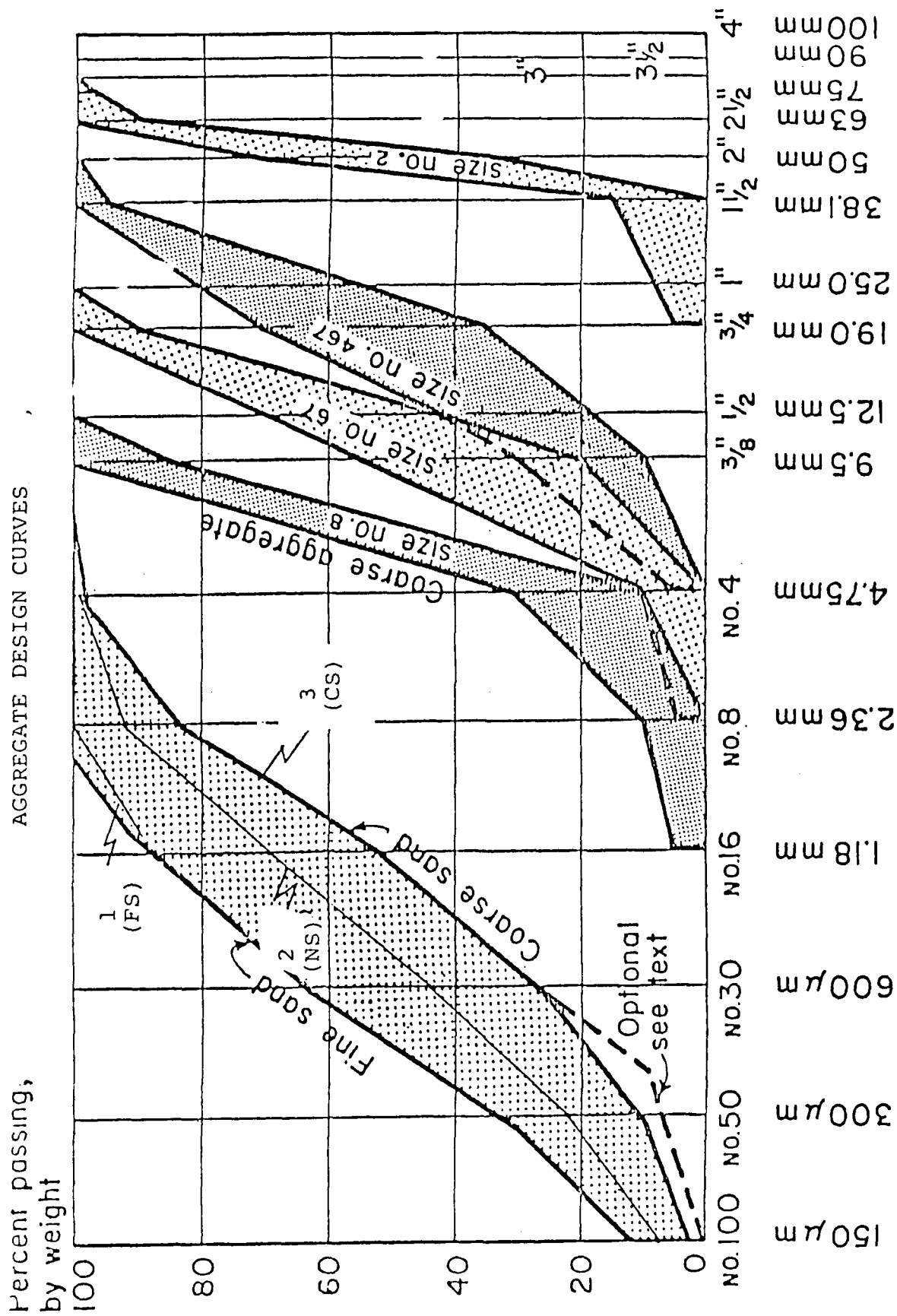


Figure 11. Curves indicate the limits specified in ASTM C33 for fine aggregates and for four size numbers (grading sizes) of coarse aggregate. (P. C. A.)

TABLE 1. FINE AGGREGATE GRADATION

SIEVE NO:	GRAMS RETAINED	% RETAINED	CUMULATIVE % RETAINED
# 4	14.60	1.5	1.5
8	169.50	17.0	18.5
16	159.60	16.0	34.5
30	151.25	15.2	49.7
50	240.80	24.1	73.8
100	192.60	19.3	93.1
PAN		69.00	6.9
	997.35		271.1
FINES MODULUS = 271.1/100 = 2.71			

TABLE 2. COARSE AGGREGATE GRADATION

CYLINDER NO:	301 - 304	305 - 320	325 -
SIEVE NO:	321 - 324		
3/4	2%	2%	1.7%
1/2	41%	41%	29.8%
3/8	21%	57%	21.8%
#4	36%	-	34.4%
PAN	-	-	12.3%
CONFORMS TO SIZE NO: 67 - ASTM - C 33			

TABLE 3. COMPRESSIVE STRESS VS. GRADATION -EPOXY

Sample #	CA/FA	% EPOXY	Max. stress
208a	1.00	6	2758
208b	1.00	6	2815
209a	1.28	6	3002
209b	1.28	6	3395
211a	1.41	6	4880
211b	1.41	6	4597

TABLE 4. COMPRESSIVE STRESS VS. GRADATION - MMA

Sample #	CA/FA	% MMA	Max. stress
260	1.00	8	3183
262	1.22	8	3400
272	1.50	8	4530

TABLE 5: COMPRESSIVE STRESS VS. GRADATION - POLYESTER

Sample #	CA/FA	% Polyester	Com. stress
402	1.17	10	1768
401	1.28	10	3253
400	1.38	10	3890
398	1.41	10	4739
512	1.41	10	6400

Effect of Temperature on Curing

The ambient temperature is an important factor to consider in the curing of any polymeric system. This is because the energy required to initiate the curing reaction is a function of the ambient temperature. Identical epoxy systems were cured at two different temperatures (64 F and 42.6 F). After 24 hours, the samples kept at the lower temperature were not sufficiently cured to evaluate the strength of material (compressive stress) of the specimen.

In the methacrylate system, the cure rate can be adjusted for different ambient temperatures by varying the content of Dimethyl Toluidine (DMT) promoter in the mix design. For example, at 75 - 79 F, the following concentrations of additives gave an effective cure time of 55 minutes to one hour.

Benzoyl Peroxide	3.0%
Dimethylaniline	1.6%
Dimethyl Toluidine	0.33%

However, when the ambient temperature was reduced to 43.2 F, the same mixture cured only after 5 hours. By increasing the Dimethyl Toluidine to .99% the curing time was reduced to 2 hours at 43.2 F.

For the curing reaction studies, a standard aggregate mix was used in preparing the specimens. The gradation used was slightly finer than the P-501 combined gradation specified in the FAA Advisory Circular 150/5370-10 CHG 2, page 319. The polymer content in the samples varied from 10 to 15%. At low temperatures (below 30 F), the curing reaction was either very slow or did not occur. This was true in the case of both Epoxy and MMA. In the preliminary studies, it was observed that after the temperature reached an optimum (45-60 F), there was no noticeable effect of polymer concrete curing time on compressive stress.

The above experiments suggest that temperatures below 45 F are not suitable for laying polymer concrete.

Specimens containing 14.2% of the MMA polymer were prepared for testing mechanical properties. Compressive stress was measured after two hours and 24 hours of specimen preparation. A 25% increase in compressive stress was noticed with the increased amount of polymer content.

Determination of the Amount of Polymer Required for Optimal Mechanical Properties

The amount of polymer required minimum voids was determined as follows. An empty mold was filled to the top with aggregates. The void space in the mold was then filled with water and the amount of water required was measured. This amount of polymer is required to fill the voids in the cylinder and prepare a good specimen. In certain mixes the polymer used was less than the optimum required to fill the voids. This was done to examine whether the mix designs having less than the optimum polymer content could be considered as a subgrade composition. Data presented in this study will reveal that reducing the polymer content below the optimum amount gives poor compressive stress values and increased moisture absorption. This can be due to excessive void space within the polymer concrete matrix and the entrapment of water in the void space. Furthermore, the entrapped water will apply stresses on isolated areas during freezing and thawing resulting in unequal stress distribution in the entire matrix. In fact, freezing and thawing is the cause of premature failure in flexible (asphaltic) and rigid (concrete) pavements in many cases. However, the possibility exists for the use of less than optimum amounts of resin for application as subgrade material due to the increased adhesive and mechanical properties of the polymeric binder.

Five polymer systems have been investigated in the laboratory during the course of this study. These are,

1. Epoxy from Shell Chemical, Ciba-Giegy and Dow Chemical
2. Methylmethacrylate(MMA) from Rohm & Haas
3. Polyester, Styrene from Dow Chemical, Union Carbide, W.R.Grace
4. Latex Emulsion from Air Products, Rohm Haas
5. Furan Polymer, from QUAKER OATS COMPANY

Of the five polymer systems initially investigated in the polymer concrete mixes, Epoxies, MMA, and Polyesters showed advantages in mechanical properties. Therefore these three systems were investigated more thoroughly. Experimental data obtained in Pandalai laboratory on all polymer systems are given below.

Epoxy Polymer Concrete

Data obtained using epoxy systems are given in tables 6 through 9. Table 6 contains data correlating cure time with compressive stress for mix designs containing 8% and 9% epoxy polymer. The polymer used is 100% solids material containing no solvents. The product used was a shell chemical product under the trade name epon 815 and the cross linking agent used was diethyl triamine (DETA) made by Union Carbide company. It can be seen from Table 6 that about 80% of the curing reaction is complete in 24 hours. Curing reaction is dependent on the type of amine curing agent used in the mix design. In order to get good workability a low viscosity curing agent (DETA) has been selected along with 100% solid high viscosity epoxy binder material.

The amount of polymer to be used in the mix design will depend on the gradation of the aggregate. Table 7 shows data which correlate percentage polymer in the mixture with compressive stress developed in a 3" x 6" cylinder. Epoxy contents of 6, 8, 9 and 10 percent were used in making samples. Data are available at different gradations having variable coarse to fine aggregate ratio (CA/FA). Compressive stress values have been found to increase with increasing polymer content.

Amount of moisture present in the aggregate has great influence on mechanical properties. The relationship between moisture content and compressive stress is shown in Table 8. It can be seen that increasing moisture content in the aggregate reduces compressive stress in the polymer concrete.

Table 9 gives experimental data on moisture absorption of polymer concrete with variation in percent polymer. The amount of water absorbed increases with decrease in polymer content.

Figure 12, 13 and 14, show the relationship between cure time, percent epoxy content and amount of moisture in aggregate with compressive stress.

Some additional observations are in order at this time. On highly humid days, the epoxy binder remained tacky for a long period of time. To study the effect of low humidity, several specimen were cured in plastic bags. It was found that those specimen in the plastic bags cured properly in 24 hours. Certain accelerators, such as dimethyl aniline and amino ethyl propanol, increases the rate of reaction even at higher humidities.

It can be seen from Figure 14, that as the water content

increases, the compressive stress decreases at the same polymer concentration. The amount of polymer used in this data set was 10%. From results obtained it was found that 10% polymer in the mix design developed a compressive strength of over 11000 psi. This is at least twice the strength of the normal portland cement concrete.

TABLE 6. COMPRESSIVE STRESS VS. CURE TIME - EPOXY

Sample #	% Epoxy	Cure time days	Comp. stress
80A	8	1	4314
80B	8	7	6430
80C	8	15	6011
80D	8	28	6223
81A	9	1	4880
81B	9	7	7000
81C	9	15	7248
81D	9	28	7496

TABLE 7. COMPRESSIVE STRESS VS. PERCENT POLYMER - EPOXY

Sample #	% Epoxy(CA/FA)		Comp. Stress
305-308	6(1.14)	~	2000 psi
325-328	6(1.41)	~	4226 psi
309-312	8(1.14)	~	4000 psi
330-332	8(1.41)	~	7120 psi
317	9(1.14)	~	7638 psi
322	9(1.41)	~	8769 psi
313	10(1.14)	~	11883 psi
333-335	10(1.41)	~	12707 psi

TABLE 8. COMPRESSIVE STRESS VS. MOISTURE CONTENT - EPOXY

SPECIMEN (1)	CA/FA (2)	% EPOXY (3)	CURE-TIME (4)	AVG STRESS PSI (5)	WATER GM/KGM (6)	TEMP. F (7)
300	47/47	6	21 HRS	2815	0	76
301	66/26.7	6.46	24 HRS	1752	5.69	70
302	67.4/26.85	6	72 HRS	983	5.69	70
303	60/34	6	24 HRS	1068	5.69	70
304	55/39	6	72 HRS	3000	0	70
305	50/44	6	5 DAYS	1697	0.94	70
306	50/44	6	5 DAYS	1782	1.87	70
307	50/44	6	5 DAYS	1386	2.68	70
308	50/44	6	4 DAYS	1344	3.74	70
309	48.9/43	8	4 DAYS	3480	0.92	71
310	49/43	8	4 DAYS	3947	1.87	71
311	49/43	8	3 DAYS	2077	2.80	71
312	48.9/43	8	3 DAYS	2759	3.74	70

Table 8: Continued.....

SPECIMEN	CA/FA	% EPOXY	CURE-TIME	AVG STRESS PSI	WATER GM/KGM	TEMP. F
(1)	(2)	(3)	(4)	(5)	(6)	(7)
313	47.9/42.1	10	1 DAY	11,883	0.93	68
314	47.9/42.1	10	1 DAY	11,318	1.87	68
315	47.9/42.1	10	1 DAY	6366	2.80	68
316	47.9/42.1	10	1 DAY	6508	3.74	68
317	48.43/42.56	9	2 DAYS	7639	0.93	69
318	48.43/42.56	9	2 DAYS	8488	1.86	67
319	48.43/42.56	9	1 DAY	6366	2.80	66
320	48.43/42.56	9	2 DAYS	5517	3.74	66
321	53.25/37.76	9	3 DAYS	7958	0	65
322	53.25/37.76	9	3 DAYS	8665	0.83	65
323	53.25/37.76	9	19 HRS	6614	1.66	68
324	53.25/37.76	9	19 HRS	6473	2.49	68

TABLE 9. MOISTURE ABSORPTION VS. PERCENT POLYMER - EPOXY

Sample #	% Epoxy	Moisture Absorption Average Percent
325 - 328	6	4.11
309 - 312	8	2.58
317 - 323	9	2.14
313 - 316	10	0.64

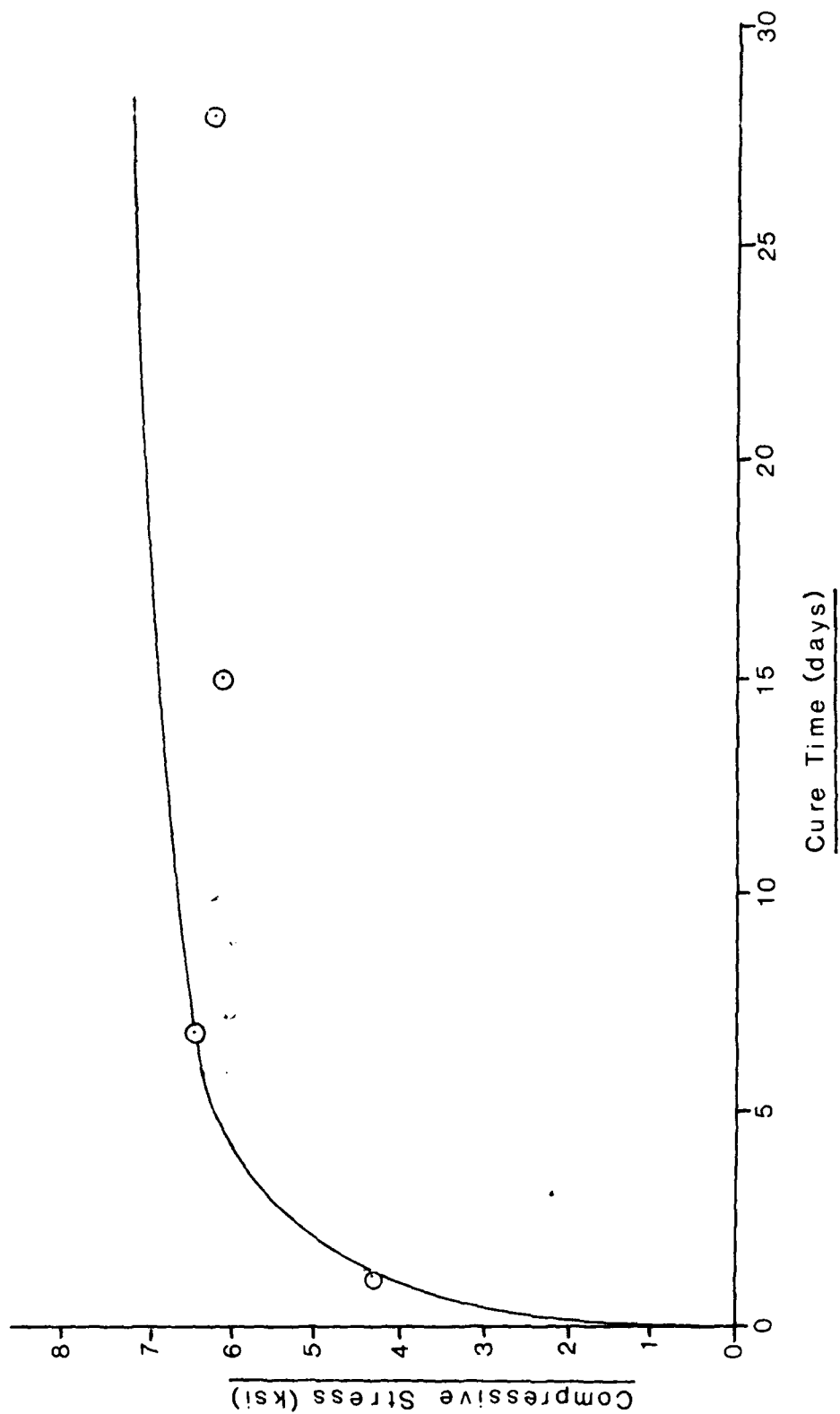


Fig.12 - Compressive Stress vs. Cure Time (epoxy -8%)

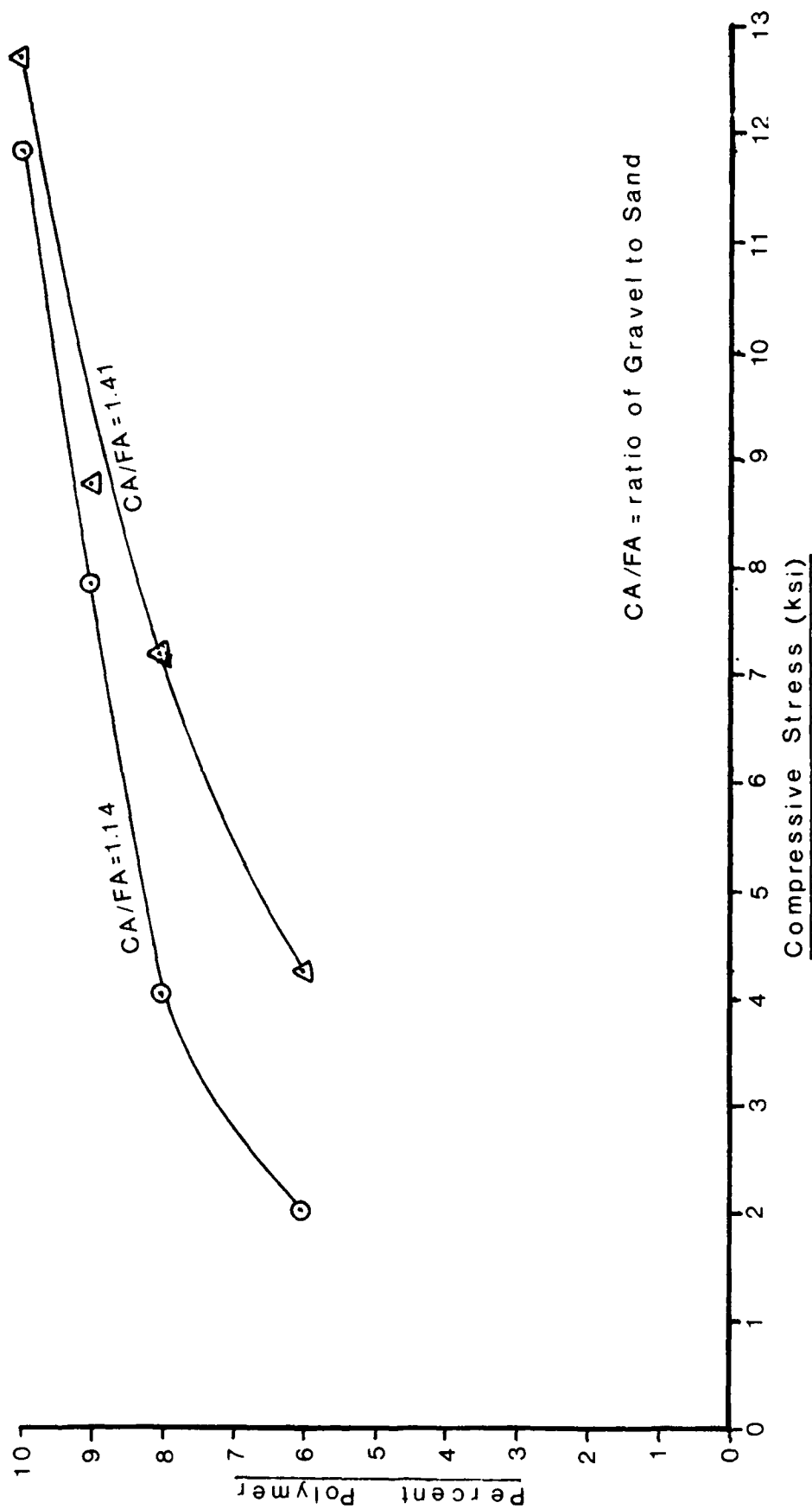


Fig.13-Compressive Stress vs. % Polymer
(Epoxy)

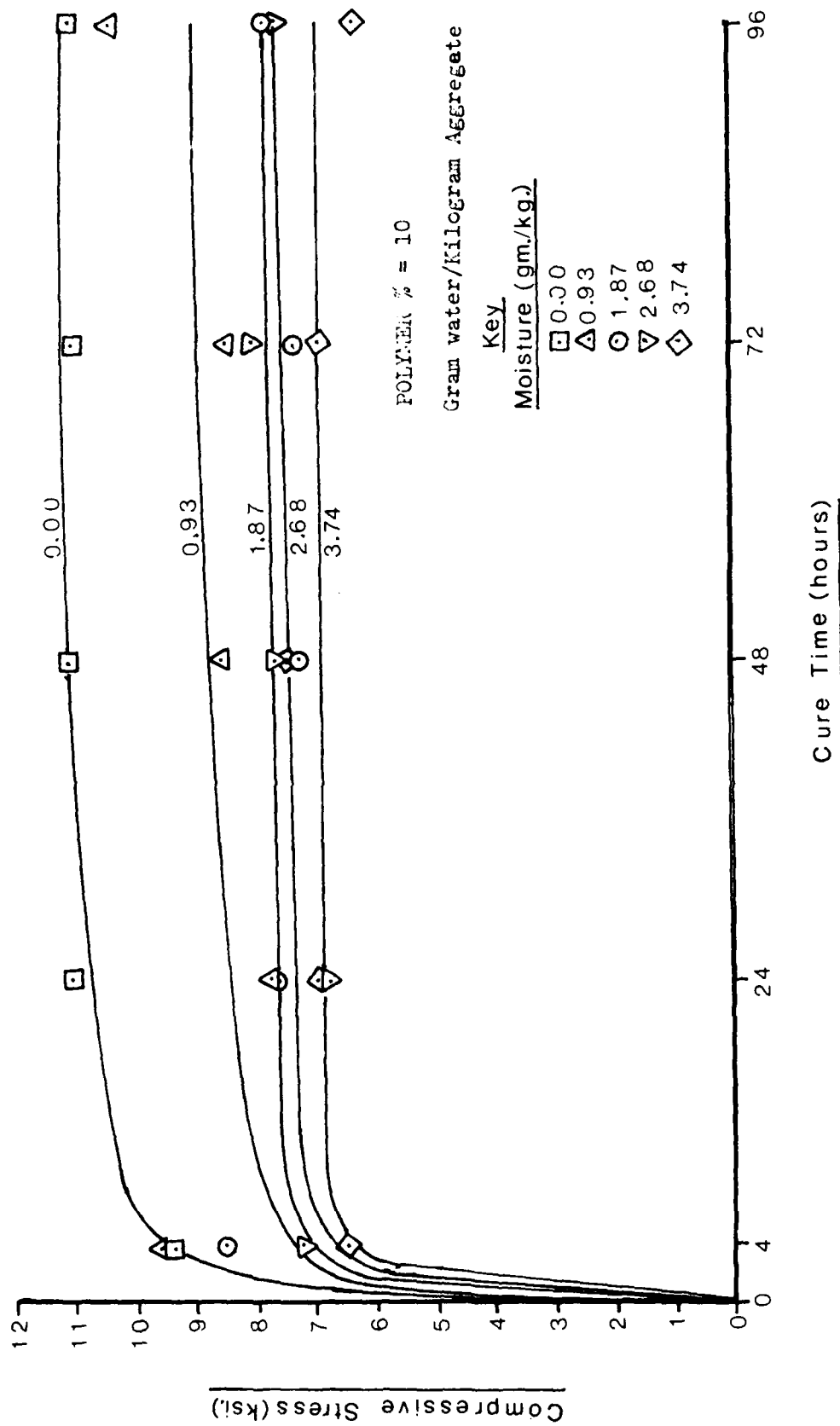


Fig 14 - Compressive Stress of Epoxy vs Water Content

Methyl Methacrylate [MMA] Polymer Concrete:

Data obtained on Methyl methacrylate(MMA) polymer concrete are given in the following section. Effects of percent polymer, ratio of coarse to fine aggregate(CA/FA) , and moisture content in the aggregate were studied to determine the relationship between these variables and mechanical properties. Data are given in ables 10 through 13.

The basic polymer mixture used in the evaluation is given below.

Dimethyl Aniline (DMA)	1.60%
N,N,-Dimethyl para-Toluidine(DMT)	0.30%
Benzoyl Peroxide (BZP)	3.00%
Methyl Methacrylate (MMA)	95.10%

Eleven percent of the above MMA polymer mix was used in the polymer concrete formulation for the result presented in table 10. The coarse to fine aggregate ratio in the polymer concrete mix was 1.41.

Table 12 shows the effect of moisture content on compressive stress for MMA polymer concrete. The data show that the compressive stress decreases as the moisture content increases.

Figures 15 and 16 correlate cure time and polymer percent with compressive stress for MMA polymer concrete. Data correlating moisture content with compressive stress are shown graphically in Figure 17. The MMA content in all the mixes in this figure has been maintained at 11%. It can be seen from the graph that 90% of the curing occurs within ten hours after mixing the polymer with the aggregates.

Table 10 and table 11 contain data correlating compressive stress with respect to cure time and percent polymer respectively. It is observed that increasing the amount of polymer and curing time increase the compressive stress. Mix designs containing as low as 8% MMA were tested. Compressive strengths between 3000 to 4000 psi were obtained for sample numbers 260, 272, 273 and 281.

The importance of using aggregates with the right gradation can be understood by an examination of table 4. By changing the CA/FA ratio from 1 to 1.5, an increase in compressive strength from 3183 to 4530 psi was obtained. Increasing percentage of

coarse aggregate in the mix design has also been found to increase the compressive stress in the case of other polymer concrete systems.

TABLE 10. COMPRESSIVE STRESS VS. CURE TIME - 11%MMA

Sample #	CA/FA	Cure Time	Max. stress
475	1.41	4 hrs.	9726
478	1.41	4 hrs.	9620
484	1.41	24 hrs.	11565
479	1.41	72 hrs.	10115
480	1.41	72 hrs.	11176
481	1.41	96 hrs.	10296
482	1.41	96 hrs.	9961
463	1.41	168 hrs.	11282

TABLE 11. COMPRESSIVE STRESS VS. PERCENT POLYMER - MMA

Sample #	CA/FA	% MMA	24 hr.stress	Max. stress
362	1.41	10		7496
345	1.41	11	6986	
386	1.41	11		9972
352	1.41	12	7922	
355	1.41	12		11105
380	1.41	13	9125	
382	1.41	13		12025
349	1.41	15	10504	

TABLE 12. COMPRESSIVE STRESS VS. MOISTURE CONTENT - MMA

Sample #	Cure Time (Hrs.)	Stress (psi)	Temp. (oF)	Gram water/Kilogram Aggregate
475(11%MMA)	4	9726	70	0.00
478	4	9655	70	0.00
484	24	11565	70	0.00
479	72	10115	70	0.00
480	72	11176	70	0.00
481	96	10292	70	0.00
482	96	9691	70	0.00
483	168	11282	70	0.00
488(11%MMA)	4	9903	70	0.93
491	24	8736	70	0.93
486	48	8700	70	0.93
487	72	8312	70	0.93
490	96	10716	70	0.93
493(11%MMA)	4	8559	70	1.87
496	24	7781	70	1.87
497	48	7215	70	1.87
494	72	7286	70	1.87
492	96	7993	70	1.87
509(11%MMA)	4	7568	70	2.68
499	24	6684	70	2.68
498	48	6932	70	2.68
504	72	8064	70	2.68
502	96	7746	70	2.68
510(11%MMA)	4	6472	70	3.74
506	24	7002	70	3.74
500	48	7356	70	3.74
505	72	6932	70	3.74
503	96	6366	70	3.74
511	24	11671	70	0.00
508	48	9620	70	0.00

TABLE 13. MOISTURE ABSORPTION VS. PERCENT POLYMER - MMA

Sample #	% MMA	Moisture Absorption Average Percent
363 - 364	10	6.4
346 - 347	11	4.2
353 - 354	11	4.0
377 - 378	12	3.6
386 - 388	13	3.2

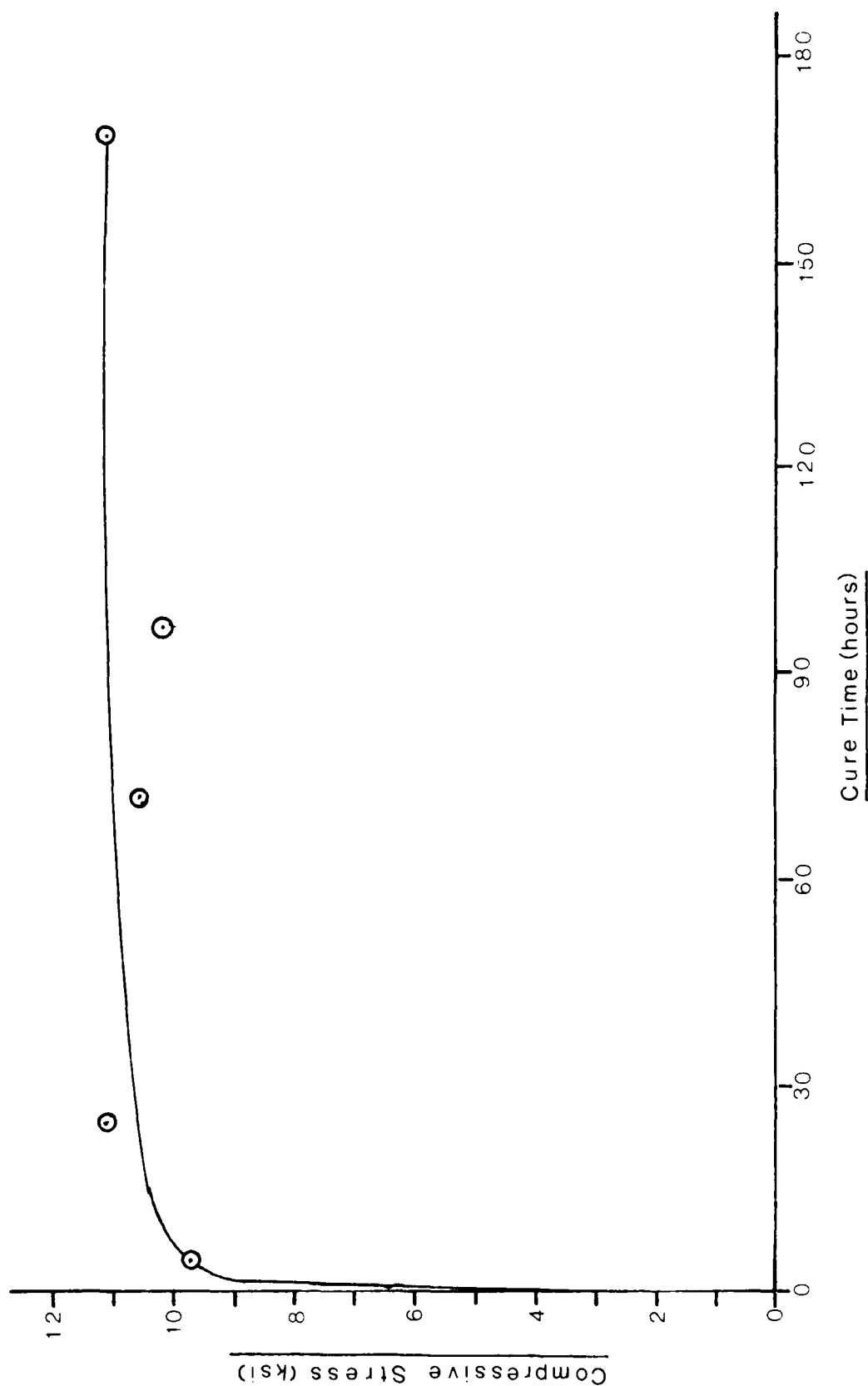


Fig.15 - Compressive Stress vs. Cure Time (MMA-11%)

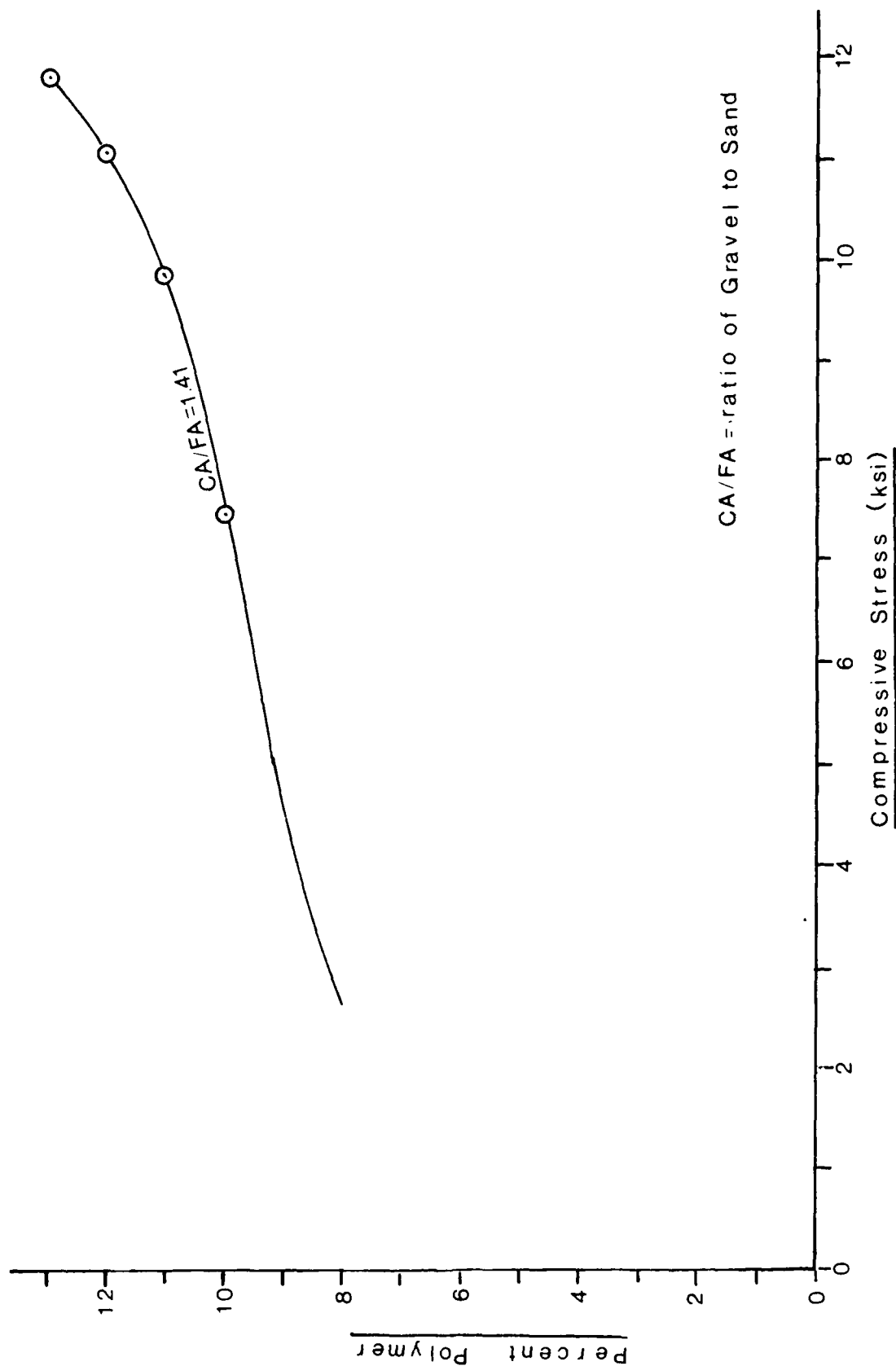


Fig.16-Compressive Stress vs. % Polymer
(MMA)

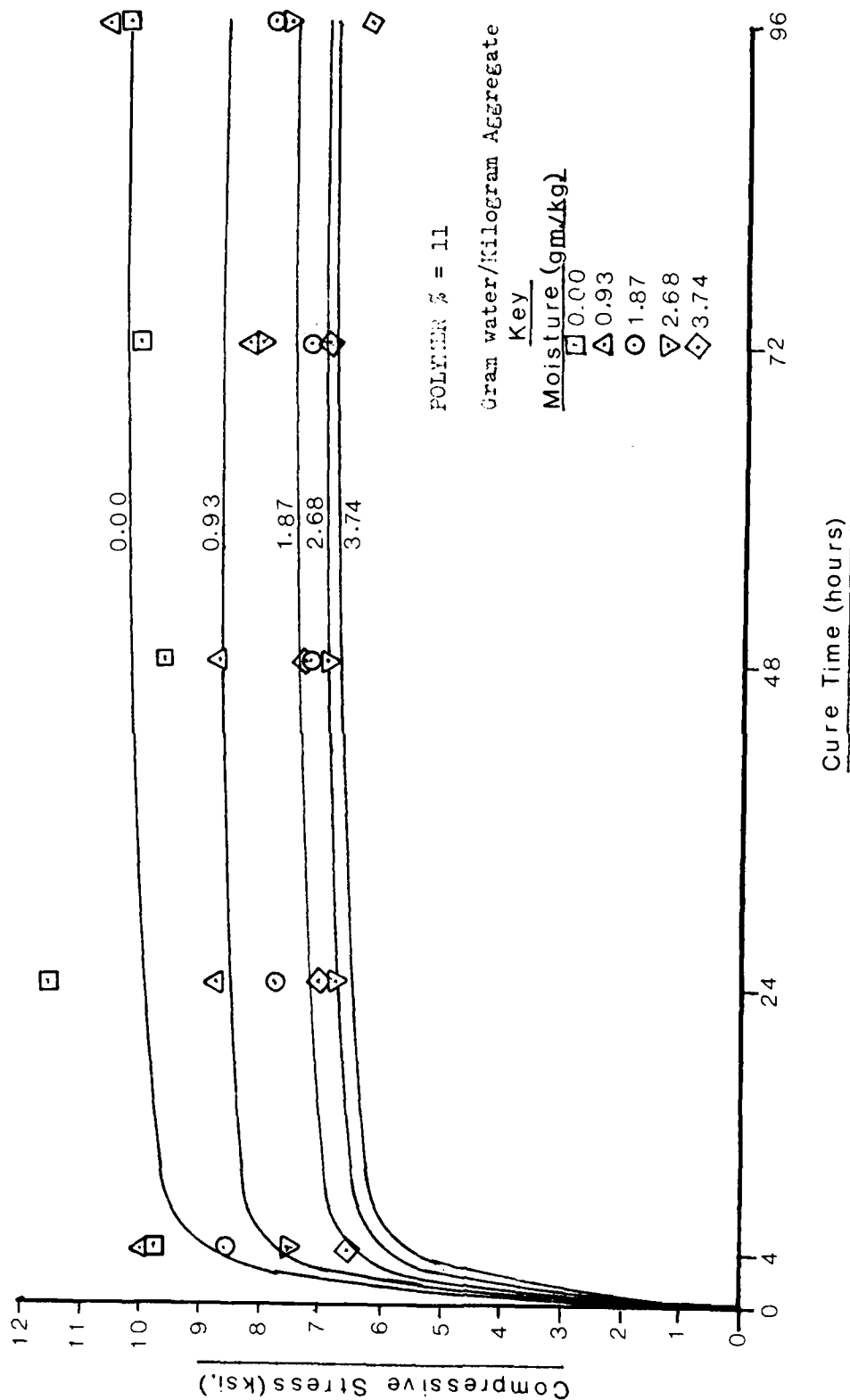


Fig.17-Compressive Stress of MMA vs. Water Content

Polyester Polymer Concrete:

Tables 14 through 17 contain data obtained in the Pandalai laboratories using polyester as the binder material in the polymer concrete matrix. Relationships between the ratio of polymer to aggregate, gradation, moisture content in the aggregate and mechanical properties were investigated in this study.

Table 15 gives the relationship between the percent polymer in the mix and the ultimate stress developed in a 3" diameter by 6" long cylinder. The percent polymer was varied from 8% to 11%. It can be seen that the ultimate stress developed gradually increases for 8% to 11% polymer samples. This behavior is similar to that of epoxy and MMA containing polymer concretes.

Table 14 shows the relationship between curing time and mechanical property development for 10% polymer containing samples. It can be observed that most of the curing takes place with the first ten hours and the curing reaction is almost complete in about a day.

The relationship between aggregate size and mechanical properties is shown in table 5. The ratio of coarse aggregate to fine aggregate (CA/FA) has been varied from 1.17 to 1.41. The relationship follows the pattern of epoxy and MMA based polymer concretes, in that the compressive stress increases with higher amount of coarse aggregates. The values reported are for 10% polymer content.

The relationship between moisture content and compressive stress is tabulated in table 16. Known amount of moisture had been added to the surface dried aggregates before preparing the samples. The moisture content was varied from zero to 3.74 grams per kilograms of aggregate. It can be seen that the compressive stress decreases with increase in moisture content for the same mix design.

One of the major problems with Portland Cement Concrete is the porous nature of the matrix and the resulting water absorption. Polymer Concrete prevents water absorption and therefore eliminates or reduces considerably problems associated with freeze thaw damage. Table 14 gives the amount of water absorbed by polyester polymer concrete. It can be seen that the water absorbed by polyester polymer concrete is practically negligible.

Figures 18 through 20 is the graphic representation of the effect of cure time, percent polymer and water content in

aggregate on the compressive stress for polyester polymer concrete.

TABLE 14: COMPRESSIVE STRESS VS. CURE TIME - 10% POLYESTER

Sample #	CA/FA	Cure Time, Hrs.	Stress
430	1.41	4	6543
433	1.41	18	7639
435	1.41	24	8664
507	1.41	24	8206
436	1.41	48	9549
439	1.41	72	10256
437	1.41	96	10539

TABLE 15: COMPRESSIVE STRESS VS. PERCENT POLYMER - POLYESTER

Sample #	CA/FA	% Polyester	Max. stress
428	1.41	8	4739
419	1.41	9	5376
427	1.41	9	6508
436	1.41	10	9549
437	1.41	10	10539
439	1.41	10	10256
414	1.41	11	10045*

*sample cured only 24 hrs.

TABLE 16: EFFECT OF MOISTURE - POLYESTER

Sample #	Cure time	% moisture	com. stress
430	4 hrs.	0.00	6543
433	18 hrs.	0.00	7639
435	24 hrs.	0.00	8664
436	48 hrs.	0.00	9549
439	72 hrs.	0.00	10256
437	96 hrs.	0.00	10539
445	4 hrs.	0.93	5942
441	24 hrs.		8453
442	48 hrs.		9019
444	72 hrs.		8984
448	96 hrs.		9230
451	4 hrs.	1.87	5872
450	24 hrs.		7604
452	48 hrs.		8912
455	72 hrs.		8700
456	96 hrs.		8912
463	4 hrs.	2.68	5765
454	24 hrs.		7215
466	48 hrs.		7286
464	72 hrs.		7746
460	96 hrs.		7640
457	4 hrs.	3.74	5234
459	24 hrs.		6542
458	48 hrs.		6720
465	72 hrs.		7286
461	96 hrs.		7180

TABLE 17: MOISTURE ABSORPTION FOR POLYESTERS

Sample #	dry wt. gms.	hrs. in H2O	wet wt. gms.
431-1	1520.0	24	1520.6
		48	1520.9
431-2	1550.4	24	1551.1
		48	1551.3
		72	1551.3

Average moisture absorption = .0585 gms.

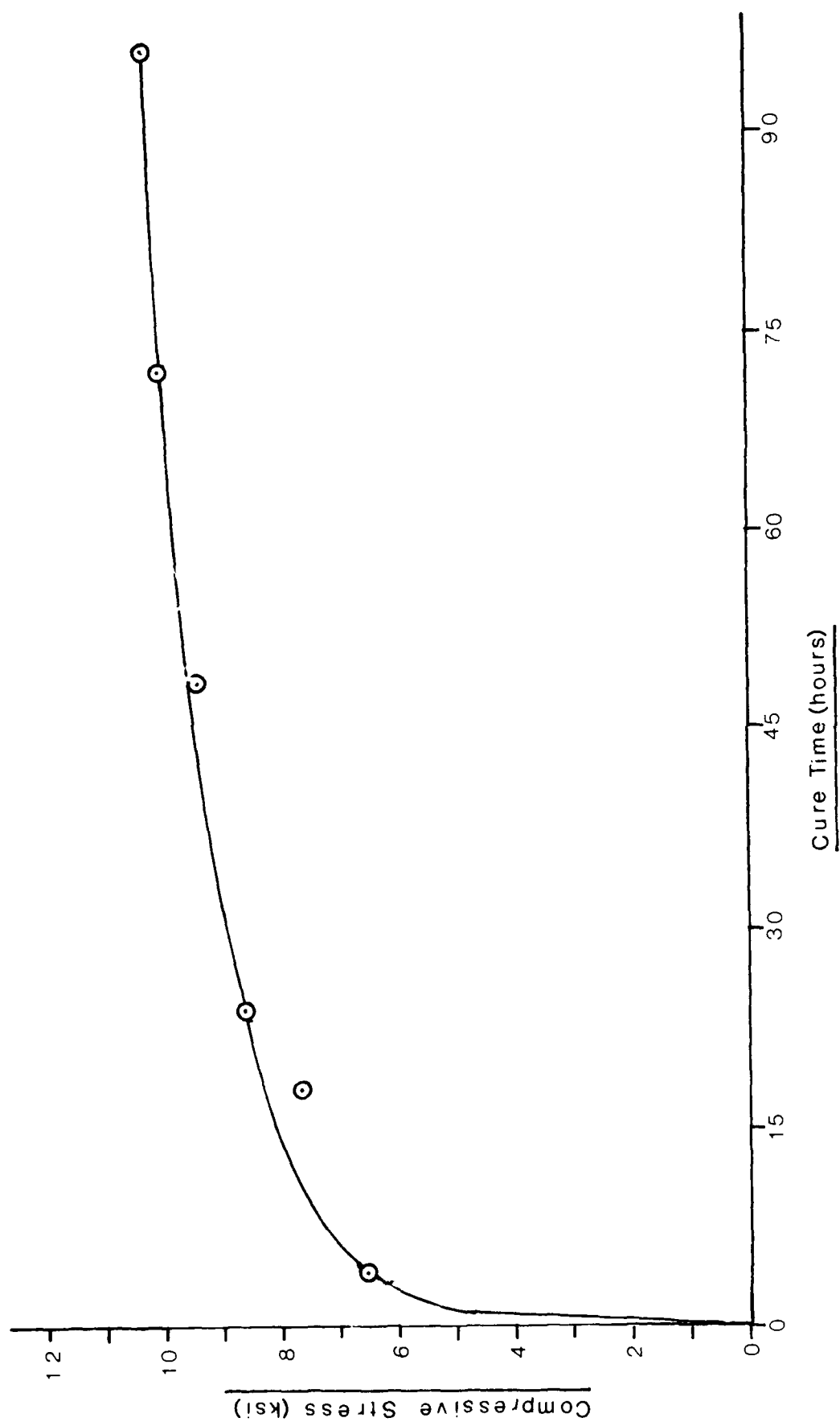


Fig.18 - Compressive Stress vs. Cure Time (polyester-10%)

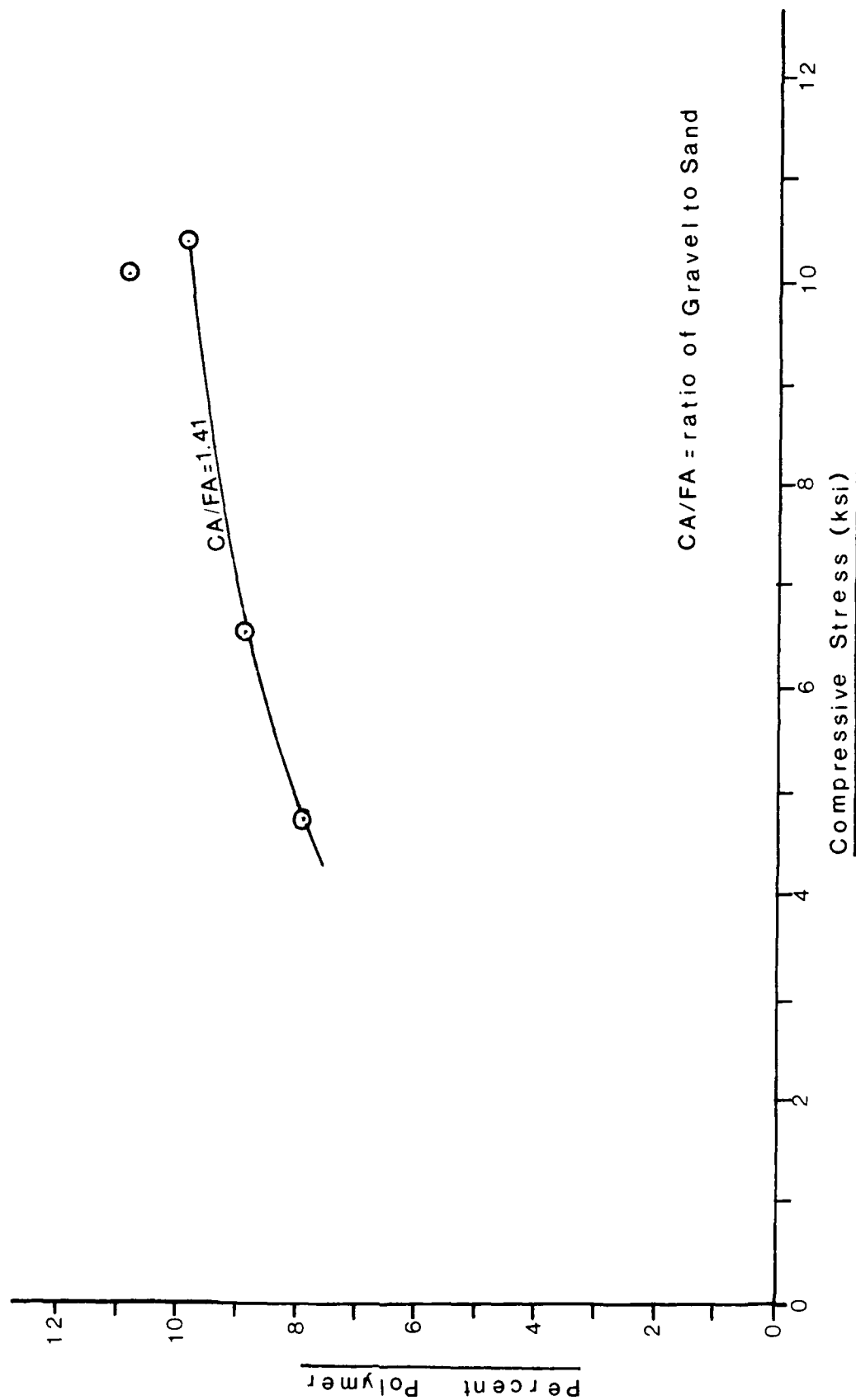


Fig.19-Compressive Stress vs. % Polymer
(Polyester)

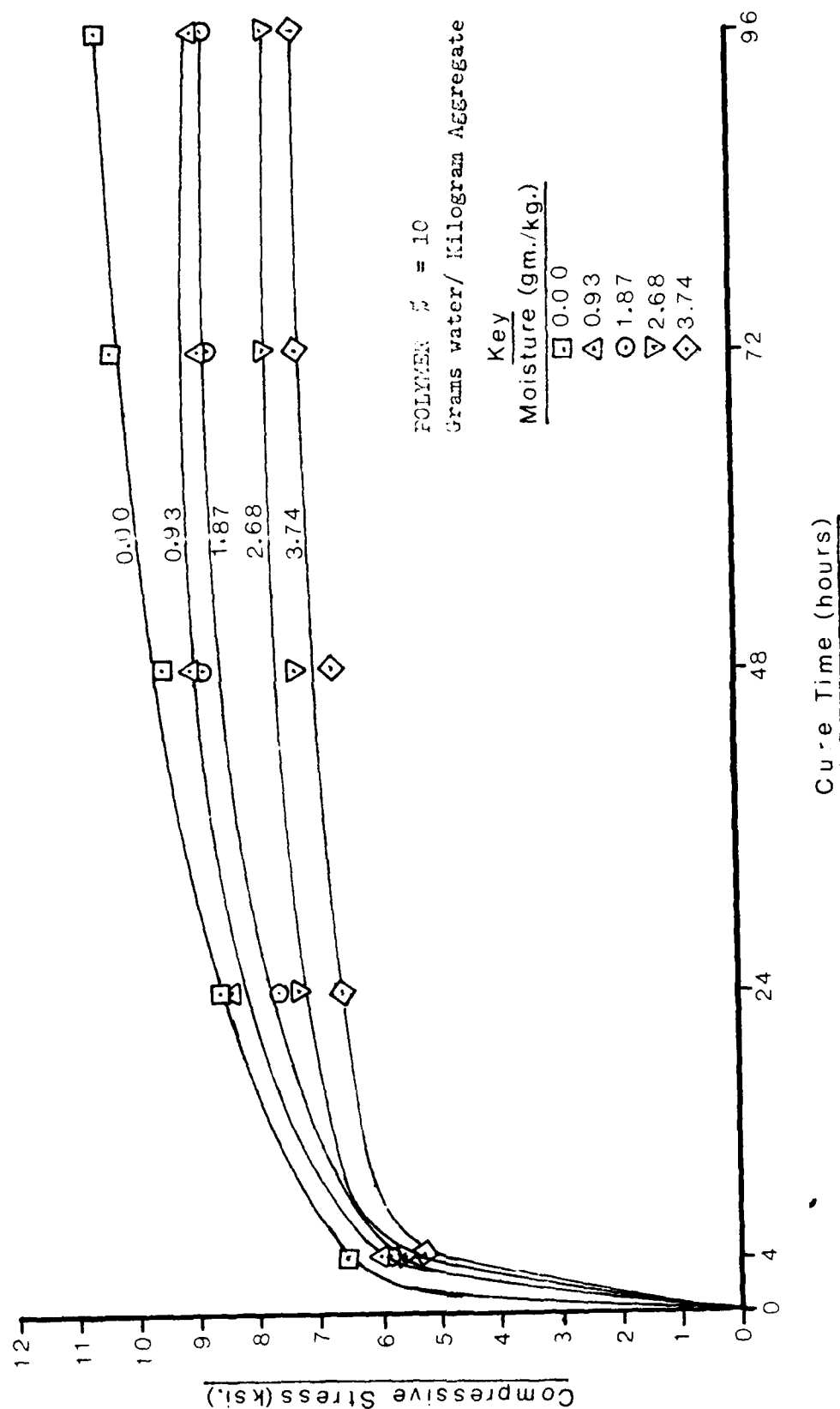


Fig. 20-Compressive Stress of Polyester vs. Water Content

CHAPTER 4

DEVELOPMENT OF MECHANICAL SPECIFICATIONS

In order to develop material specifications, the mechanical properties of the various polymer concrete mixes were experimentally determined. The following mix design was used to prepare samples that were used to perform the various tests.

A. MIX DESIGN

A mix design for polymer concrete was prepared using locally available coarse and fine aggregate. The coarse aggregates used were #57 and #8 crushed gravel and the fine aggregate used was natural sand. The physical properties of the material were according to FAA Advisory Circular requirements for P-501 concrete mixes. Based on various trial mixes, the final selected blend of coarse and fine aggregates is as below.

1. Aggregate Blend

Crushed gravel #57	-	25%
Crushed gravel #8	-	25%
Natural sand	-	50%

2. Polymer Blend

DETA	-	1 part
Epon-815	-	9 part

3. Blend of Mix

Aggregates	-	87.5%
Polymer	-	12.5%

The gradation of natural sand and aggregate blend was

compared with the FAA P-501 mix requirement and was found to fall within the specification limits (Tables 18 and 19). The aggregate gradation of the mix is presented in Table 20. The gradation is marginally coarser as compared to P-501 requirements for normal cement concrete mix.

4. Sample Preparation

Sample preparation was performed according to ASTM standard procedures with appropriate modification as considered necessary. The coarse and fine aggregates were oven dried before use in the mix. All proportioning was done by weight. The two polymer components were weighed separately and then blended together, before mixing with the pre-weighed aggregates. Mixing was performed using a mechanical mixer for about 60 to 90 seconds and then the mix was transferred to the mold for sample preparation. The workability of the mix was good as the polymer dispersed uniformly within the aggregate matrix. Initial curing time of the specimen as measured by the drop in the reaction temperature was found to be between two to three hours. Final curing time was measured by the drop in the rate of strength gain and is indicated in the compressive strength test results. Samples were prepared for the following laboratory tests:

1. Modulus of Elasticity
2. Compressive Strength
3. Flexural Strength
4. Modulus of Resilience
5. Dynamic Modulus
6. Fracture Toughness
7. Splitting Tensile Strength
8. Freeze Thaw Resistance
9. Fatigue Test
10. Creep Test

Table 18. Fine Aggregate Gradation (Mech. Property Studies)

Sieve Size	% Passing	P-501 Specification Limits
3/8"	100	100-
#4	97.5	95-100
#8	85.0	---
#16	62.5	45-80
#30	42.5	25-55
#50	17.5	10-30
#100	5.0	2-10
#200	2.1	---

Table 19. Coarse Aggregate Gradation (Mech. Property Studies)

		P-501 Specification Limits
1 1/2"	100	100
1"	99	100
3/4"	95	90-100
3/8"	45	20-55
#4	8	0-10
#8	1.6	0-5

Table 20. Combined Aggregate Gradation of the Mix

GRADATION LAB NOS.

LAB NO. 84-2709

#1 Crushed Gravel #57 #3 Natural Sand

#2 Crushed Gravel #8 #4

MATERIAL FROM <u>Columbus, Ohio</u>		DATE <u>9-25-86</u>		TYPE OF MIX <u>Polymer Concrete Mix</u>							
FOR PROJECT <u>Polymer Concrete</u>		#2		#3		#4					
Material	#1	#2		#3		#4		Total % Retained	Total % Passing	Total % Retained	Total % Passing
		Percent Failing	Percent Batch	Percent Failing	Percent Batch	Percent Failing	Percent Batch				
2											
1-1/2		100	25	100	25	100	50	100	100		
1		97.5	24.4	100	25	100	50	99.4	99		
3/4											
1/2		43	10.75	100	25	100	50	85.8	86		
3/8											
No. 4		5	1.25	20	5.0	97.5	48.8	55.0	55		
No. 8		2.5	0.62	5	1.25	85	42.5	44.4	44		
No. 16				2.5	0.63	62.5	31.3	31.9	32		
No. 30						42.5	21.3	21.3	21		
No. 60						17.5	8.8	8.8	9		
No. 100						5	2.5	2.5	3		
No. 200						2	1	1.0	1		

B. LABORATORY TESTS

1. Test for Static Modulus of Elasticity of Concrete in Compression:

This test method, performed according to ASTM C 469, was to determine the modulus of elasticity of molded polymer concrete cylinders under longitudinal compressive stress. The tests were performed on 3" x 6" cylindrical specimens and the test load ranged from 2 to 28 kips. All tests were performed at room temperature ($73\text{ }^{\circ}\text{F} \pm 3$). In all, eight samples were tested at loads ranging from 2 to 28 kips and the strain values were recorded at each load. Tests were performed on the compression testing machine with a rate of loading of about 0.05 inch per minute, which was equal to about 35 ± 5 psi per second. Without interruption of the load, the applied load and the longitudinal strain were recorded when the longitudinal strain was 50 millionths and the applied load was equal to 40 percent of the ultimate load. Longitudinal strain is defined as the total longitudinal deformation divided by the gauge length. The rest of the test procedure was according to ASTM C 469. Table 21 presents the results of static modulus of elasticity for polymer concrete. The average value, based on tests on eight samples, is 3.107×10^6 psi with a standard deviation of 0.465. For normal concrete with a compressive strength in the range of 7000 to 10,000 psi, the modulus of elasticity is about 5.7×10^6 psi. Polymer concrete has a lower modulus than normal concrete, but a much higher compressive strength. This lower modulus is due to the damping effect of the polymer ingredients in the matrix and this effect is desirable for most intended use.

2. Tests for Compressive Strength:

This test, performed according to ASTM C 39, was for the determination of compressive strength of polymer concrete specimens of dimensions 3" x 6". This test method consists of applying a compressive axial load to molded concrete cylinders at a rate of 1000 lb/second until failure occurs. Eleven samples were prepared and tested for compressive strength. Test results are presented in Table 22.

The average compressive strength of the eleven samples tested is 1.046×10^4 psi with a standard deviation of 857.3. However, eight out of eleven samples tested have strength greater than 1×10^4 psi, and this was achieved within 24 hours of molding the sample. The increased strength and the increased rate in gain in strength as compared to normal concrete makes PC an ideal

Table 21. Modulus of Elasticity Test Results

APPLIED LOAD (LB)	STRESS (psi)	STRAIN *E-04 (IN/IN)								STRAIN AVERAGE VALUE *E-04	STANDARD DEVIATION
		SAMPLE #									
		1	2	3	4	5	6	7	8		
2000	283.1	0.6187	0.5625	0.7031	0.5063	0.8156	0.7594	0.4781	0.7594	0.6500	0.127
4000	566.2	1.3781	1.3207	1.3781	1.2082	1.7156	1.6031	1.1531	1.5750	1.4160	0.190
5000	849.3	2.1656	2.2218	2.2500	2.0520	2.6156	2.5031	1.9406	2.3344	2.2600	0.222
8000	1132.3	3.0656	3.0375	3.1500	2.8687	3.5437	3.4594	2.7562	3.2062	3.1300	0.255
10000	1415.4	3.9656	3.9656	4.1062	3.6270	4.5562	4.3593	3.6281	4.1062	4.0390	0.322
12000	1698.5	4.9781	4.8938	5.1469	4.5270	5.5125	5.3156	4.4437	4.9781	4.9740	0.350
14000	1981.6	5.8500	5.7375	6.1312	5.3730	6.4969	6.2719	5.2875	5.8500	5.3750	0.412
16000	2264.7	6.7500	6.8625	7.0312	6.3270	7.4250	7.0875	6.1875	6.6937	6.7960	0.400
18000	2547.8	7.5937	7.7625	8.0437	7.2000	8.4375	7.9875	7.1437	7.5375	7.7130	0.418
20000	2830.9	8.5500	8.5625	9.0562	7.9312	9.4500	9.0281	7.6500	8.6062	8.6040	0.524
22000	3113.9	9.4500	9.5063	9.9562	8.8312	10.4062	9.9562	8.7187	9.1687	9.4990	0.526
24000	3397.0	10.1250	10.5188	10.9687	9.6750	11.4187	10.8562	9.3937	10.1812	10.3920	0.661
25000	3680.1	10.9687	11.3625	12.0375	10.5188	12.4875	12.0937	10.2937	10.9687	11.3410	0.741
26000	3963.2	11.9250	12.3750	13.1625	11.5875	13.3312	13.1062	11.2500	11.9812	12.3400	0.724
MODULUS OF ELASTICITY (PSI)		3,195,327	2,875,908	3,004,299	3,145,444	2,960,418	3,195,327	3,246,817	3,300,187		
AVERAGE VALUE OF MODULUS OF ELASTICITY (PSI)		3,115,466									

material, for its intended use. Normal concrete if it has to be designed for 1×10^4 psi compressive strength would need special aggregates and high content of cement, and would also take 14 to 28 days to develop an equivalent strength of PC.

Compressive Strength of MMA

Three samples of PC were prepared for this test using the following mixture:

MMA

133.14	grams of methylmethacrylate monomer
2.24	gm of DMA
0.42	gm of MT
4.2	gm of BZP catalyst

Aggregates

341	gm #57
341	gm # 8
682	gm sand

MMA polymer : aggregate ratio = 10%

Test results on these samples were 4571 psi, 4286 psi, and 4571 psi with an average value of 4476 psi. As can be seen from these results, MMA PC will exhibit compressive strength value equal to that of normal strength portland cement concrete after only 24 hours curing.

3. Flexural Strength:

This test, performed according to ASTM C 78 covers the determination of flexural strength of concrete by the use of a simple beam with third point loading. The test was performed in such a way to ensure that the forces applied were perpendicular to the face of the specimens and without eccentricity. The load was applied continuously at a rate of 150 psi/min. which resulted in a constant increase in the extreme fiber stress at the same rate. Eight samples were prepared and tested for flexural strength and test results are presented in Table 23.

The average flexural strength of polymer concrete based on eight samples is 2.124×10^3 psi with a standard deviation of 256. For normal concrete the compressive strength is about 5 to 7 times the tensile strength, and the same ratio applies to PC also. The major difference being that most of the strength of PC develops at 24 hours or less, which is a great advantage for its

Table 22. Compressive Stress Test Results

3" X 6" CYLINDERS

Sample #	Actual Area (in)	Failure (lb)	Compressive Strength/psi
1	7.07	68000	9618
2	7.07	64000	9052
3	7.07	73500	10396
4	7.07	74500	10537
5	7.07	75000	10608
6	7.07	75500	10679
7	7.07	77100	10905
8	7.07	86000	12164
9	7.07	74000	10467
10	7.07	79000	11174
11	7.07	67000	9477
AVERAGE VALUE			10462
STANDARD DEVIATION			857.3

Table 23. Flexural Strength (FS) Test Results

$$F_s = \frac{2Pl}{bd^2}$$

$$l = 18"$$

Sample No.	Beam Dimensions (in) bxdxL	Failure Load P (lb)	Flexural Strength FS (psi)
1	6x6x22	15000	2500
2	6x6x22	12500	2085
3	6x6x22	11500	1920
4	6x6x22	11250	1870
5	6x6x22	14500	2420
6	6x6x22	12000	2000
7	6x6x22	11250	1870
8	6x6x22	14000	2330
AVERAGE VALUE			2124
STANDARD DEVIATION			256

intended use.

4. Modulus of Resilience:

The concept of diametrical modulus has been previously applied to concrete mixes. For short duration dynamic loads, Young's Modulus (E) can be defined as the resilient modulus, a material property useful in pavement analysis. No standard ASTM test method is available for this test. In testing for modulus of resilience, a dynamic load of known duration and magnitude, lower than half the indirect tensile strength of the specimen, was applied across the vertical diameter of the specimen. The elastic deformation across the specimen was measured with displacement transducers. After recording the magnitude of the dynamic load and deformation, the modulus of resilience (MR) was calculated using the equation:

$$MR = \frac{P (v + 0.2734)}{\Delta t} \quad (1)$$

Where: P = Magnitude of dynamic load
 v = Poisson's ratio
 t = Specimen thickness
 Δ = Total deformation

Six samples were prepared and tested for deformation of modulus of resilience and test results are presented in Table 24.

The average value based on tests on six samples is 3.829×10^6 psi with a standard deviation of 0.953. For normal concrete with a compressive strength of about 10,000 psi the modulus of resilience is in the region of 3.96×10^6 psi. PC has lower MR than normal concrete, for the same reasons explained under "Modulus of Elasticity" tests.

5. Dynamic Modulus:

This test method was performed according to ASTM D 3497 with some modifications. ASTM D 3497 defines the determination of dynamic modulus of polymer concrete by application of sinusoidal axial compression stress applied to the specimen at three different temperatures and loading frequency. The resulting recoverable axial strain response was measured and used to calculate dynamic modulus. Dynamic modulus is the absolute value of the complex modulus that defines the property of a material subject to sinusoidal loading. The tests were performed at

Table 24. Modulus of Resilience Test Results

LVDT CONSTANT $F = 4.5 \times 10^{-7}$

CONSTANT - 0.5734

Sample #	Thickness T (in)	Applied Load (lb)	No. Lines	Deformation $\delta \times 10^{-5}$ (in)	Modulus of Resilience $\times 10^6$ (psi)
1	3.063	1443	(9.5+7.5)10mV	7.650	3.531
2	2.719	1281	(7+3.5)10mV	4.725	5.717
3	2.968	1399	(12+5.5)10mV	7.875	3.432
4	2.422	1141	(14.5+2)10mV	7.425	3.638
5	2.938	1384	(12.5+4)10mV	7.425	3.638
6	2.906	1369	(7+2)20mV	8.100	3.334
AVERAGE VALUE					3.882
STANDARD DEVIATION					0.907

temperatures of 25, 35 and 45 degree C and loading frequency of 1, 4, 10 and 16 Hz. The loading stress was determined as follows:

$$\sigma_0 = \frac{H_1 \times L}{H_2 \times A} \quad (2)$$

where:

H₁ = Measured weight of load
H₂ = Measured chart height
L = Full scale load
A = Cross sectional area

The recovered axial strain was determined as follows:

$$\epsilon_0 = \frac{H_3 \times S}{H_4} \quad (3)$$

where:

H₃ = Measured height of recoverable strain
H₄ = Measured chart height
S = Full scale strain amplitude

Dynamic modulus was determined by dividing the loading stress (σ_0) by the axial strain (ϵ_0).

Fifteen samples were prepared and tested for determination of dynamic modulus and test results are presented in Table 25.

The average value based on test of fifteen samples is presented below.

Dynamic Modulus at Different Frequencies(x10⁵ psi)

Temp:	1Hz	4Hz	10Hz	16Hz
25 C	41.77	49.36	82.32	142.31
35 C	36.92	41.17	60.44	95.12
45 C	34.76	37.71	50.82	74.80

The data given above indicate that the dynamic modulus is temperature dependent, which is not normally the case with

Table 25. Dynamic Modulus of Elasticity
(at 25°C)

DYNAMIC MODULUS X 10 ⁵ (PSI) (AT 25°C)				
Freq. Sample #	1Hz	4Hz	10Hz	16Hz
1	43.037	50.116	72.321	123.087
2	50.154	61.136	94.594	160.245
3	36.531	44.231	75.228	132.703
4	46.324	52.613	80.123	126.849
5	31.626	38.285	59.846	109.382
6	41.632	46.896	72.508	146.431
7	34.153	40.405	64.789	125.215
8	32.678	37.618	72.931	128.682
9	35.584	48.389	88.462	163.327
10	42.810	50.050	93.520	149.710
11	50.840	60.290	99.610	154.240
12	51.580	60.290	105.590	179.560
13	49.840	53.050	96.990	162.480
14	39.590	50.550	80.330	139.010
15	39.850	46.430	77.930	133.680
AVERAGE	41.77	49.36	82.32	142.31
STANDARD DEVIATION	6.85	7.50	13.48	19.12

Table 25. Dynamic Modulus of Elasticity (continued)
(at 35°C)

DYNAMIC MODULUS X 10 ⁵ (PSI) (AT 35°C)				
Freq. Sample #	1Hz	4Hz	10Hz	16Hz
1	36.49	41.88	66.84	100.15
2	42.27	48.31	73.28	117.96
3	36.70	41.26	61.14	102.52
4	36.06	39.32	57.84	94.79
5	38.62	43.28	66.84	102.52
6	29.88	33.25	45.75	67.77
7	38.14	41.94	59.37	94.36
8	37.17	40.13	52.42	80.90
AVERAGE	36.92	41.17	60.44	95.12
STANDARD DEVIATION	3.46	4.20	8.74	15.15

Table 25. Dynamic Modulus of Elasticity (continued)
(at 45°C)

DYNAMIC MODULUS X 10 ⁵ (PSI) AT (45°C)				
Freq. Sample #	1Hz	4Hz	10Hz	16Hz
1	27.55	31.61	54.80	84.25
2	25.69	34.75	41.26	77.74
3	26.32	31.97	45.41	97.08
4	39.13	41.04	53.96	72.42
5	39.70	42.92	54.15	72.42
6	40.42	44.61	53.85	76.10
7	37.89	41.39	49.92	60.49
8	36.82	41.94	50.33	67.11
9	30.32	47.18	53.72	65.63
AVERAGE	34.76	37.71	50.82	74.80
STANDARD DEVIATION	6.28	5.59	4.69	10.93

portland cement concrete. Also, the dynamic modulus of the normal concrete is about 20 percent higher than the static modulus. It appears that polymer concrete also behaves similarly. It could also be argued that dynamic modulus of polymer concrete is temperature dependent due to the effect of polymer matrix in concrete. Dynamic modulus values decrease with an increase in temperature.

6. Fracture Toughness:

The method used to determine fracture toughness was developed at Ohio State University. The fracture toughness (K_{Ic}) was determined by cutting a right angled wedge into a three inch diameter specimen and initiating a crack (0.125 inch long) at the apex of the notch. The specimen was set on a base with the notch pointing upwards, and a vertical load was applied to it through a three-piece set-up consisting of two plates (placed against the sides of the wedge) and a semicircular rod placed between the two plates to transmit the load by "wedging" to the sides of the wedges.

The results of (tests conducted at room temperature) allowed the calculation of the fracture toughness, K_{Ic} through the equation[35]

$$K_{Ic} = F_{\text{stress}} * F_{\text{geom}} * \sqrt{C} * \frac{P}{t * R} \quad (4)$$

Where:

F_{stress} = stress factor
 F_{geom} = geometry factor
 C = crack length (inches)
 P = maximum vertically applied load (lbs)
 t = thickness of specimen (inches)
 R = radius of specimen (inches)

Also from reference 19:

$$F_{\text{stress}} = 6.153078e^{4.30577(c/R)^{2.475}}$$

$$F_{\text{geom}} = 3.950373e^{-3.07103(c/R)^{0.25}}$$

The fracture toughness test provides engineers with an additional parameter for evaluating cracking potential. K_{Ic} has been found to be a material constant independent of slight changes in the crack length, loading conditions, and other geometrical variables.

Table 26. Fracture Toughness K_{Ic} Test Results

$$K_{Ic} = F \text{ stress} \times F \text{ geom.} \times \sqrt{C} \times \frac{P}{t \times r}$$

$$F \text{ stress} = 6.53078 \times e^{4.30577 \left(\frac{C}{r}\right)^{2.457}}$$

$$F \text{ geom.} = 3.950373 \times e^{-3.07103 \left(\frac{C}{r}\right)^{0.25}}$$

Sample No.	Length of Initial Crack	Radius r(in)	Thickness t (in)	Failure Load P (lb)	Fracture Toughness K_{Ic} (psi√in)
1	0.125	1.50	2.50	6200	1032.5
2	0.125	1.50	2.31	5150	928.2
3	0.125	1.50	2.33	7000	1250.8
4	0.125	1.50	2.34	4450	791.7
5	0.125	1.50	2.60	5000	800.6
6	0.125	1.50	2.50	6450	1074.1
7	0.125	1.50	3.00	3500	485.7
8	0.125	1.50	3.00	4000	555.0
AVERAGE VALUE					864.8
STANDARD DEVIATION					260.2

Table 27. Splitting Tensile Test Results (σ_y)

$$\sigma_y = \frac{2P}{\pi dt}$$

Sample	Dia d(in)	Thickness t(in)	Failure Load P(lb)	σ_y (psi)
1	3.00	2.53	18500	1552.5
2	3.00	2.63	20200	1630.7
3	3.00	2.52	19400	1634.5
4	3.00	2.51	17200	1454.9
5	3.00	2.53	12400	1040.7
6	3.00	2.28	14000	1303.7
7	3.00	2.27	14600	1365.5
8	3.00	2.48	16750	1457.4
AVERAGE VALUE				1430.0
STANDARD DEVIATION				196.45

Eight samples were prepared and tested for determination of fracture toughness. The test results are presented in table 26. The average value based on eight samples tested is 865 psi $\sqrt{\text{in.}}$ with a standard deviation of 260.2. For normal concrete, the fracture toughness is about 1200 psi/ $\sqrt{\text{in.}}$. It could be argued that fracture toughness of PC is slightly lower due to high compressive strength and ductile fracture behavior of the material.

7. Splitting Tensile Strength:

This test was performed according to ASTM C 496 standard which covers the determination of the splitting tensile strength of cylindrical concrete specimens. The specimens were tested on a compression testing machine by applying the load continuously and without shock at a constant rate of 150 psi per minute until failure of the specimen. The maximum load applied to the specimen was recorded and splitting tensile strength was calculated as follows:

$$\sigma_y = \frac{2P}{\pi dt} \quad (5)$$

where:

P	=	Maximum load, (lbs)
d	=	Specimen diameter, (inches)
t	=	Specimen length, (inches)

Eight samples were prepared and tested for determination of splitting tensile strength and test results are presented in table 27. The average value based on eight samples tested is 1430 psi with a standard deviation of 196. This appears to be about 30% higher than for normal concrete.

8. Poisson Ratio:

The value of Poisson ratio is not directly observed through experimentation but rather is calculated from data obtained through other experimental tests. The data used for the calculation of Poisson ratio resulted from the resilient modulus and modulus of elasticity tests. That is, the value of Poisson's ratio was calculated using the following expressions from [36]

Table 28. Poisson Ratio Value

Sample No. No.	Sample Thickness	Load (lb)	Deformation * _{10⁻⁵} (in)	Poisson Ratio	Comments
1	3.063	1443	7.650	0.2360	
2	2.719	1281	4.725	0.0426	Discussed
3	2.968	1399	7.875	0.2506	
4	2.422	1141	7.425	0.2211	
5	2.938	1384	7.425	0.2211	
6	2.906	1369	8.100	0.2657	
Average Value				0.2389	
Standard Deviation				0.0194	

$$F = \frac{S_H}{t} (0.9976 + 0.2692) \quad (6)$$

t = Poisson ratio
 E = Modulus of elasticity, psi
 t = Specimen thickness, inches
 S_H = P/x_t
 P = Load, lbs.
 x_t = Total horizontal deformation for the load P , inches

The results are presented in Table 28. One entry (second row of Table 28) was ignored in calculating the average value. A close look at Table 28 shows that the ignored value is about five times smaller than that of the other listed values. This is due to the corresponding value for the horizontal deformation used in the formula to calculate the Poisson's ratio from the resilient modulus tests, listed in Table 24, being excessively low compared to the remaining values listed in the same Table. The average value of Poisson's ratio for polymer concrete is 0.2389 with a standard deviation of 0.0193. Comparison of Poisson's ratio values for polymer concrete and cement concrete show they are similar.

9. Freeze and Thaw Tests:

This test performed according to ASTM C 666 standard that covers the determination of the resistance of concrete specimens to rapidly repeated cycles of freezing and thawing in water. If results indicate that the specimens are unaffected by the rapid freeze-thaw cyclic action, then it can be concluded that the concrete samples were made with sound aggregates and a proper air void system. The test procedure determined the length change, weight change, and durability factor after 300 cycles of freezing and thawing.

Three samples were prepared and tested for freeze-thaw effect and test results are presented in table 29. the test results indicate that polymer concrete is much more durable than normal concrete, under adverse freeze-thaw cyclic conditions.

Table 29. Resistance To Rapid Freezing and Thawing Test Results

Sample No.	Length Change, %	Weight Change, %	Durability Factor
1	+0.005	+0.2	98
2	+0.005	+0.2	99
3	+0.003	+0.2	99
Average Value	+0.004	+0.2	99

10. Fatigue Properties of PC:

Beams of three different dimensions were fabricated using the mix design proportions described earlier. Testing began with 3" x 3" x 15" beams which did not break after about 700,000 cycles with a load of 1700 lbs. Consequently the thickness was changed and tests were performed on specimens that were 2" x 3" x 15" and 1.75" x 3" x 15". the 2-inch and 1.75 inch values are beam depth. Tests were performed at different stress levels such that the ratio σ/MR varied from 0.60 to 0.92 of the ultimate flexural strength. The haversine load was applied with a duration of two pulses per second. The number of cycles to failure and stress level were recorded for each sample (see Table 30)

The results were used to calculate fatigue for the polymer concrete specimens. The general mathematical form of the fatigue equation is:

$$\text{Log } N_f = K_1 + K_2 \left(\frac{\sigma}{MR} \right) \quad (7)$$

where:

N_f	=	number of cycles to failure
σ	=	stress level, psi
MR	=	modulus of rupture
K_1, K_2	=	regression constants

For typical portland cement concrete this equation is

$$\text{Log } N_f = 17.61 - 17.61 \left(\frac{\sigma}{MR} \right)$$

Results obtained from the tests on polymer concrete samples are shown in Table 30 and can be used according to (7) to yield

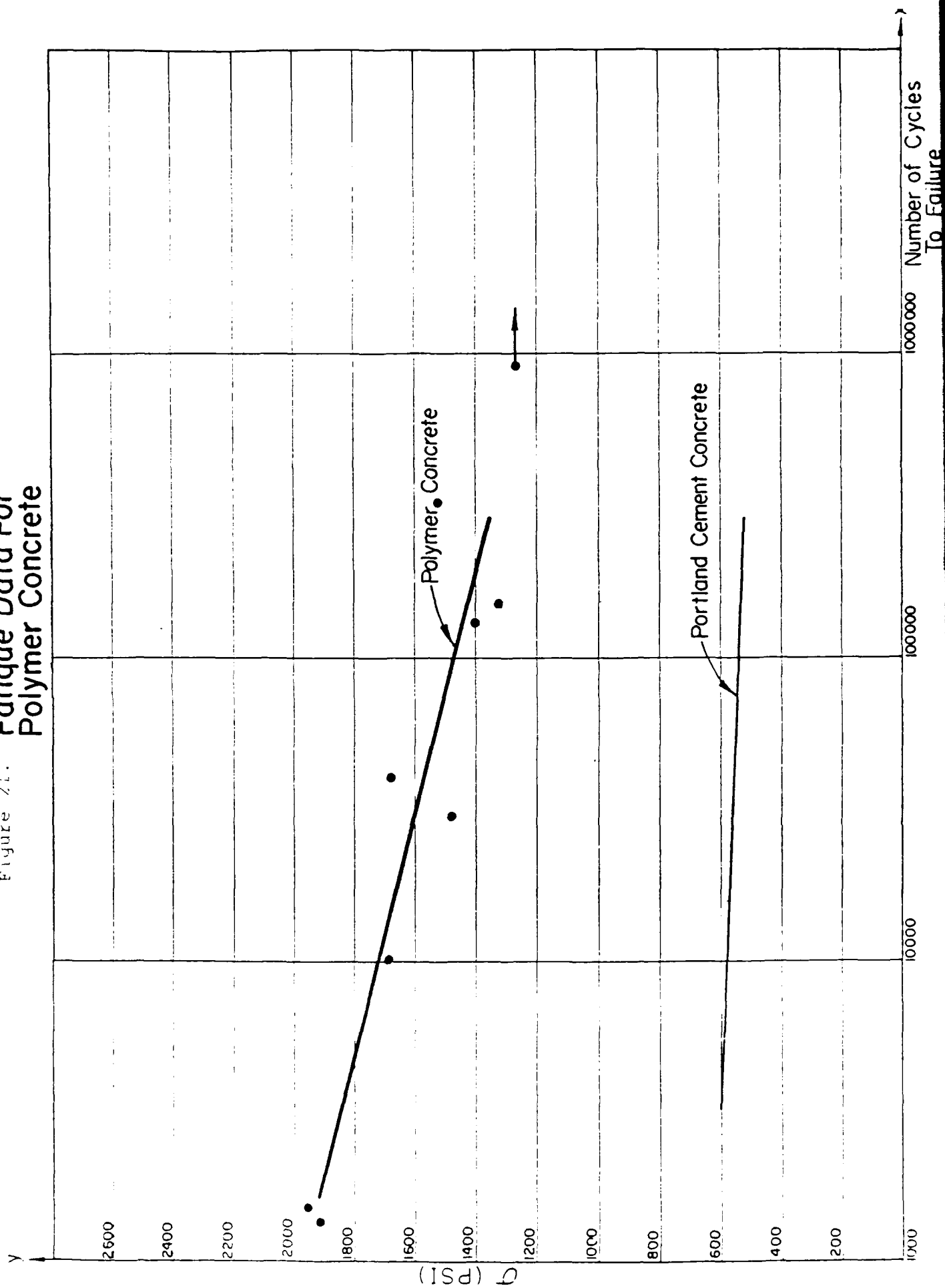
$$\text{Log } N_f = 10.17 - 7.51 \left(\frac{\sigma}{MR} \right)$$

The correlation coefficient (R) for this equation is -0.93. The curves of stress versus number of cycles for polymer concrete and portland cement concrete are presented in Figure 21. Flexural strength, σ , and number of cycles to fracture for both polymer concrete and normal concretes are also given in Figure 21. Since the ratio σ/MR is about the same for both polymer and normal concretes, ability to longer resist fatigue failure is better illustrated by the display of σ , and not σ/MR for polymer and normal concretes. As can be seen from the figure, PC will provide higher resistance to fatigue cracking than conventional PCC and hence more service life can be expected.

Table 30. Fatigue Data

Sample	Stress	σ /MR	No. Cycles	Log No.
1	1969	0.92	1518	3.18
2	1930	0.91	1326	3.12
3	1896	0.90	2000	3.51
4	1690	0.80	9893	4.00
5	1670	0.79	39024	4.59
6	1517	0.71	334300	5.52
7	1486	0.70	30122	4.48
8	1380	0.65	130100	5.11
9	1300	0.61	152500	5.18
10	1275	0.60	Not broken after 900000	At least 5.95

Figure 21. Fatigue Data For Polymer Concrete



11. Creep Behavior of PC:

A creep test was conducted in accordance with the method described in VESYS' IIM structural subsystem [34]. In this method cylindrical samples were prepared and tested in compression loading mode. Loading was applied first to condition the sample and thereafter to perform the experiment for calculating permanent deformation and creep behavior of the material. Of importance in this study is to obtain the creep deformation characteristics of PC at different temperatures. Three different temperatures were chosen in this study, namely: 25 C, 35 C, and 45 C. Results of this test are presented in Table 31 and average results plotted in Figure 22. The general equation for fitting the creep compliance data is:

$$J(t) = \beta_0 + \beta_1 t + \beta_2 (1 - e^{-\beta_3 t})$$

where:

$$\begin{aligned} J(t) &= \text{creep compliance, psi}^{-1} \\ t &= \text{time, seconds} \\ \beta_i &= \text{regression constants} \end{aligned}$$

Results of the regression constants at different temperatures are tabulated below:

Temp(C)	β_0	β_1	β_2	β_3	SE
25	3.13	.0001	.279	.08	.0068
35	3.18	.0006	.232	.08	.0038
45	3.98	.0004	.487	.08	.0121

It can be seen from these results that polymer concrete will tend to exhibit creep behavior as the room temperature increases. The magnitude of creep deformation is not considered significant if compared with materials such as sulfur/asphalt mixtures; however, it is an indication of a behavior that should be considered in the design of a structural member using PC. Tolerances on permissible deformation will dictate the temperature limits under which PC could be utilized in the field. The other aspects of creep behavior is that most of the epoxy/resin systems are

therosetting polymers, and hence deformation characteristics of PC may not be reversible. How tough PC becomes when subjected to cyclic thermal stresses is an area that needs further investigation.

Compressive stress values obtained at Pandalai laboratories and Resource International are in agreement within experimental error. In order to calculate the pavement thickness for a given load and number of repetitions, design charts will have to be developed for the various types of aircrafts and different wheel configurations. Data obtained in this study will be used to solve the Westergaard equation to obtain relationship between pavement thickness and axle load for various subgrade reaction constant values. The fatigue equation will now be introduced to correlate number of landings and applied load for various thicknesses of the polymer concrete pavement. The material properties required are modulus of elasticity, flexural stress, Poisson's ratio and fatigue equation constants. All these required material properties are available from the phase 1 study to proceed to the second phase investigation.

Table 31. Creep Compliance Data (continued)
(at 250C)

SAMPLE NO.	HEIGHT (in.)	LOAD (lbs)	(psi)	$J(t)10^{-7}$						(psi^{-1})		
				1	3	10	30	100	1000			
1	2.125	775	109.7	2.6	2.80	2.89	2.89	2.89	3.28			
2	2.125	850	120.3	2.31	2.39	2.44	2.49	2.49	2.49			
3	2.063	825	160.8	2.57	2.61	2.61	2.71	2.90	3.18			
4	2.125	775	109.7	3.09	3.25	3.33	3.33	3.33	3.33			
5	2.125	800	113.2	2.57	2.74	2.76	2.76	2.81	2.90			
6	1.772	975	138.0	3.26	3.41	3.62	3.63	3.63	3.77			
7	2.125	875	123.9	3.42	3.59	3.76	3.80	3.80	3.80			
8	1.750	775	109.7	3.69	3.98	4.10	4.10	4.10	4.40			
9	1.722	775	109.7	3.69	3.93	4.05	4.11	4.11	4.18			
10	1.734	750	106.2	3.55	3.80	3.91	3.91	3.91	3.91			
			Average	3.08	3.25	3.35	3.37	3.40	3.52			
			S	0.52	0.58	0.63	0.62	0.59	0.59			

Table 31. Creep Compliance Data (continued)
(at 350C)

SAMPLE NO.	HEIGHT (in.)	LOAD (lbs)	(psi)	$J(t)10^{-7}$						(psi ⁻¹)
				1	3	10	30	100	1000	
1	2.00	925	130.83	3.10	3.19	3.23	3.23	3.27	3.53	
2	2.00	975	137.90	2.94	3.02	3.06	3.10	3.10	3.51	
3	2.00	950	134.57	4.01	4.18	4.35	4.44	4.52	4.85	
4	2.00	975	137.90	2.86	3.10	3.18	3.26	3.26	4.00	
5	2.00	975	137.90	2.78	2.86	2.94	3.02	3.02	3.92	
			Average	3.14	3.27	3.35	3.41	3.43	3.96	
			S	0.50	0.52	0.57	0.58	0.62	0.54	

Table 31. Creep Compliance Data (continued)
(at 45°C)

SAMPLE NO.	HEIGHT (in.)	LOAD (lbs)	(psi)	$J(t)10^{-7}$						(psi^{-1})		
				1	3	10	30	100	1000			
1	1.79	1100	155.6	4.80	5.14	5.47	5.66	5.91	7.01			
2	1.71	925	130.9	4.18	4.53	4.73	4.88	4.98	5.28			
3	1.79	1100	155.6	4.61	5.09	5.38	5.57	5.95	6.72			
4	2.00	950	134.37	3.43	3.64	3.72	3.77	3.85	4.19			
5	2.00	975	137.91	3.18	3.35	3.43	3.47	3.59	3.84			
6	2.00	975	137.91	3.26	3.43	3.59	3.59	3.59	3.84			
7	2.00	975	137.91	3.75	3.92	3.96	3.96	4.00	4.24			
8	2.00	963	136.14	4.58	4.79	4.83	4.88	4.88	4.96			
9	2.00	975	137.91	3.51	3.71	3.79	3.84	3.84	3.92			
			Average	3.92	4.18	4.32	4.40	4.51	4.94			
			S	0.63	0.67	0.79	0.85	0.95	1.26			

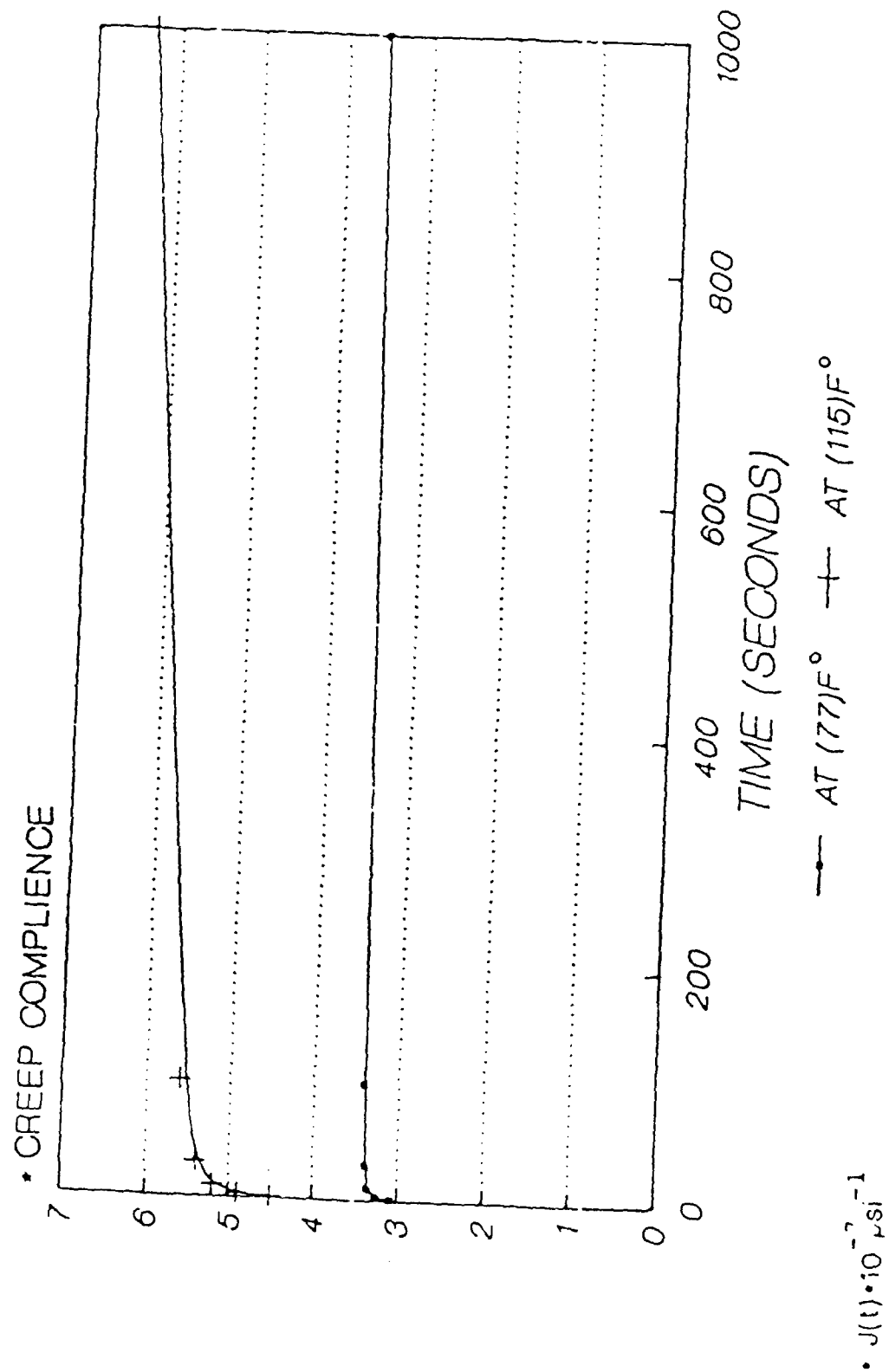


Figure 22. Polymer Concrete Creep Compliance

CHAPTER 5

ANALYSIS OF RESULTS

The objective of the present study was to develop specifications and design charts to calculate airport runway pavement thickness for various aircraft gear configurations and loads. In the phase 1 work, mix designs and material constants have been determined experimentally and this data will be used in phase 2 to develop design charts.

Three polymer systems have been found to have good adhesive and binding characteristics, when used with properly graded aggregates, to give superior mechanical properties for the pavements in comparison to normal strength portland cement concrete.

The three polymer systems are:

- Epoxy based polymer
- Methyl Methacrylate Polymer
- Polyester Polymer

The optimum percent polymer for each mix design has been found to vary depending upon the type of polymer used. This is due to the rheological, adhesive, and wetting characteristics of the polymer.

For example, it was possible to make epoxy polymer concrete with 6% polymer in the mixture with a 24 hour compressive stress of 2000 to 3000 psi. However, when a 6% polymer content was used for the MMA and polyester polymer concrete, there was no homogeneity or integrity for the samples.

The epoxy binder has a much higher viscosity at identical temperatures when compared to MMA and Polyester. This is a contributing factor in the difference in the behavior of the epoxy polymer concrete and the MMA and Polyester based polymer concrete.

Using FAA's P-501 specification for the fine and coarse aggregate, A good mix design can be developed utilizing a range of binder concentrations. It has been found that too low a binder concentration, leaves too many void spaces, and should be

avoided. Very high amounts of binder concentration can cause rutting problems, especially at elevated temperatures. This is because the polymer concrete with large amounts of polymer undergoes permanent deformation to a greater extent than the normal strength concrete.

A better understanding of the effect of cyclic loading on permanent deformation of polymer concrete at different temperatures will give valuable information to reduce problems associated with rutting.

Based on the work carried out in this study, the following percentages of polymers are recommended for optimum quality polymer concrete mix design.

- epoxy polymer concrete 8-12.5%
- MMA 10-12.5%
- Polyester 10 - 12.5%

The basis for this recommendation are:

- Appearance
- Honeycomb structure
- Void formation
- Mechanical Properties

The aggregate and polymer combined will make 100% of the pavement mixture. The composition of each of the polymer system and the sources of each chemical are given in Chapter 3 for the benefit of those interested in pursuing additional work in this area. A major factor in favor of polymer concrete pavement is its superior fatigue behavior compared to normal strength concrete. It can be seen from figure [19]* that the number of cycles for failure at the same applied load for polymer concrete is two to three orders of magnitude higher than normal strength concrete. While it is difficult to translate the superior fatigue behavior of polymer concrete in quantitative terms, a qualitative analysis suggests that polymer concrete pavement will last two to three times longer than the normal strength concrete pavement. Field data is required to confirm the laboratory data.

CHAPTER 6

CONCLUSIONS AND RECOMMENDATIONS

Many investigators have been active in the field of polymer concrete research for several decades. Most of these efforts have been directed toward highway pavement applications where the load applied is many times lower than that of an aircraft landing runway. Use of polymer concrete for airport runway application has been limited to tests carried out by the Air Force for bomb damaged runway repairs. The objectives of the present study is to develop mix designs based on readily available polymeric binder systems. Three viable mix designs using epoxy, MMA and polyester material have been developed in this study. Material properties have been developed for the mix designs to calculate polymer concrete pavement thicknesses for various Aircraft loads and axle configurations.

Based on the laboratory test results provided in this report, the following conclusions can be made:

1. In comparison to normal strength portland cement concrete, polymer concrete provides two to three times higher compressive and flexural strength, about 30 percent higher tensile strength, and about 30 percent lower fracture toughness.
2. In comparison to normal strength portland cement concrete, polymer concrete about the same or slightly lower static modulus of elasticity and modulus of resilience. However, the dynamic modulus of PC is both frequency and temperature dependent. The higher the temperature, the lower the dynamic modulus value.
3. Polymer concrete provides excellent resistance to freeze-thaw cyclic action for both volume and linear change behavior.
4. Polymer concrete will exhibit creep deformation behavior especially at elevated temperatures. the significance of this behavior depends on specific field application and permissible design tolerances.
5. Polymer concrete provides substantial resistance to fatigue

cracking in comparison to normal strength portland cement concrete. This property could be interpreted in the sense of providing more service life than PCC concrete or reduced thickness design requirements for equal service life.

The data obtained in this study will be used in the second phase work to develop design charts to correlate polymer concrete pavement thickness with gear loads. Life cycle cost analysis will also be carried out to determine the viability of polymer concrete for airport runway application. Material specifications and laydown conditions and procedures will also be developed in the second phase work.

The Westergaard analysis assumes that the material behavior is linear elastic. This is a first approximation of the viscoelastic characteristics of polymeric materials. Further work needs to be done to determine the nonlinear and viscoelastic response of polymer concrete to cyclic loading and shear deformation to simulate field conditions which exist at runway exits. More work is also required to determine the creep behavior of polymer concretes especially at higher temperatures. The above topics are beyond the scope of the present study and needs separate investigation.

PART II-DESIGN THICKNESS CHARTS, QUALITY CONTROL,
CONSTRUCTION PROCEDURES, AND COST ANALYSIS

Chapter 1 - Introduction

Part II report contains information gathered by Pandalei Coatings Company during the second phase of the contract #DTFA 01-86-Y-01015. The main thrust of the second phase work includes the development of design thickness charts, quality control aspects, construction procedures, and cost estimates. During Phase I work, mix design based on three polymer systems were developed. These polymers are:

1. Epoxy-amine type
2. Methyl methacrylate addition polymer
3. Polyester-Styrene cured system

The optimized mix designs were used to determine the elastic modulus, poisson's ratio, flexural strength and fatigue properties. The mechanical properties of polymer concrete (PC) is taken advantage of in developing the design thickness charts. Initial work considered three scenarios which include:

1. Polymer concrete replacing portland cement concrete completely
2. Polymer concrete used as an overlay
3. Polymer concrete used as an underlay

These aspects are discussed in Chapter 2 - Preliminary Pavement Thickness Calculations Based on Polymer Concrete and Comparison with Portland Cement Concrete. Based on this data, detailed design thickness calculations were carried out and design thickness charts were developed. These charts are presented in Chapter 3 - PCC Overlay Over PC Underlay for four types of aircrafts. Chapter 4 contains quality control methods which are significant factors in the development of optimal mechanical properties. There are three categories of properties which are used to determine the quality of the polymer systems. They are:

1. Physical properties such as density, viscosity, molecular weight and molecular weight distribution.
2. Chemical properties such as the presence of functional groups before and after the chemical reaction. Infrared analysis techniques are used to determine the degree of completion of a chemical reaction. These are test methods

which are more complex than the determination of physical properties.

The Illi-slab computer code is used to calculate pavement thickness in the present study. The method of treatment of a composite layer according to the Illi-slab program is based on the following transformation principle. The Illi-slab program transforms two composite layers into an equivalent layer and develops the strain fields in the transformed section. The strain fields developed in the equivalent layer can then be retransformed into stresses for the two composite layers (A detailed discussion of the treatment of the composite layer using the Illi-slab program is given in Appendix A). Presently, the design procedures are based on assumptions such as continuous slabs which are infinite in length. By calculating the stresses and deflections for these continuous slabs and then superimposing the system on the design slab, and then using the two dimensional finite element model, it is possible to analyze pavements which have prescribed size and load characteristics in a realistic fashion.

It is impractical to determine all these properties before starting an actual construction job and the minimum number of tests for an acceptable quality control program is suggested in Chapter 4.

Construction procedures will be different from those followed for portland cement concrete at the present time. Depending on the size of a job, the raw materials will have to be shipped to the job site in the appropriate quantities and mixed on-site. Also, the mixing technique for these raw materials must be done according to a standard procedure in order to avoid any premature curing or reactions taking place in mixing containers. These procedures are outlined in Chapter 5 - Construction Procedures.

The final factor is the cost. When a workable system is developed, the cost determines whether or not that system can be economically pursued. This cost analysis is carried out in Chapter 6 - Cost Analysis and the concluding remarks and recommendations are discussed in Chapter 7 - Conclusions and Recommendations.

Chapter 2 - Preliminary Pavement Thickness Calculations Based on Polymer Concrete and Comparison with Portland Cement Concrete

Work carried out to date has been concentrated in the following three areas:

1. Polymer concrete completely replacing portland cement concrete
2. Polymer concrete being used as an overlay material
3. Polymer concrete being used as an underlay material

However, before these three areas can be expanded on, the method of attack on this problem or design methodology would have to be described. Section 2.1 describes the FAA design methodology and an analysis of how the design methodology for this project was determined.

2.1 - FAA Design Methodology

According to the design procedure given in the FAA Advisory Circular, AC 150/5320-6c, determination of slab thickness for PCC pavements is based on the level of stress in the concrete slab and the flexural strength of the slab. Calculation of the stresses is based on slab theory and is determined for the condition that the loads are adjacent to a joint with no load transfer across the joint. These stresses are then reduced by 25 percent to compensate for load transfer. In this procedure, only the load stresses are considered. A factor of safety is considered to compensate for stresses not specifically calculated such as stresses due to shrinkage, curl, loss of support, rate of loading, etc. The factors of safety, sometimes implied, have been established from experience from pavements with proven performance records with known pavement properties and loading conditions.

Polymer concretes have properties which are similar in many

ways to PCC concretes. Thus it seems logical that the thickness requirements for polymer concrete slabs could be determined by comparing stress to strength ratios for polymer concretes with those for ordinary PCC concrete slabs. Therefore, such a procedure should give a good indication of the relative slab thickness requirements for polymer concrete slabs.

Polymer concretes have a number of properties which are sufficiently different from those of PCC concrete to warrant a closer look at this approach before finalizing thickness design procedures. As indicated above, there are a number of sources for stresses in concrete pavements which are not implicitly taken into account in the design procedure, but are compensated for through the use of an appropriate factor of safety, based primarily on experience. Chief among these are the stresses due to temperature gradients through the slab. It is known that temperature gradients will cause stresses in PCC slabs which are a function of slab length, and properties of the concrete such as its modulus of elasticity and coefficient of thermal expansion. It is also known that polymer concretes have similar properties, but the characteristics for these properties for the polymer concretes are sufficiently different from those of ordinary PCC that it cannot be stated with certainty how much the temperature gradients will affect the performance of the polymer concrete slabs in service.

Polymer concretes are more sensitive to rates of loading and temperature than ordinary PCC. What is not known is whether the difference in these properties will affect the relative performance of ordinary PCC and polymer concretes. Intuitively, they should since both the modulus of elasticity and modulus of rupture for the polymer concrete are influenced by both the rate of loading and temperature. For ordinary PCC, the modulus of elasticity is influenced somewhat by the rate of loading, but not by temperature. Therefore, the relative effect on slab thickness requirements should be different.

Fatigue characteristics of ordinary PCC have been studied extensively, whereas, the fatigue characteristics of the polymer concretes have relatively little data to support their assumed characteristics. What little data are available suggest that the polymer concretes are less susceptible to fatigue damage than ordinary concretes. This would indicate that more energy is needed to cause failure of these materials. This is consistent with their improved fatigue performance characteristics. What is uncertain is the relative effect of temperature changes on the fatigue failure characteristics. Data are also needed on the shrinkage characteristics of polymer concrete and the influence of shrinkage on performance.

With its greater strength, it is logical that slab thickness with polymer concrete could be significantly less without

resulting in slab failure due to concrete overstress. If this is so, then alternate failure criteria might also have to be considered. Wide bodied aircraft such as the DC-10, L-1011, B-747 and others cause a much greater slab deflection so the maximum stress on the subgrade might become a more significant parameter than slab fatigue. This would be especially true in areas where slow moving or standing aircraft are anticipated.

The above discussion merely points out the need to study the thickness design criteria and procedures with great care before drawing final conclusions. As a first step it is recommended that the relative slab thickness can be established by comparing the ratio of stress and strength. The relative thickness should then be evaluated by field testing and analysis to establish those parameters which are most critical to pavement performance prior to establishing final design curves.

2.2 - Replacement of PCC with PC

The first scenario examined in this study was the complete substitution of portland cement concrete with polymer concrete. The following is a table of values for both portland cement concrete and polymer concrete.

Table 1
Maximum Calculated Responses

Runs 1 - 4: $E_1 = 3$ Mpsi, Top Layer: $E_2 = 4$ Mpsi, Bottom Layer
 $F = 90000$ lb, $v = 0.25$ $k = 200$ psi/in. One layer

Run	Material	Thickness (in)	Deflection (mils)	Bending Stress (psi)	% Strength
1	PCC	14	100	664	94.86
2	PC	14	108	624	29.71
3	PC	8	160	1243	59.67
4	PC	4	246	3277	156.04

Note that in this set of data, the last column represents the percent strength, that is the bending stress of the concrete divided by its maximum tensile strength. For PCC, the maximum

tensile strength is assumed to be 700 psi and for PC, the value is taken at 2100 psi. These data are plotted on Figure 1 with thickness as the abscissa and percent strength as the ordinate. Upon further examination, this graph shows that 14" thickness of PCC is close to its loading limit. By drawing a horizontal line from the PCC point to the PC line, the corresponding value for PC can be found. Then looking down at the thickness, it is seen that in order to get approximately 95 percent capacity, a PC thickness of about 6 inches is required, which is less than half of the required thickness for PCC.

% Strength vs Thickness

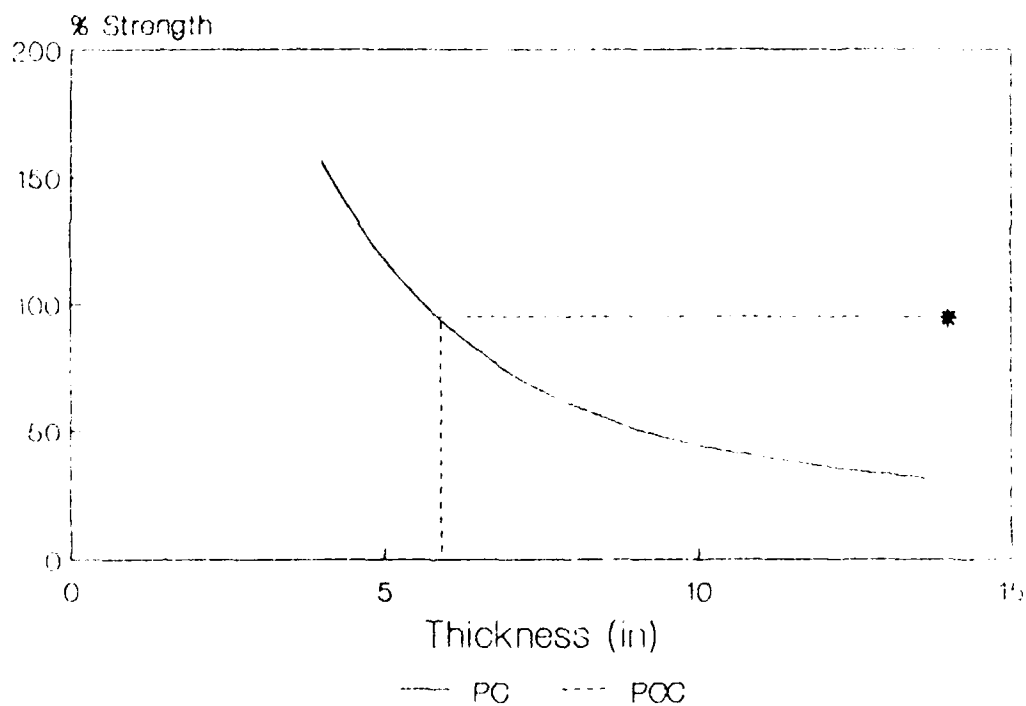


FIGURE 1

2.3 - PC Used as an Overlay

Table 2

Runs 5,6 : PC used as an Overlay of 2" thickness;
k=200psi/in

Run	Thickness (inches)	Deflection (mils)	Bending Stress	
			PC (psi)	PCC (psi)
5	8	134	219	1039
6	6	155	246	1366

Table 2 contains data for PC as an overlay with PCC used underneath. Obviously, from these data it can be seen that the tensile stress of PC reaches a maximum value of 246 psi which is about 12 percent of the maximum attainable value. Therefore, this configuration does not take advantage of the superior strength of PC. It can also be seen that the stress on PCC is well above the maximum tensile strength of PCC which would in all probability result in pavement failure. Therefore, further work along these lines with PC as an overlay has not been explored.

2.4 - PC Used as an Underlay

Table 3

Runs 7-11 : PC used as an Underlay of varied thickness; $k=200$ psi/inch

Run	Thickness		Deflection (mils)	Bending Stress	
	PCC (inch)	PC (inch)		PCC (psi)	PC (psi)
7	6	2.0	155	778	1157
8	8	2.0	134	688	868
9	7	2.0	144	734	993
10	5	2.5	162	607	1280
11	7	1.0	154	1075	1102

Table 4

Runs 20-23 : PC used as an underlay of varied thickness; $k=100$ psi/inch

Run	Thickness		Deflection (mils)	Bending Stress	
	PCC (inch)	PC (inch)		PCC (psi)	PC (psi)
20	7	1.0	265	1290	1332
21	7	2.5	280	725	1529
22	6	2.0	267	934	1388
23	8	2.0	227	826	1041

When examining the data in Tables 3 and 4, it is observed that the higher strength of PC is taken advantage of in this set up. In most of the runs, the stress on the PC is greater than the stress on the PCC. If this were reversed, as in the data in Table no. 1, the mechanical properties would not be used to their maximum potential. For example, in run no. 10 the stress ratios on the pavement are $1280/2100$ or 61 percent of the maximum possible load for PC and $607/700$ or 86 percent of the maximum possible load for PCC. The ideal situation would be to have both PC and PCC to have the same percentage to utilize the superior strength of PC for optimal design considerations. It can also be seen that as the PC thickness increases, the difference between the attained maximum stress of the PCC top layer and the PC bottom layer increases, this means that the superior strength of the PC is being utilized effectively. Similar results were obtained when the modulus of elasticity (E2) was increased from 3,000,000 to 6,000,000 for the PC in the design calculation. This means if the mix design for PC is modified to obtain a higher elastic modulus, a more cost effective composite design could be developed. These aspects are beyond the scope of the present work and must be investigated separately.

Chapter 3 - PCC Overlay Over PC Underlay

In chapter 3, stress calculations have been carried out for four different aircraft (B-747, B-727, DC-10 and L1011). The design configuration used is shown in figure 2 - a composite slab with PC as the underlay and PCC as the top layer. This configuration is used because it has been found to utilize the higher strength of PC.

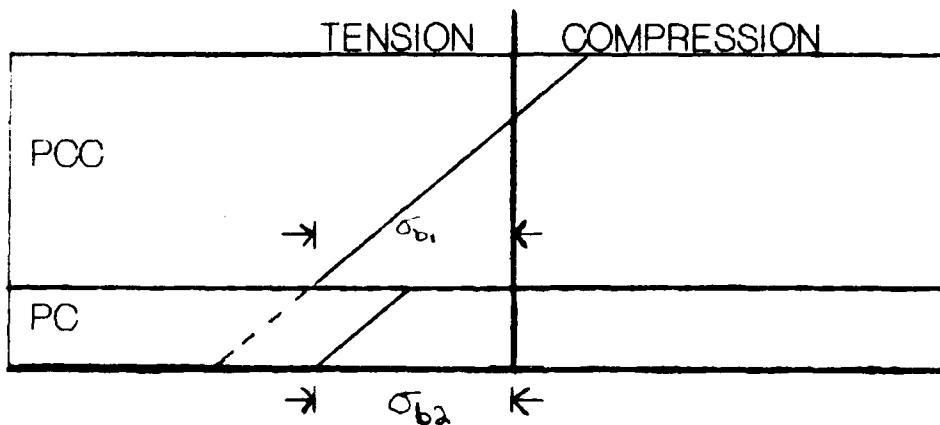


Figure 2 - Composite Pavement Slab

PCC - Overlay
PC - Underlay

Stress calculations were carried out for each of the four aircraft for various top and bottom layer thicknesses and stresses. These plots are self-explanatory and the figure numbers for the various aircrafts follow.

- B-747 data in table 5, figures 3 - 10

- B-727 data in table 6, figures 11 - 18
- DC-10 data in table 7, figures 19 - 26
- L1011 data in table 8, figures 27 - 34

Table 5
Pavement Data - B-747

h1	h2	K	S1	S2
8	1	100	1119	1071
6	1	100	1405	1457
10	1	100	910	831
6	1	300	1035	1073
8	1	300	824	789
10	1	300	670	612
8	2	100	812	988
6	2	100	1019	1344
10	2	100	660	767
6	2	300	687	970
8	2	300	539	713
10	2	300	439	553
7	0	100	2061	
8	0	100	1715	
10	0	100	1249	
14	0	200	664	

h1 - top layer thickness

S1 - max top layer stress

h2 - bottom layer thickness

S2 - max bottom layer stress

K - subgrade reaction constant

Modulus of elasticity (E) = 3 Mpsi for top layer and 4 Mpsi for the bottom layer

Table 6
Pavement Data - B-727

h1	h2	K	S1	S2
7	0	100	2061	
8	0	100	1715	
10	0	100	1249	
6	1	100	1645	1707
8	1	100	1235	1181
10	1	100	958	874
6	1	300	1288	1335
8	1	300	983	941
10	1	300	756	711
6	2	300	821	1175
8	2	300	702	855
10	2	300	511	633
6	2	100	1168	1542
8	2	100	877	1067
10	2	100	680	780

h1 - top layer thickness

S1 - max top layer stress

h2 - bottom layer thickness

S2 - max bottom layer stress

K - subgrade reaction constant

Modulus of elasticity (E) = 3 Mpsi for top layer and 4 Mpsi for the bottom layer

Table 7
Pavement Data - DC-10

h1	h2	K	S1	S2
7	0	100	1739	
3	0	100	1491	
10	0	100	1139	
6	1	100	1382	1433
8	1	100	1100	1053
10	1	100	898	819
6	2	100	926	1392
8	2	100	799	973
10	2	100	632	763
6	1	300	1082	1122
4	1	300	818	783
10	1	300	690	629
8	2	300	683	978
9	2	300	589	716
10	2	300	466	562

h1 top layer thickness S1 - max top layer stress
h2 bottom layer thickness S2 - max bottom layer stress
K subgrade reaction constant

Modulus of elasticity (E) = 3 Mpsi for top layer and 4 Mpsi for
the bottom layer

Table 8
Pavement Data - L1011

h1	h2	K	S1	S2
7	0	100	1629	
8	0	100	1349	
10	0	100	1014	
6	1	100	1303	1351
8	1	100	971	930
10	1	100	805	735
6	2	100	938	1236
8	2	100	699	851
10	2	100	579	673
6	1	300	1067	1107
8	1	300	785	752
10	1	300	654	598
6	2	300	667	955
8	2	300	557	678
10	2	300	494	466

h1 - top layer thickness

S1 - max top layer stress

h2 - bottom layer thickness

S2 - max bottom layer stress

K - subgrade reaction constant

Modulus of elasticity (E) = 3 Mpsi for top layer and 4 Mpsi for
the bottom layer

Top Thickness vs Top Tensile Stress

Bottom Layer thickness = 2 in.

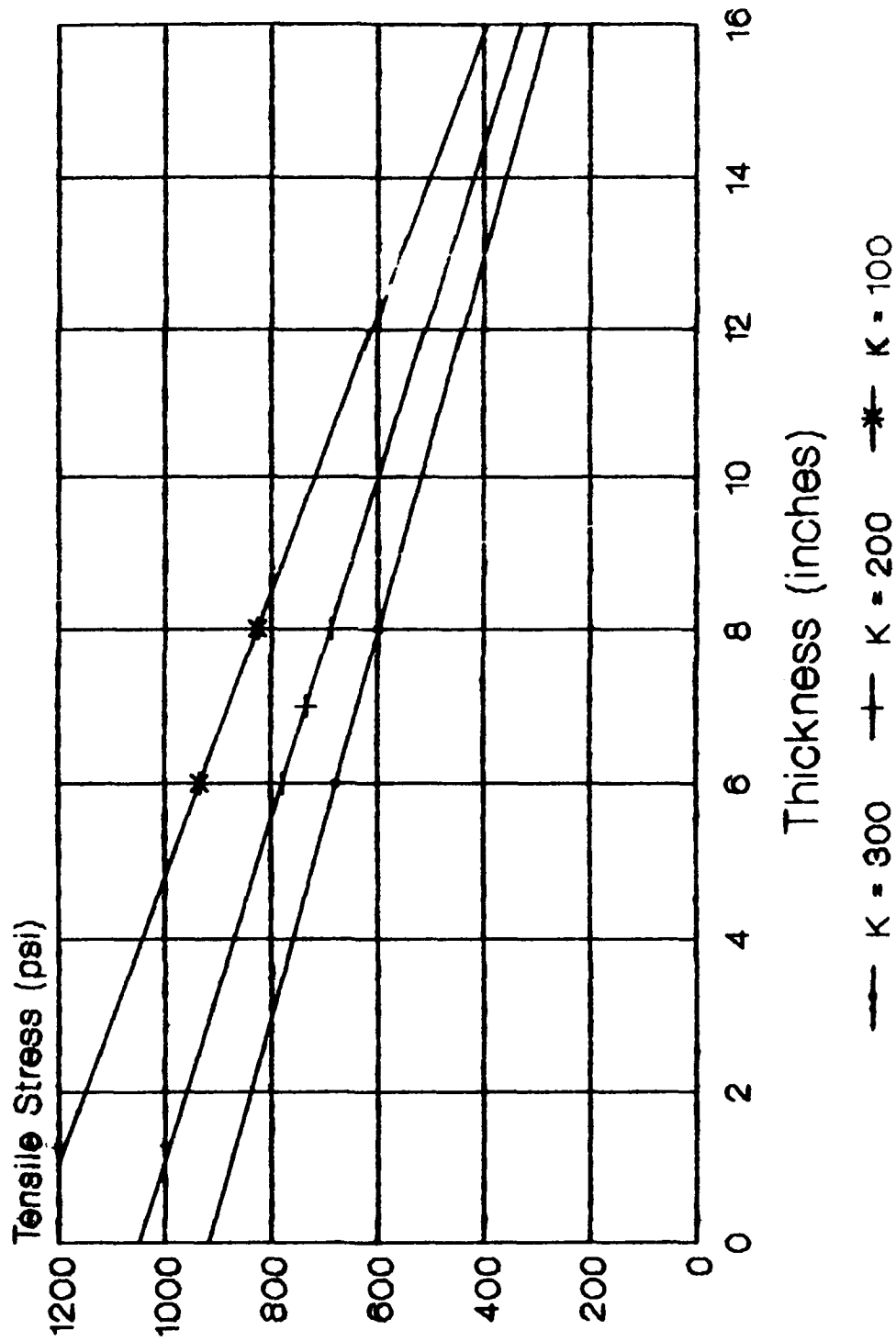


Figure 3 - chart of B-747 Data

Top Thickness vs Bottom Tensile Stress

Bottom layer Thickness = 2 in.

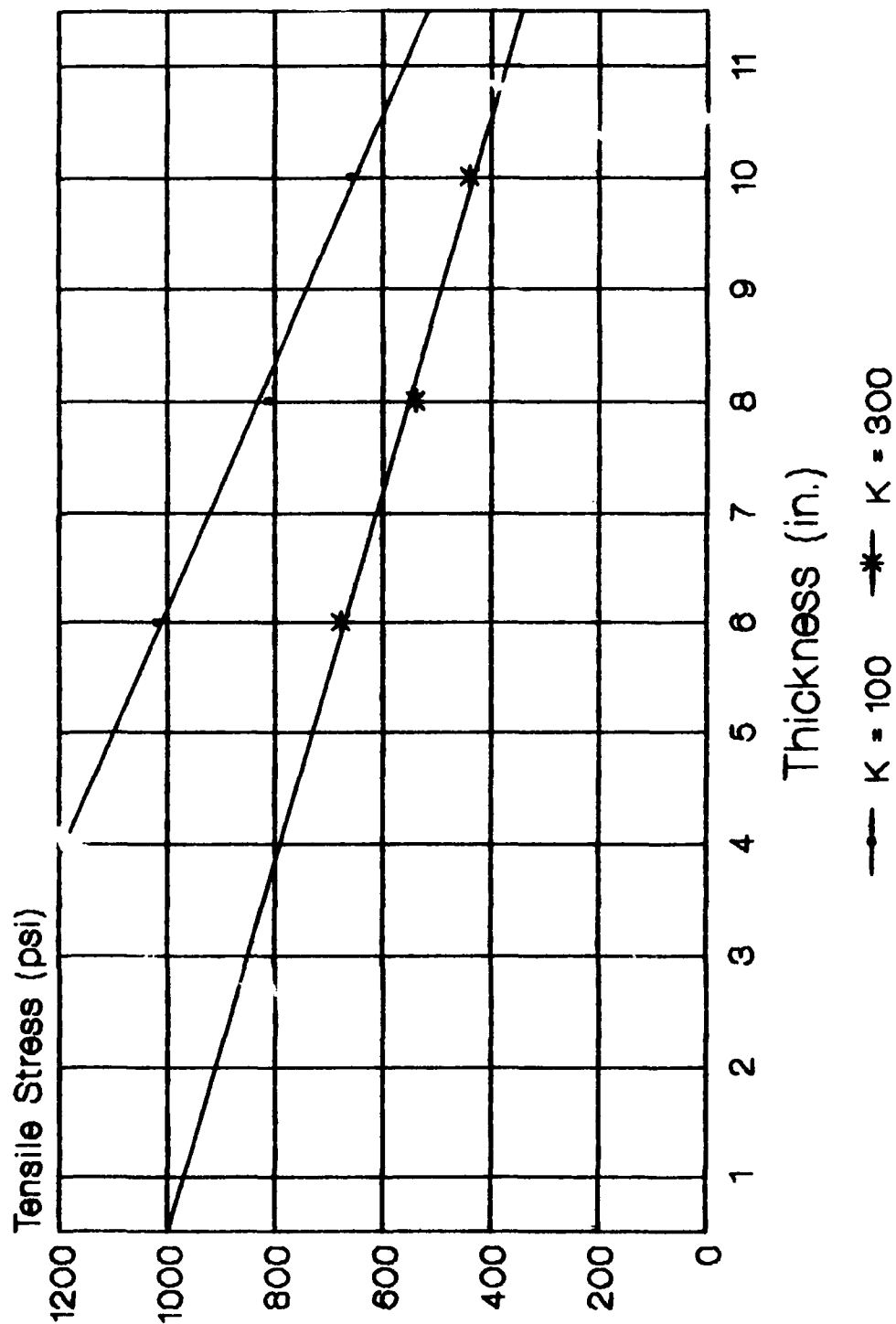
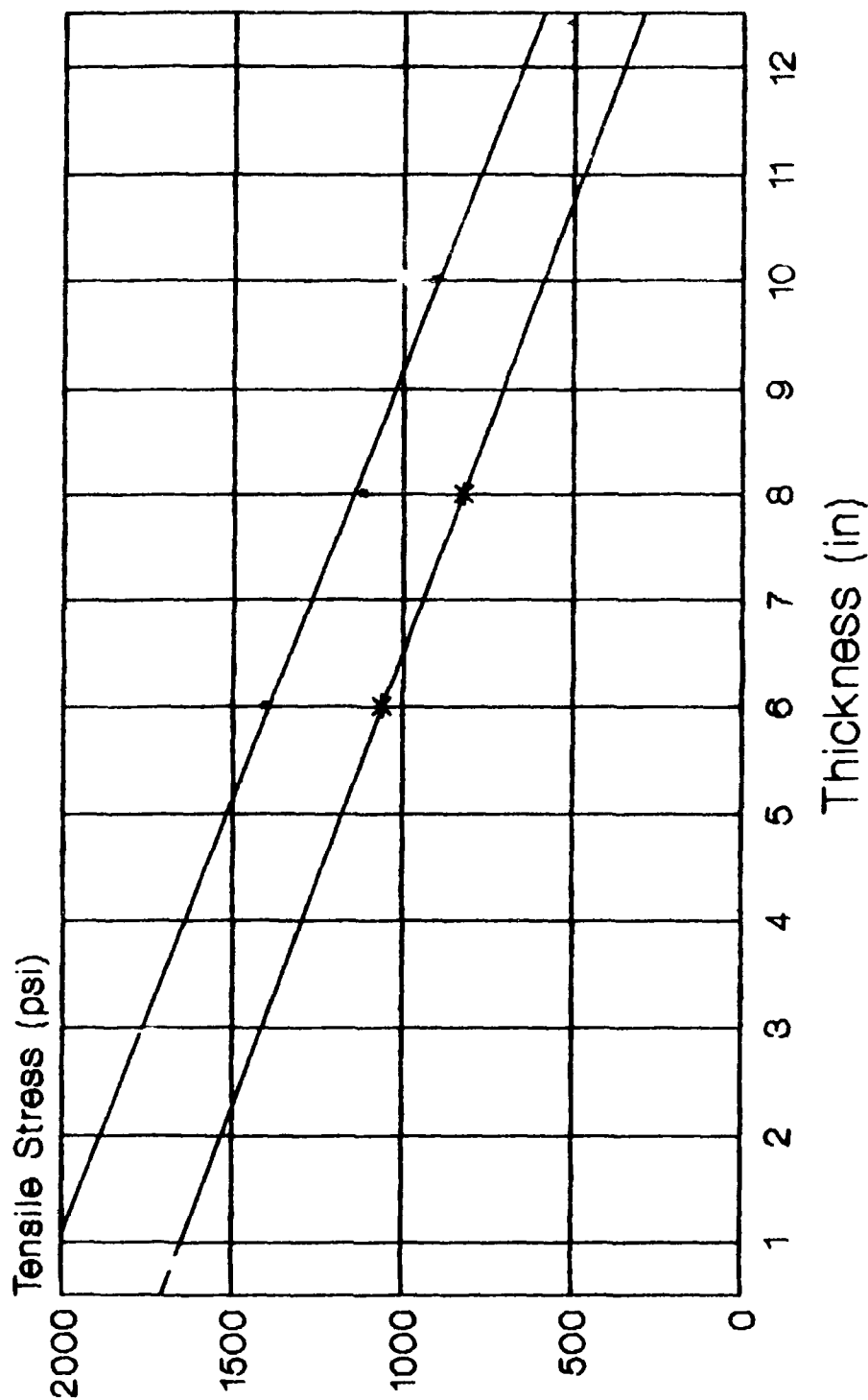


Figure 4 - chart of B-747 data

Top Thickness vs Top Stress

Bottom Layer Thickness = 1 in.

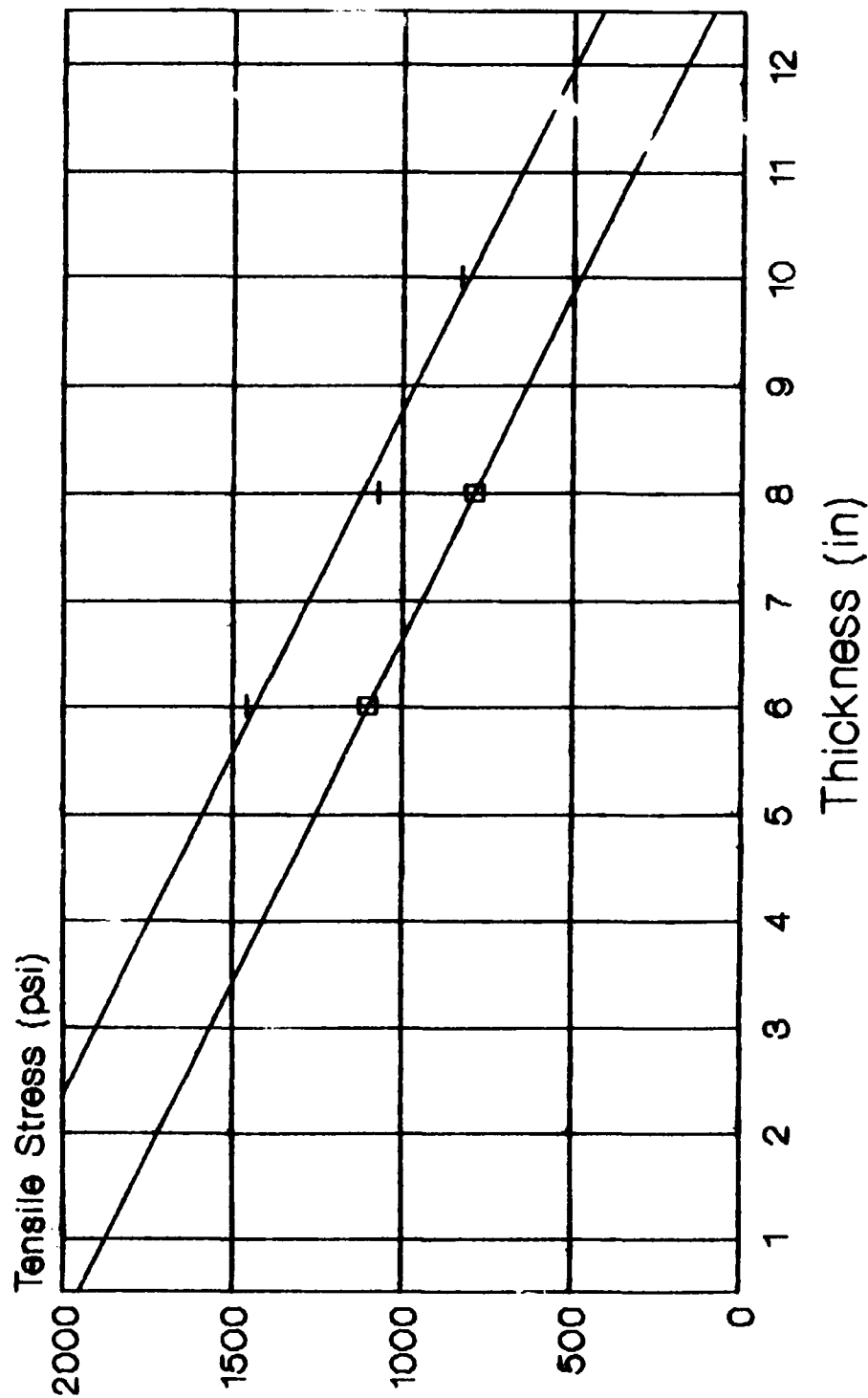


—•— K = 100 —*— K = 300

Figure 5 - chart of B-747 data

Top Thickness vs Bottom Stress

Bottom Layer Thickness = 1 in.



+ K = 100 x K = 300

Figure 6 - chart of B-747 data

Bottom Thickness vs Bottom Stress

Top Layer Thickness = 6 in

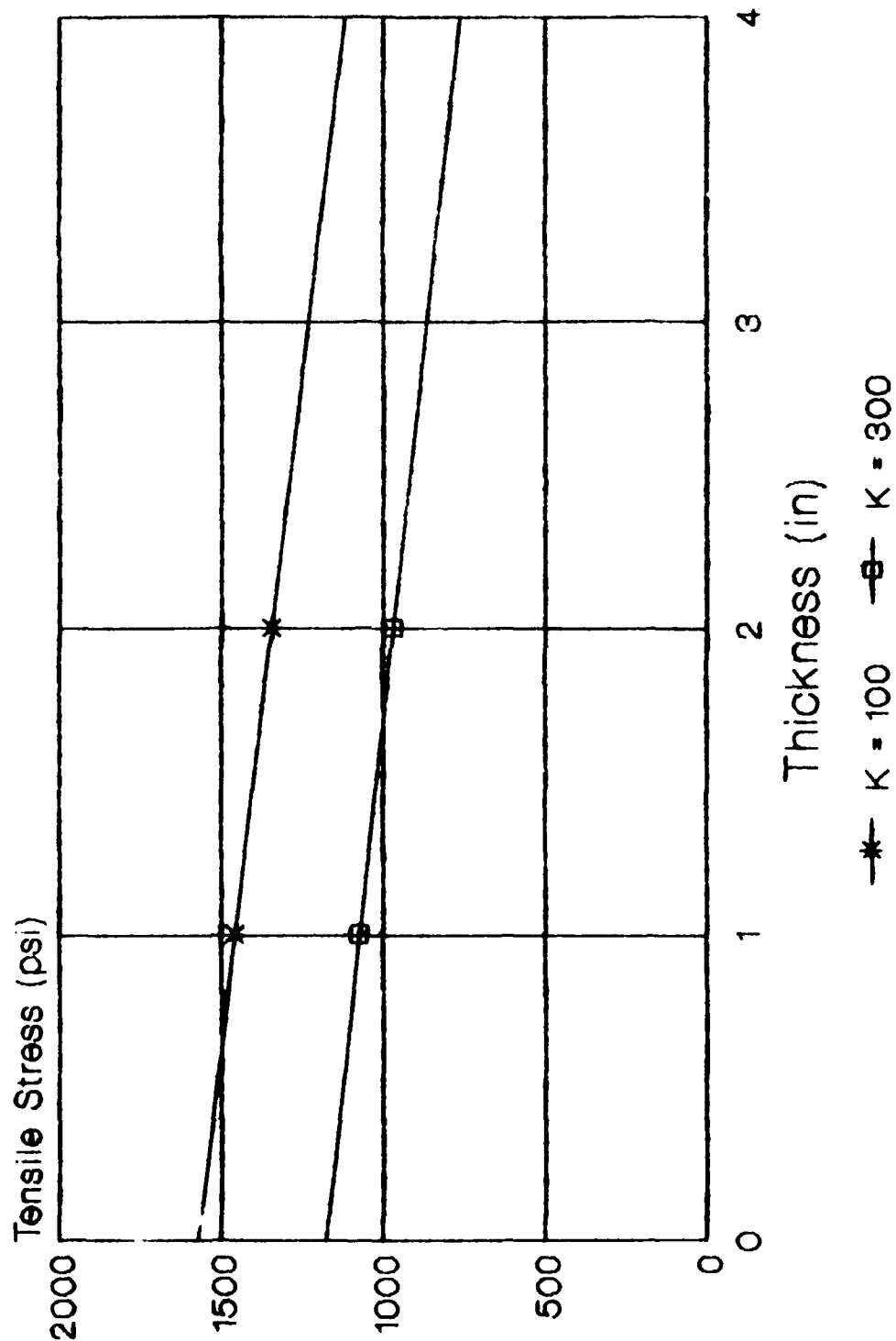
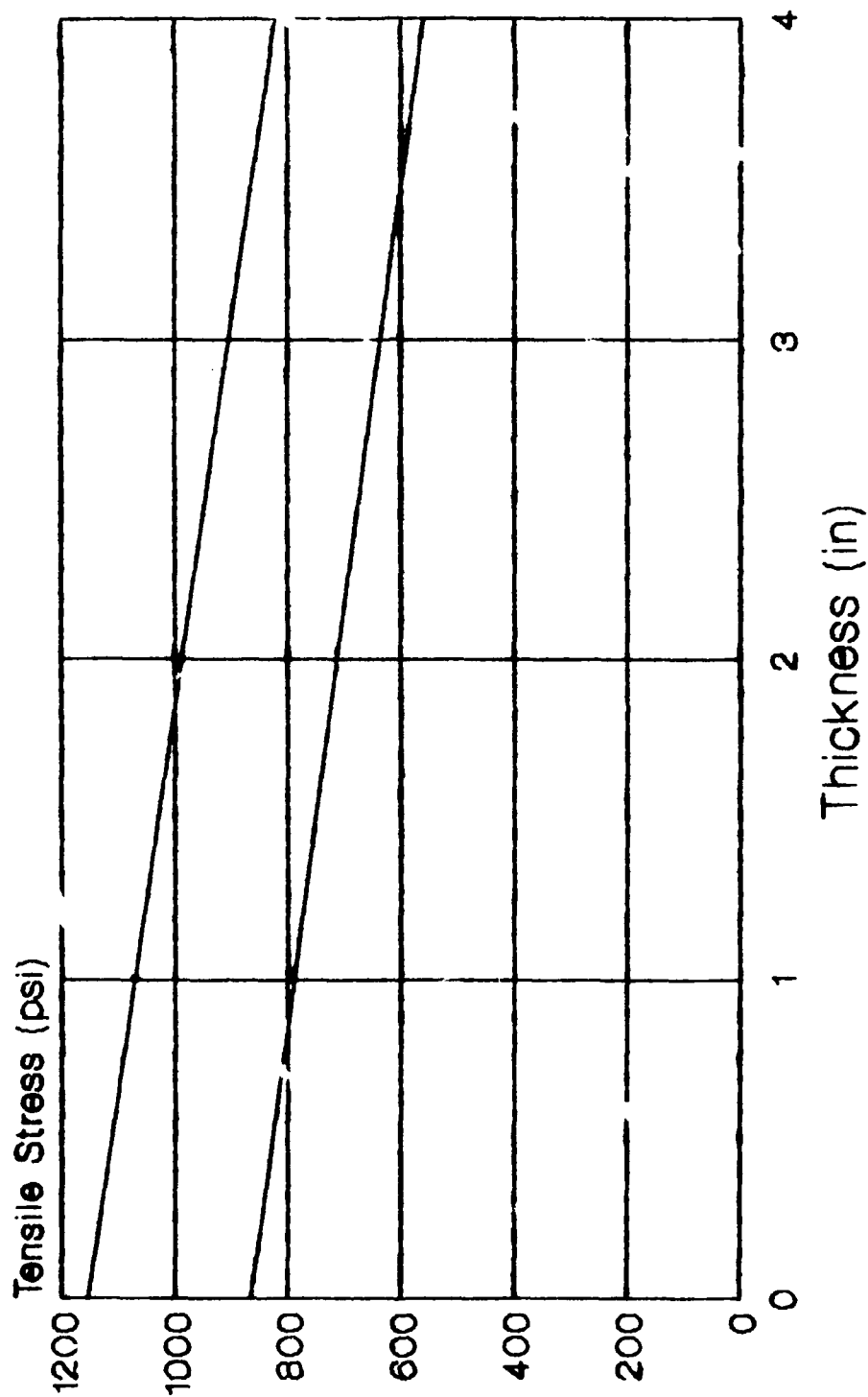


Figure 7 - chart of B-747 data

Bottom Thickness vs Bottom Stress

Top Layer Thickness = 0.8 in

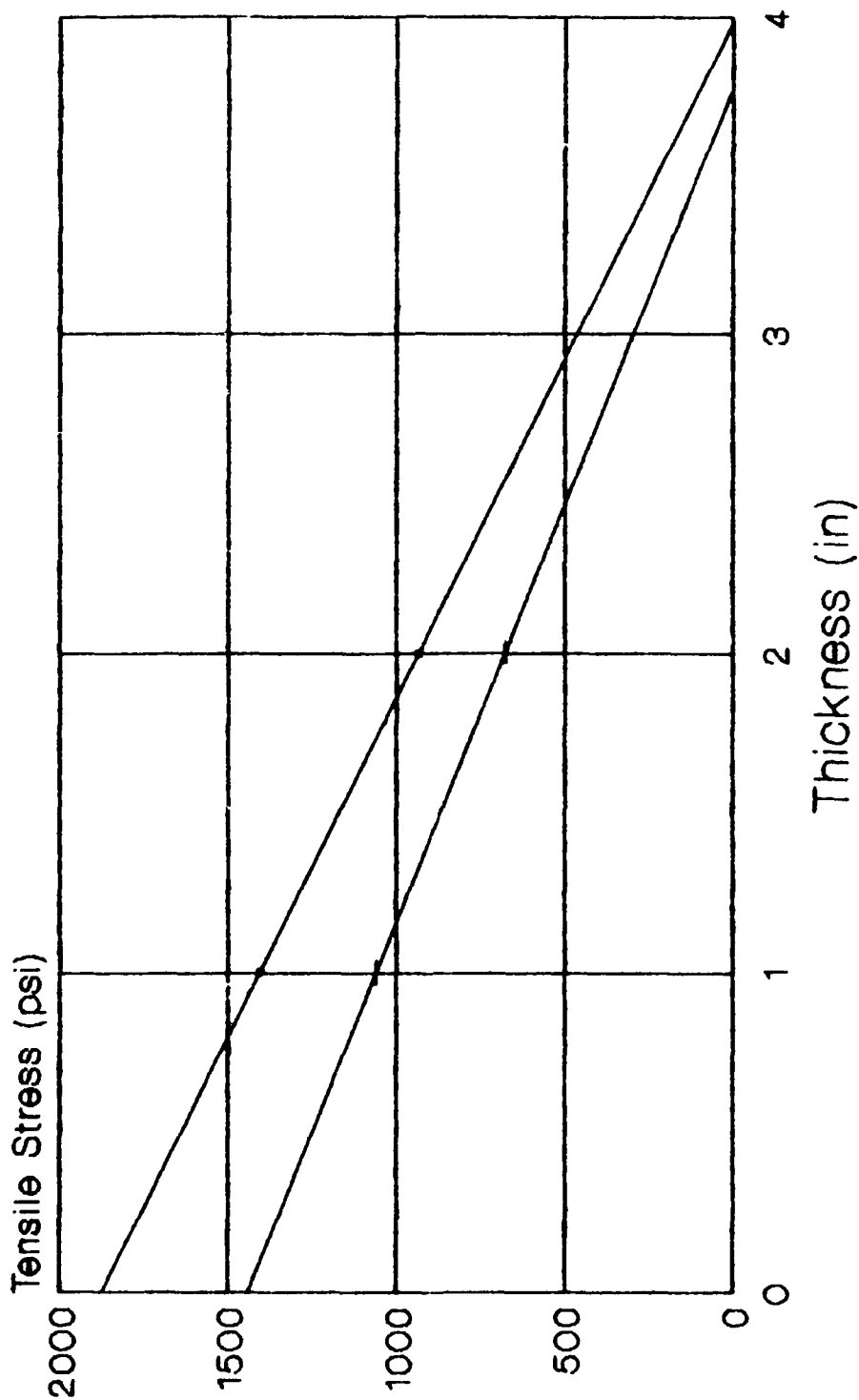


—•— K = 100 —+— K = 300

Figure 8 - chart of B-747 data

Bottom Thickness vs Top Layer Stress

Top Layer Thickness = 8 in.

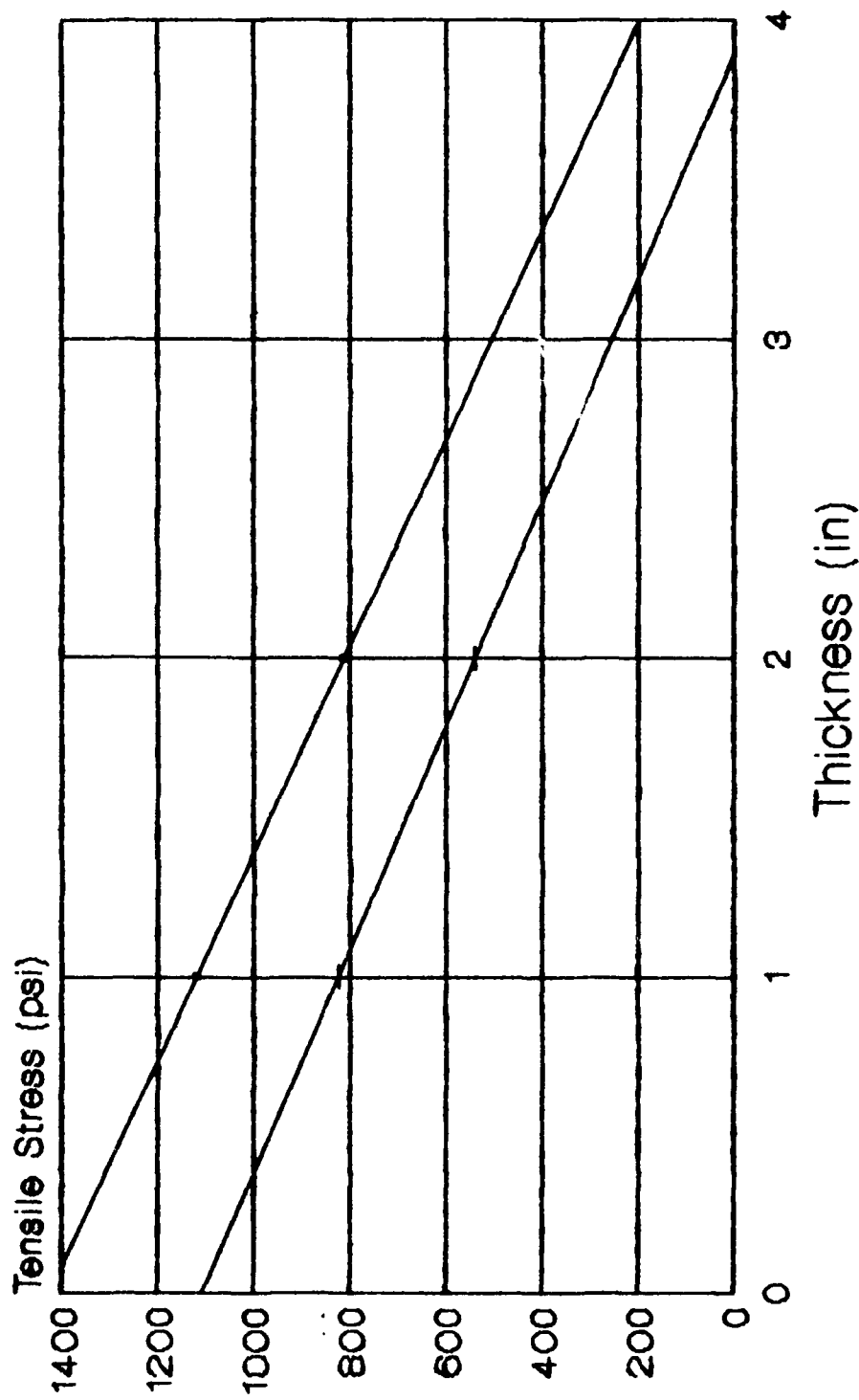


—•— K = 100 —+— K = 300

Figure 9 - chart of B-747 data

Bottom Thickness vs Top Stress

Top Layer Thickness = 8 in.

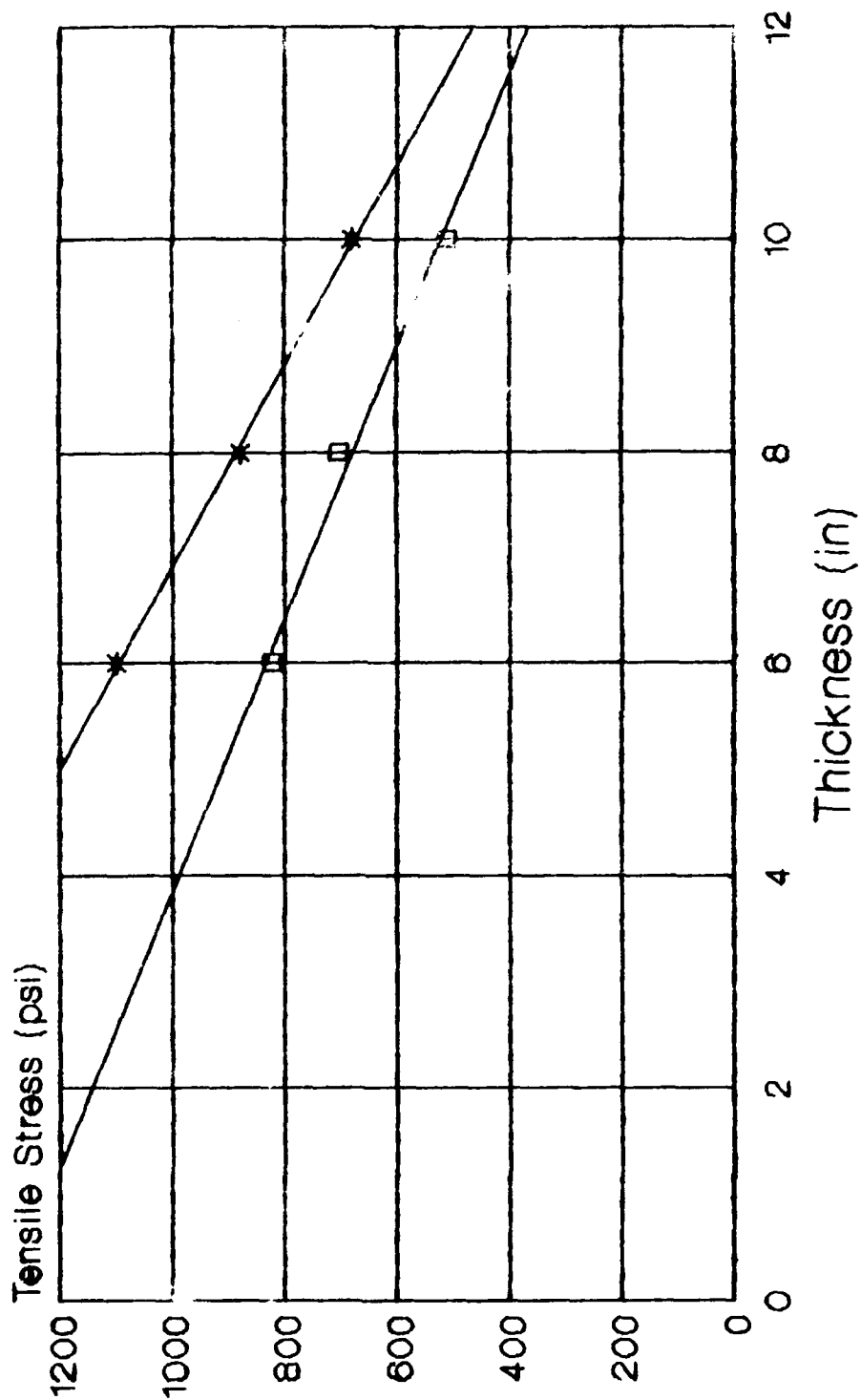


—+— K = 100 — K = 300

Figure 10 - chart of B-747 data

Top Thickness vs Top Stress

Bottom Layer Thickness = 2 in.

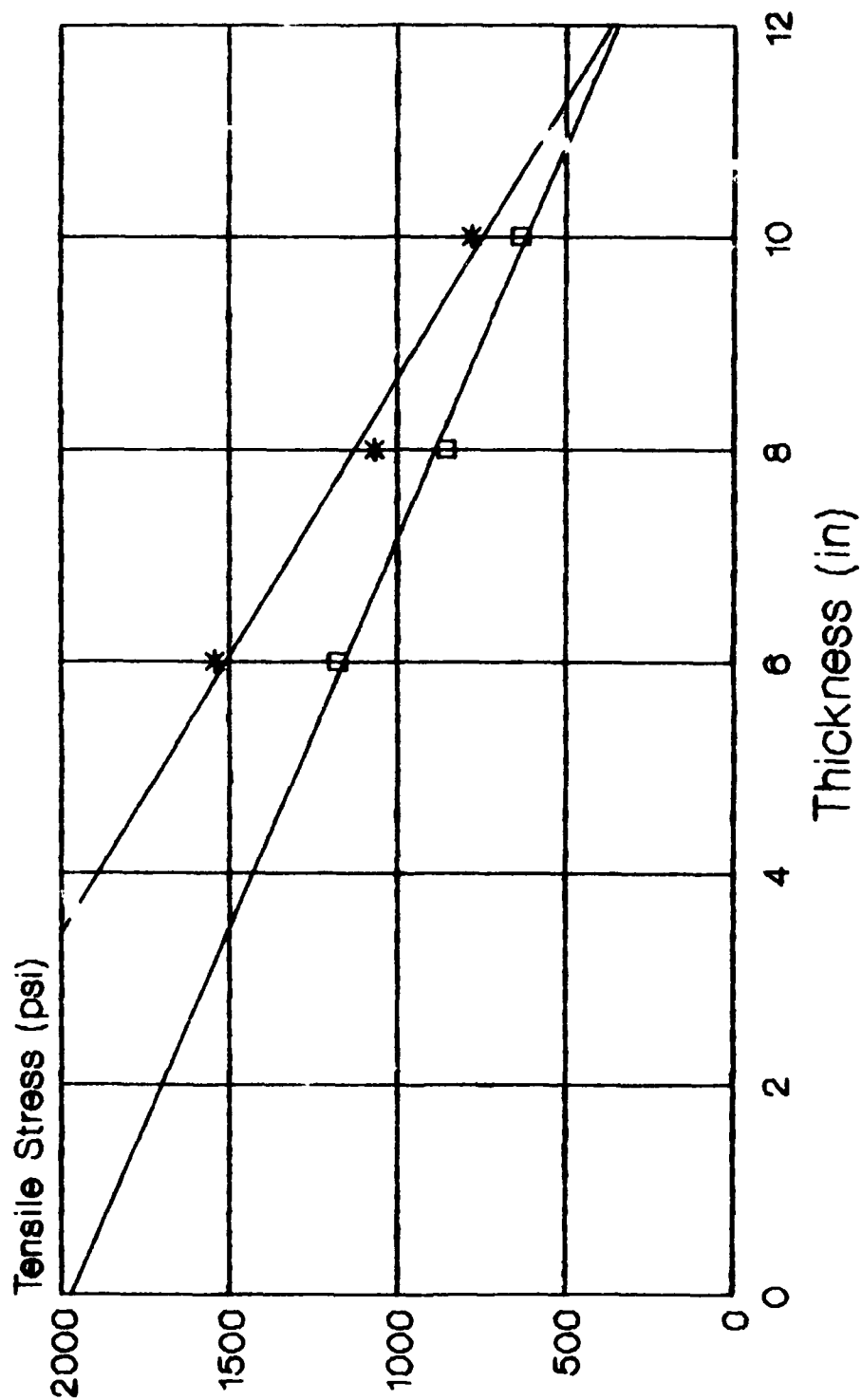


* K = 100 □ K = 300

Figure 11 - chart of B-727 data

Top Thickness vs Bottom Stress

Bottom Layer Thickness = 2 in.



* K = 100 □ K = 300

Figure 12 - chart of B-727 data

Top Thickness vs Top Stress

Bottom Layer Thickness = 1 in.

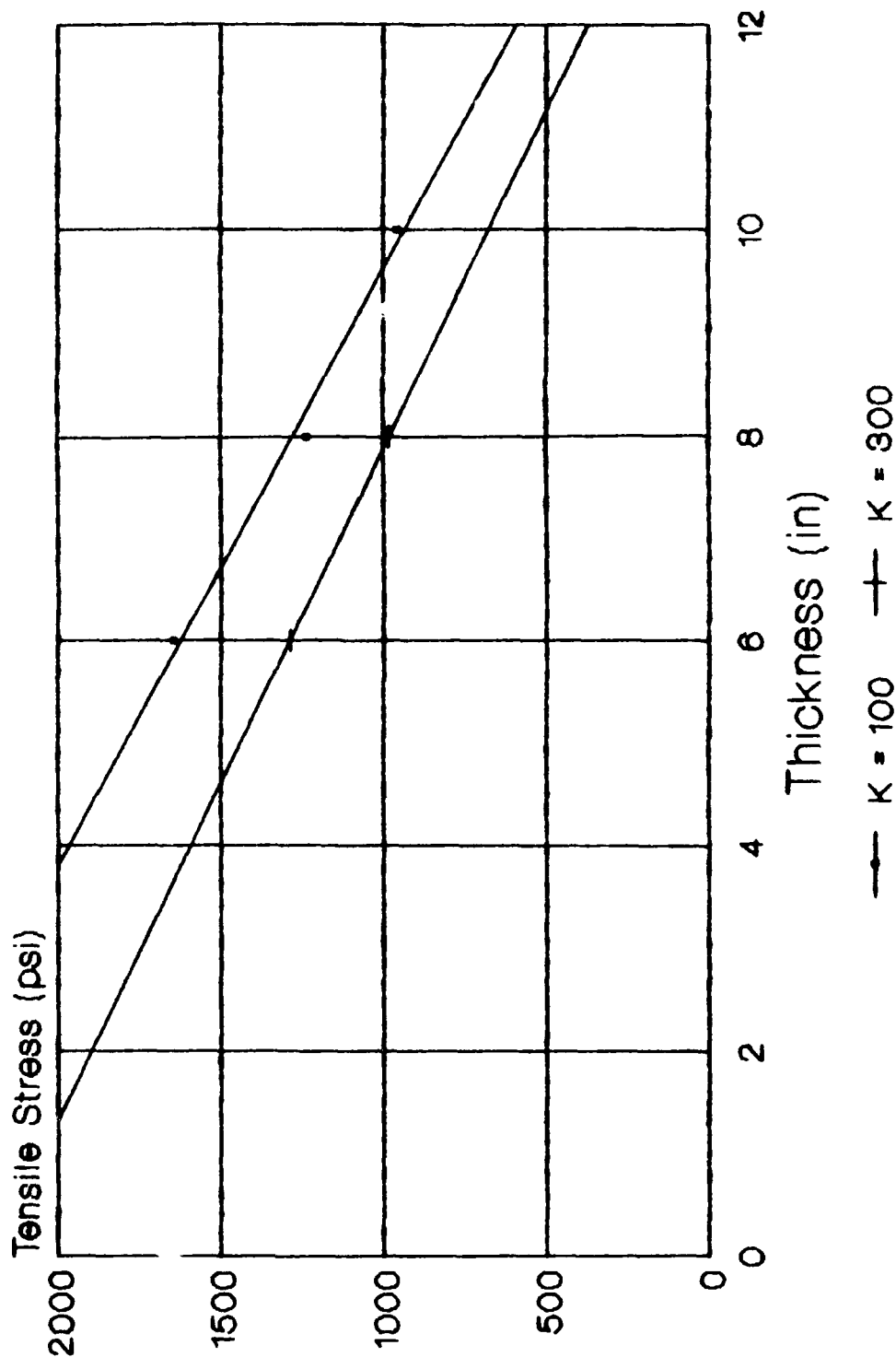


Figure 13 - chart of B-727 data

Top Thickness vs Bottom Stress

Bottom Layer Thickness = 1 in.

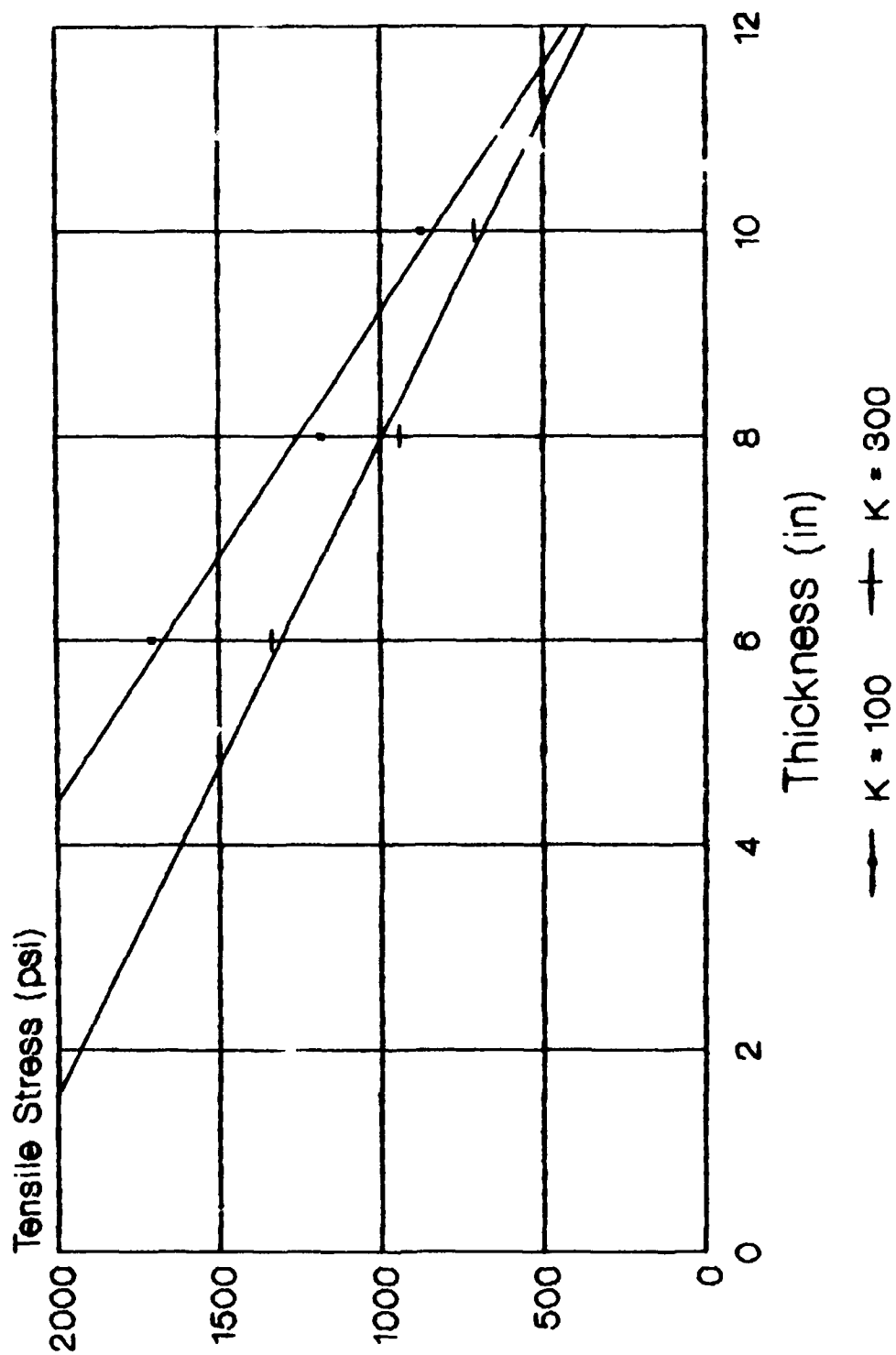
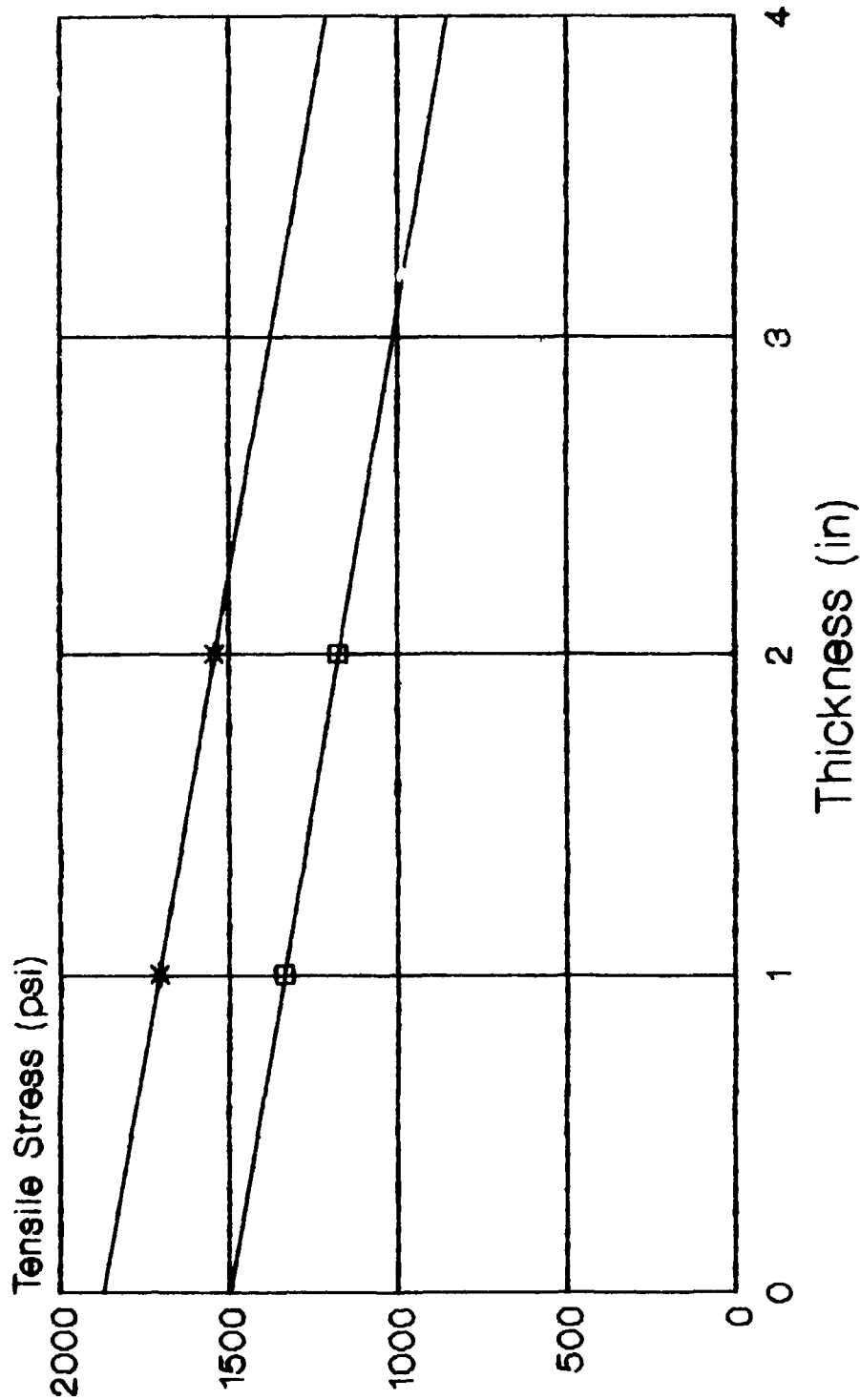


Figure 14 - chart of B-727 data

Bottom Thickness vs Bottom Stress

Top Layer Thickness = 6 in

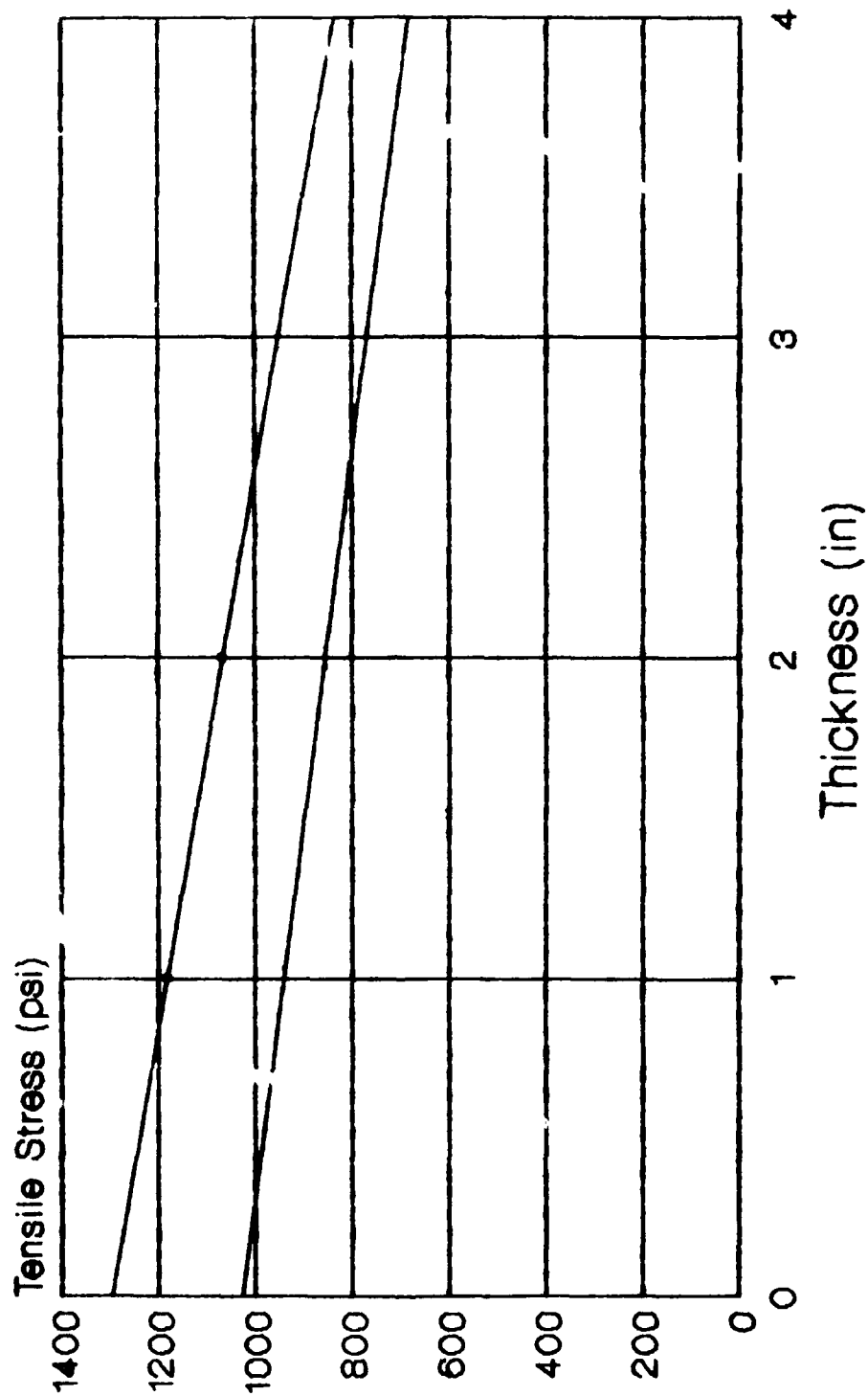


—*— K = 100 —□— K = 300

Figure 16 - chart of B-727 data

Bottom Thickness vs Bottom Stress

Top Layer Thickness = 8 in

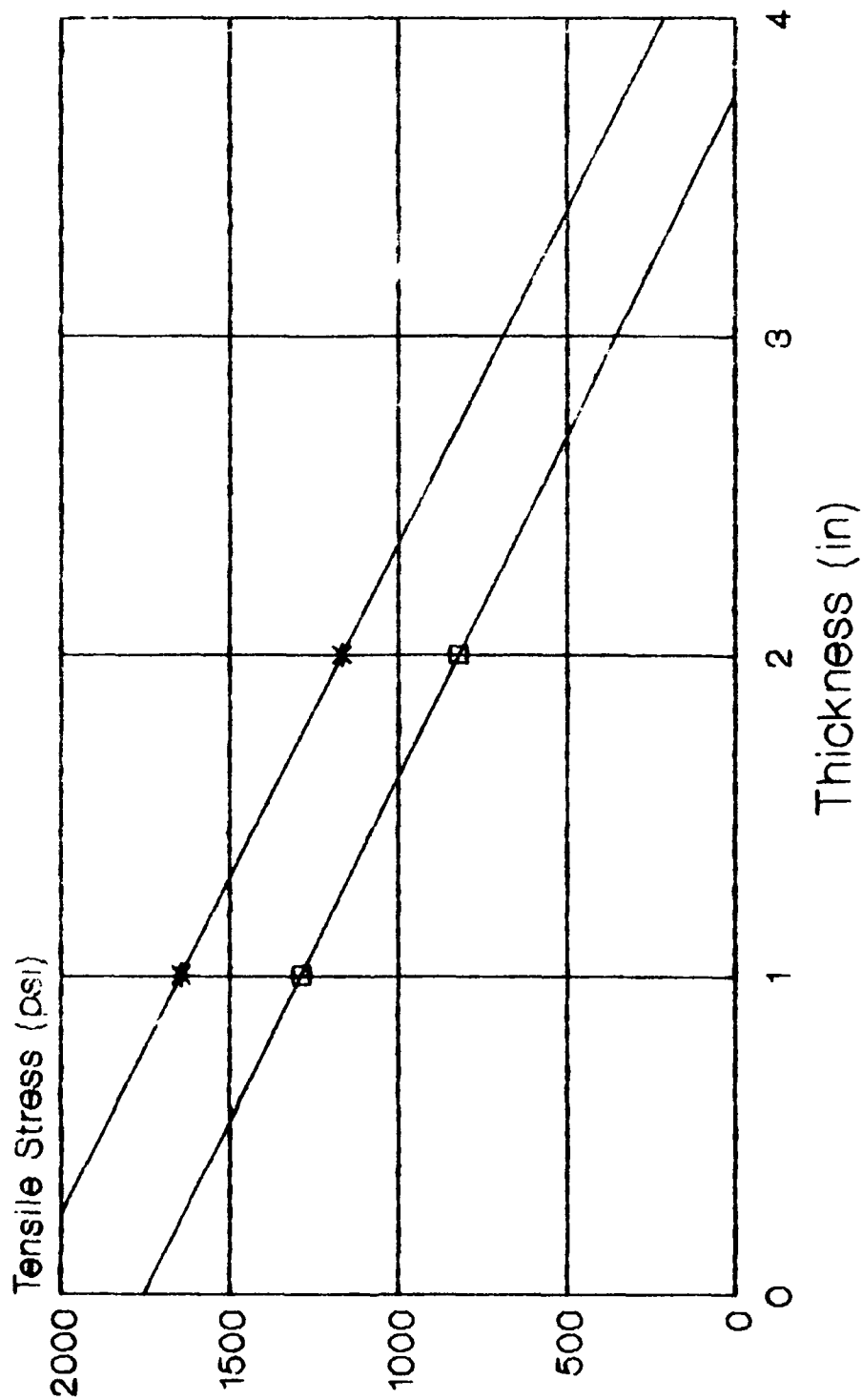


—•— K = 100 —+— K = 300

Figure 16 - chart of B-727 data

Bottom Thickness vs Top Stress

Top Layer Thickness = 6 in.

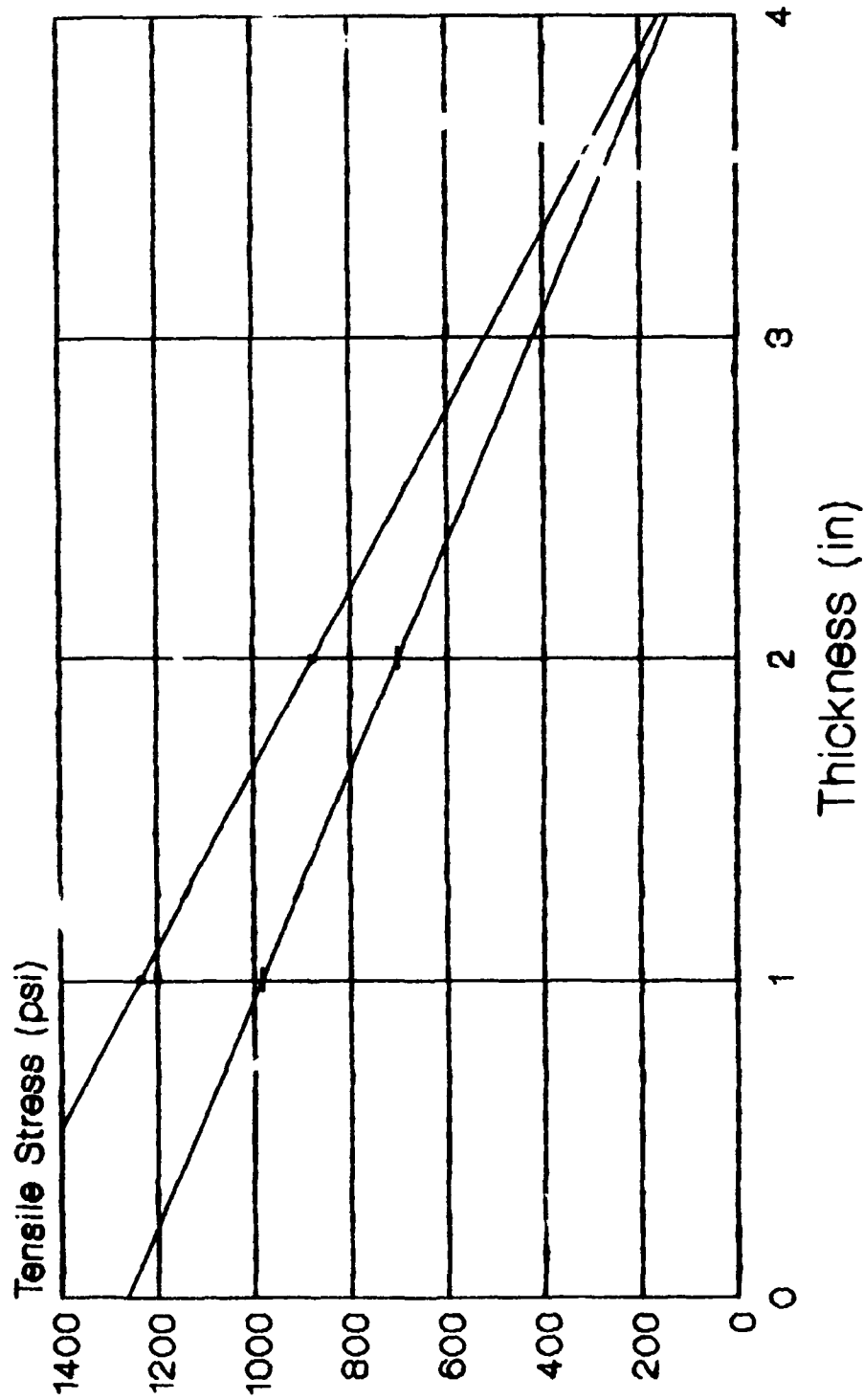


* K = 100 □ K = 300

Figure 17 - chart of B-727 data

Bottom Thickness vs Top Stress

Top Layer Thickness = 8 in.



— K = 100 — K = 300

Figure 18 - chart of B-727 data

Top Thickness vs Top Stress

Bottom Layer Thickness = 2 in

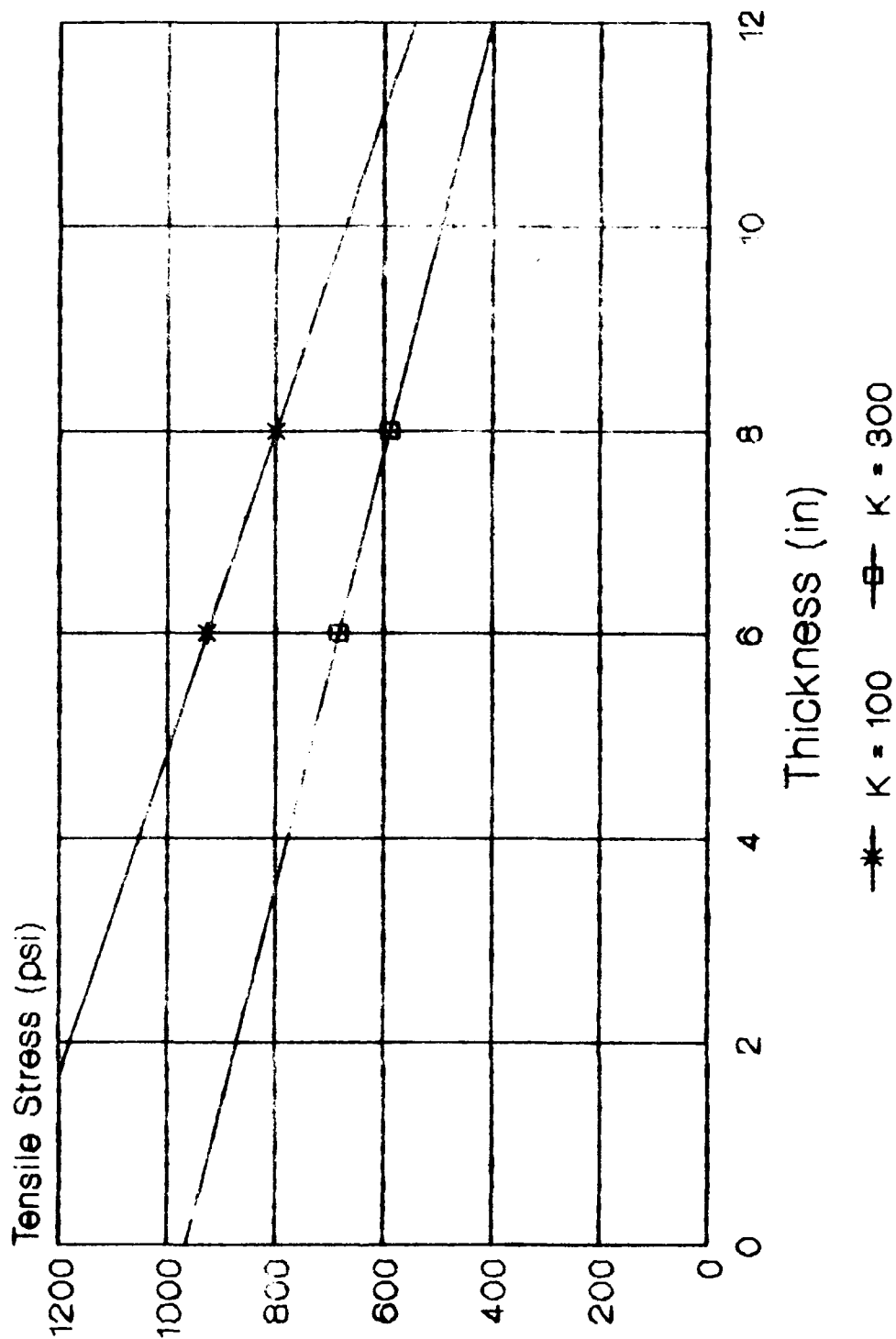
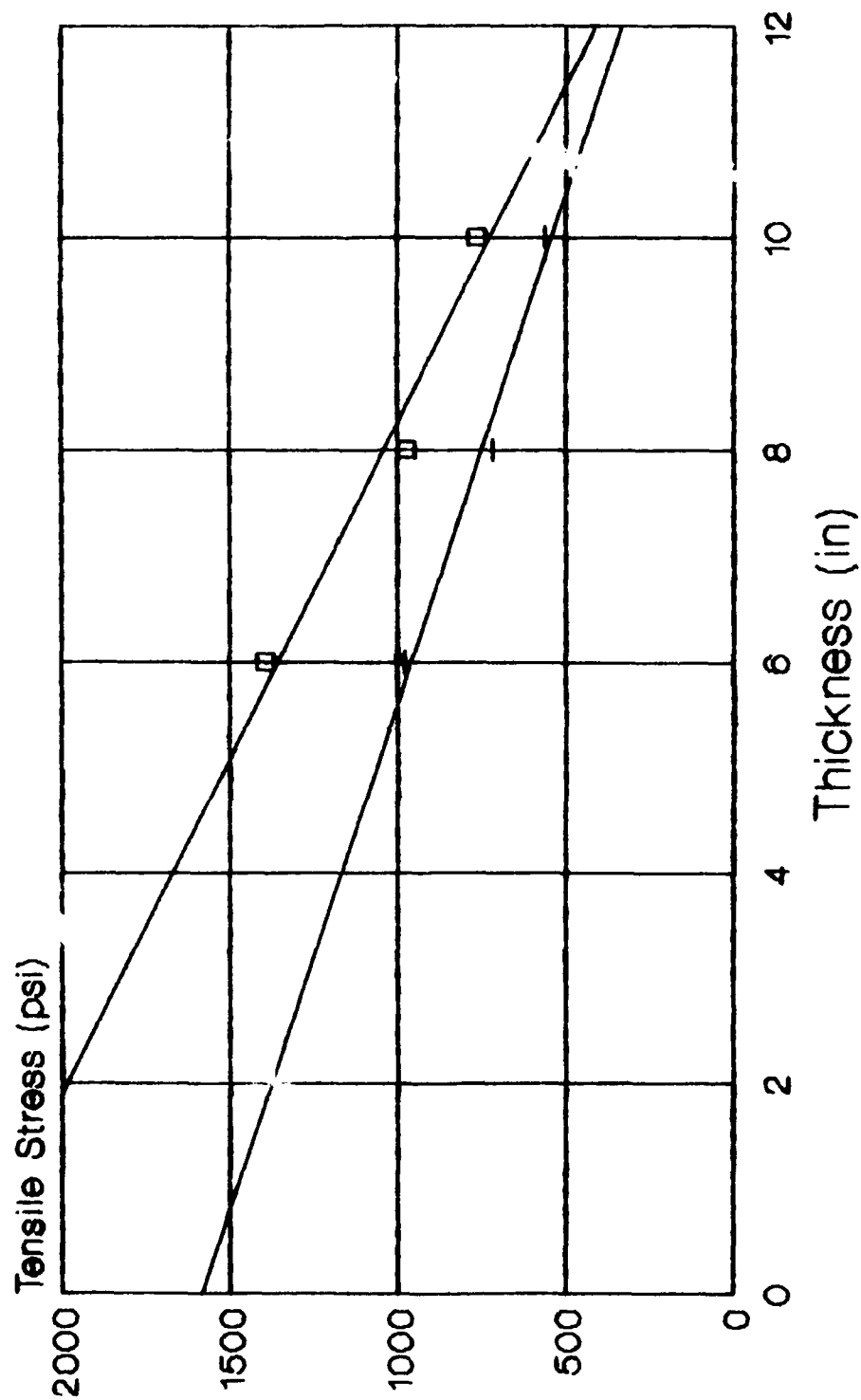


Figure 19 - chart of DC-10 data

Top Thickness vs Bottom Stress

Bottom Layer Thickness = 2 in



— K = 100 — K = 300

Figure 20 - chart of DC-10 data

Top Thickness vs Top Stress

Bottom Layer Thickness = 1 in.

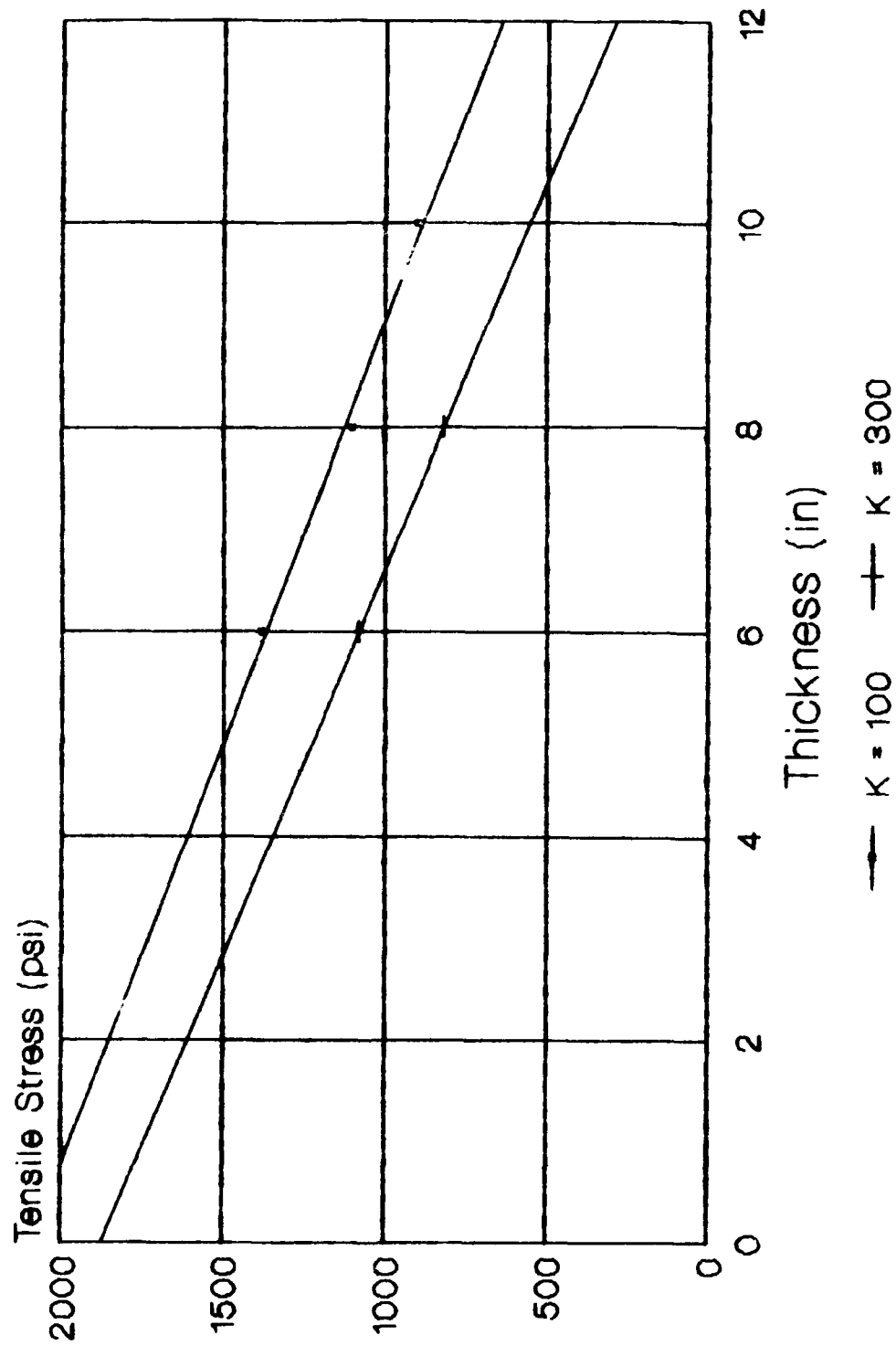
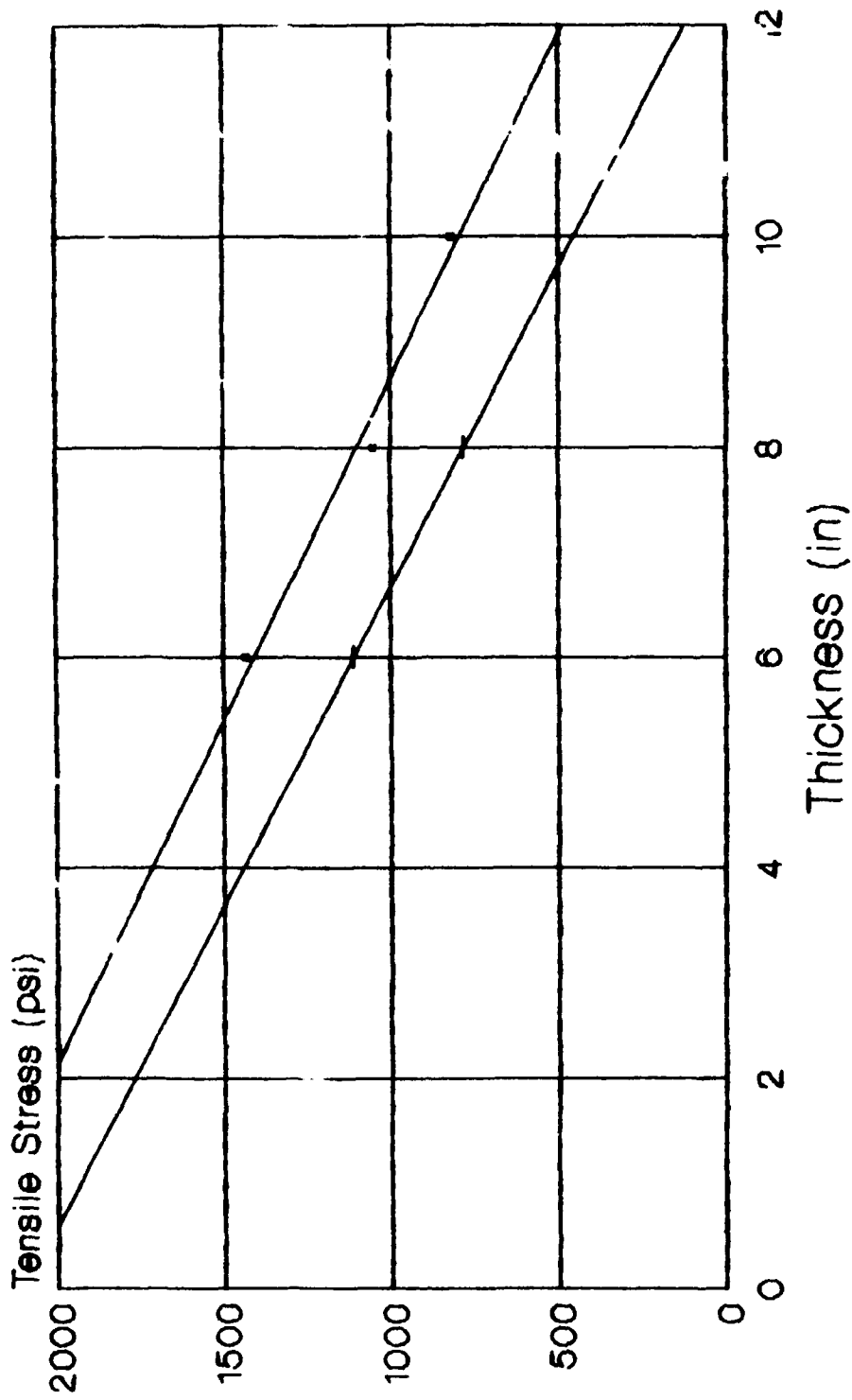


Figure 21 - chart of DC-10 data

Top Thickness vs Bottom Stress

Bottom Layer Thickness = 1 in



—•— K = 100 —+— K = 300

Figure 22 - chart of DC-10 data

Bottom Thickness vs Bottom Stress

Top Layer Thickness = 6 in.

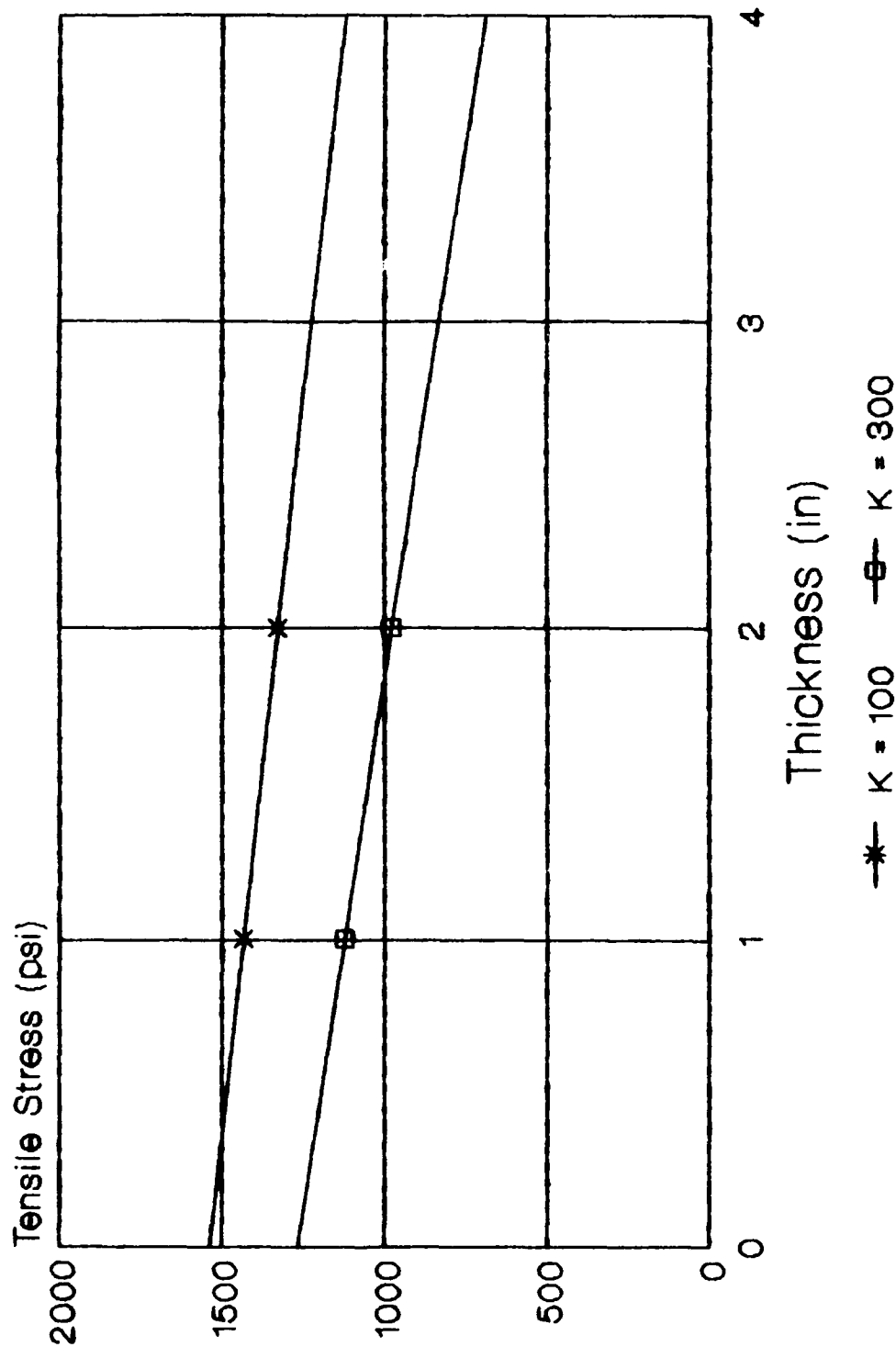
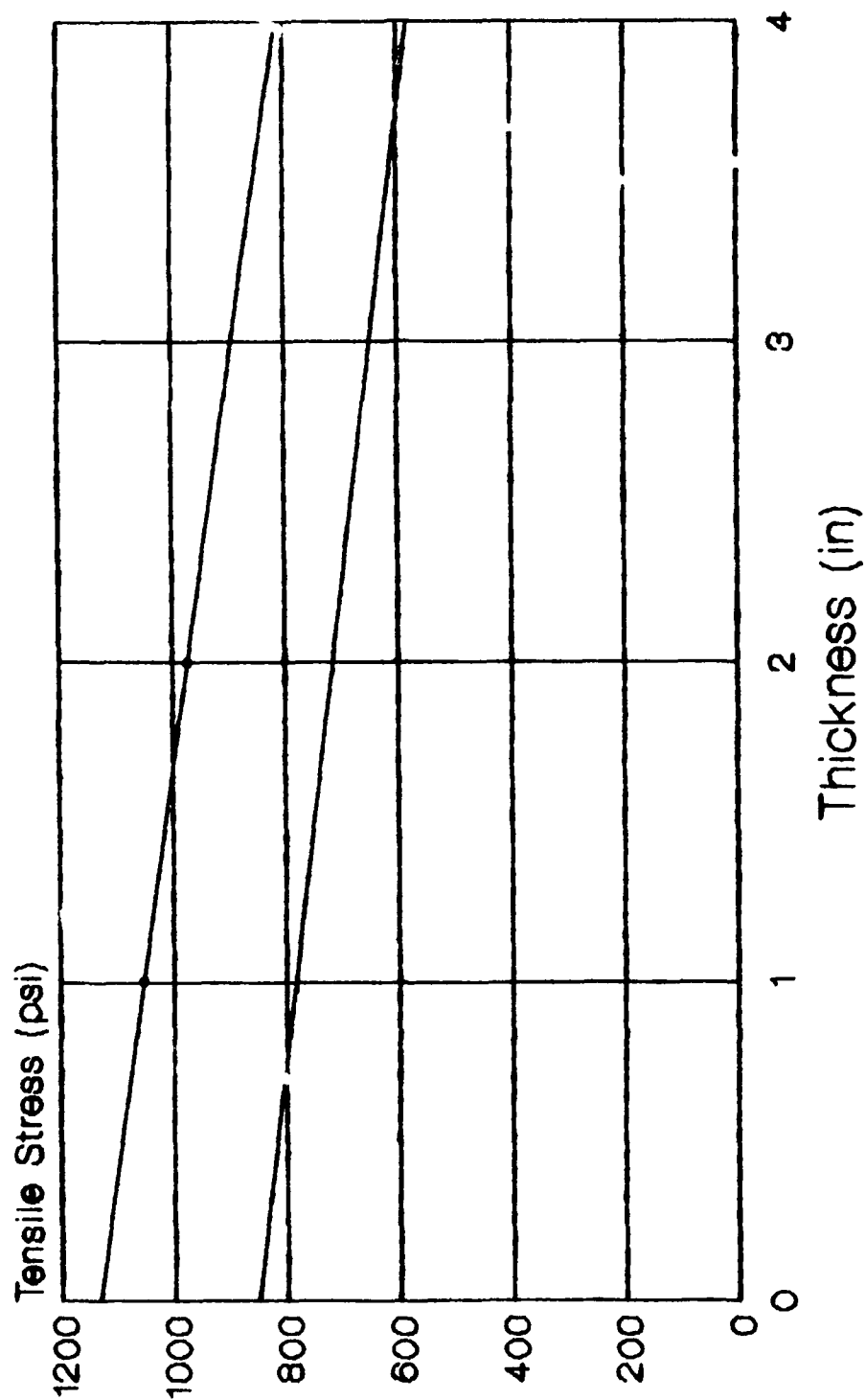


Figure 23 - chart of DC-10 data

Bottom Thickness vs Bottom Stress

Top Layer Thickness = 8 in.

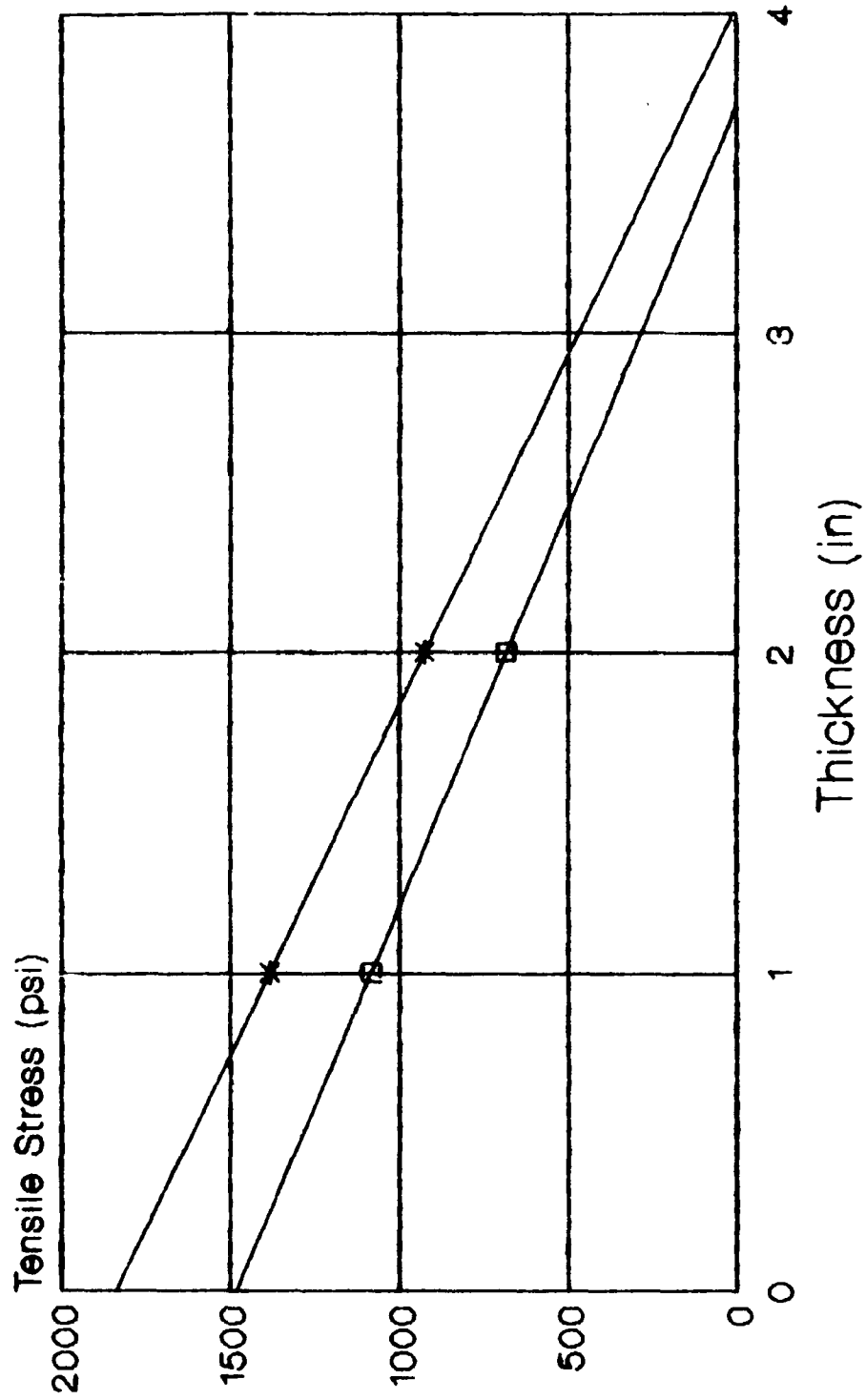


—•— K = 100 —+— K = 300

Figure 24 - chart of DC-10 data

Bottom Thickness vs Top Stress

Top Layer Thickness = 6 in.



—*— K = 100 —□— K = 300

Figure 26 - chart of DC-10 data

Bottom Thickness vs Top Stress

Top Layer Thickness = 8 in.

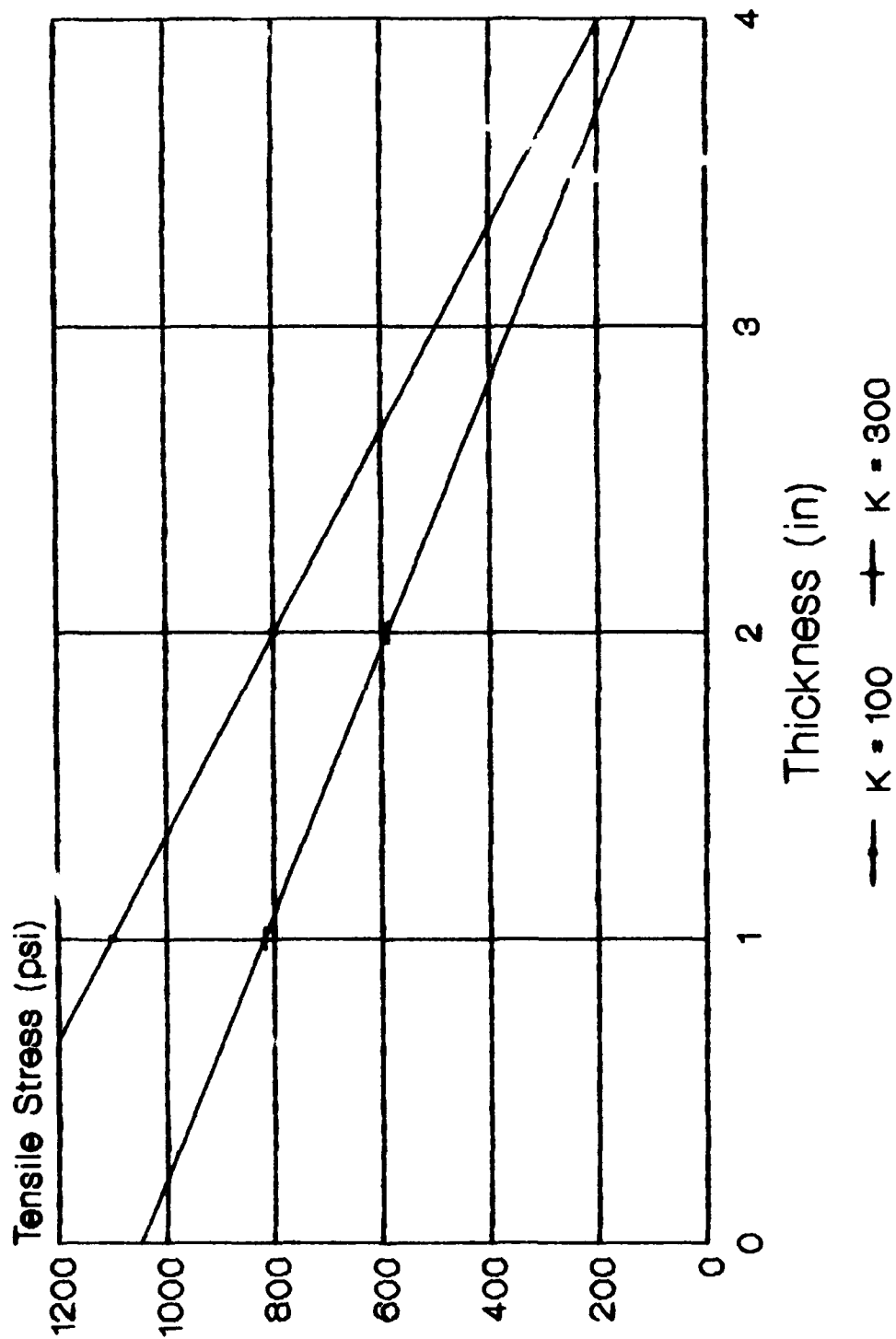
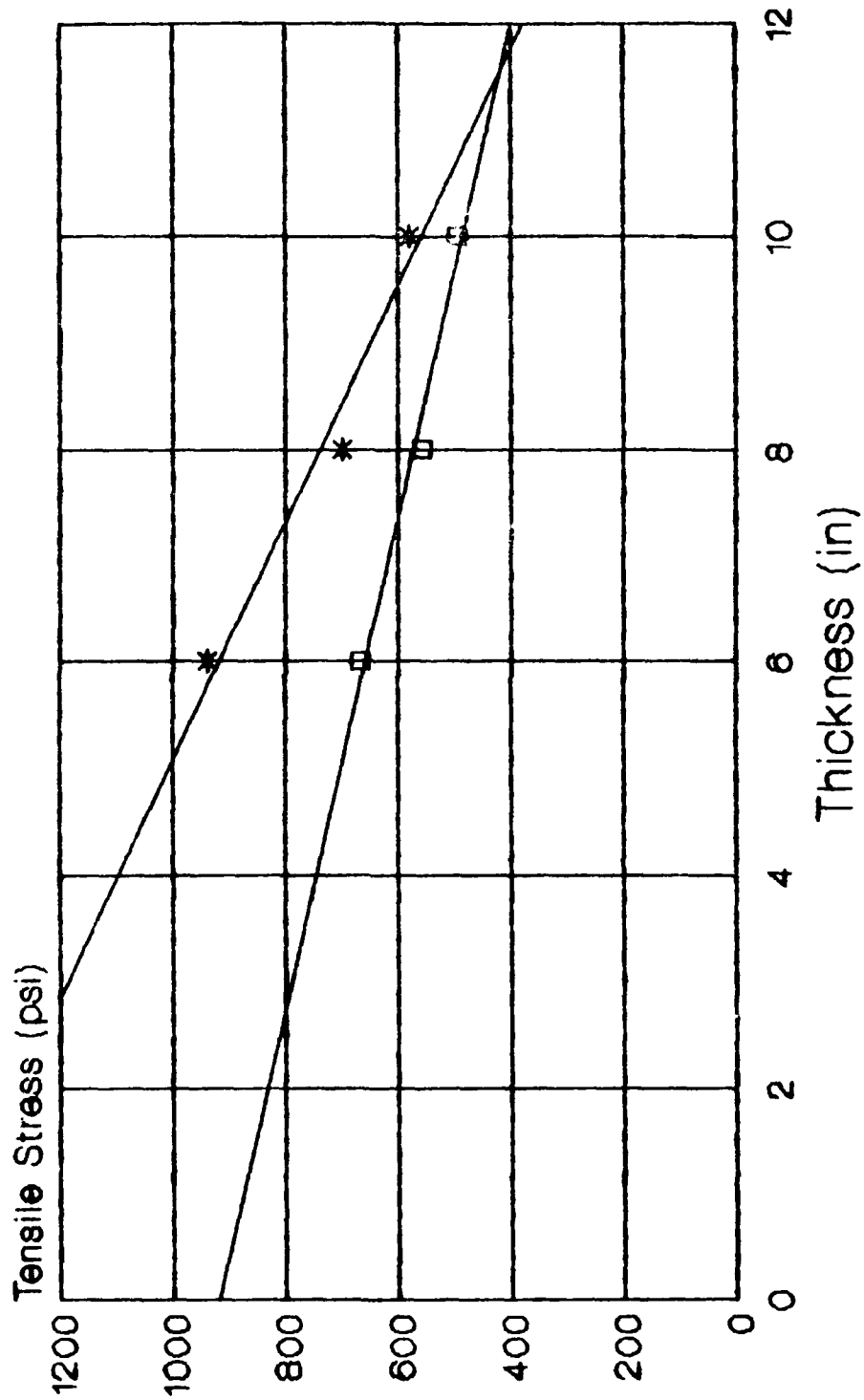


Figure 26 - chart of DC-10 data

Top Thickness vs Top Stress

Bottom Layer Thickness = 2 in.

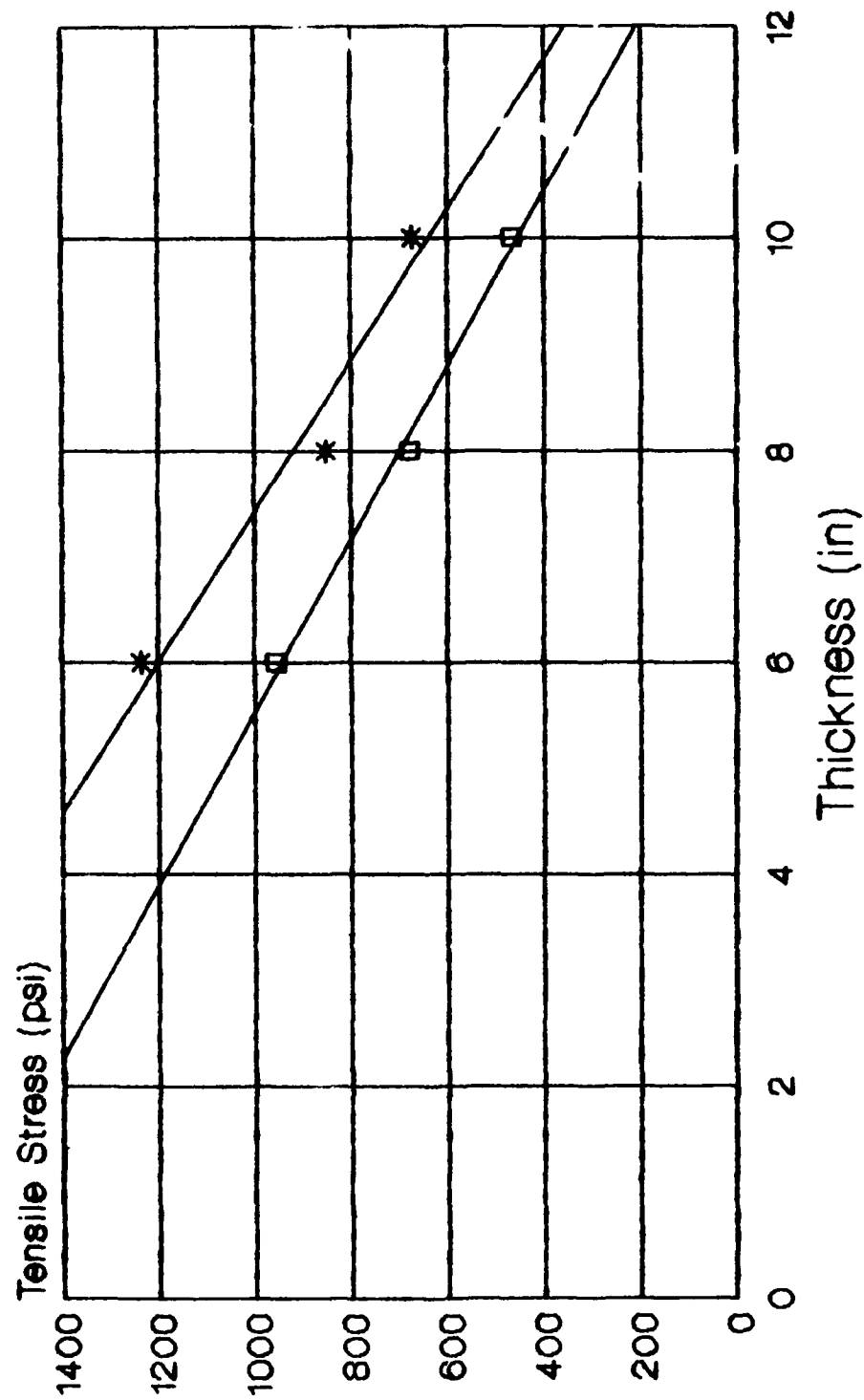


* K = 100 □ K = 300

Figure 27 - chart of L-1011 data

Top Thickness vs Bottom Stress

Bottom Layer Thickness = 2 in.



* K = 100 □ K = 300

Figure 28 - chart of L-1011 data

Top Thickness vs Top Stress

Bottom Layer Thickness = 1 in.

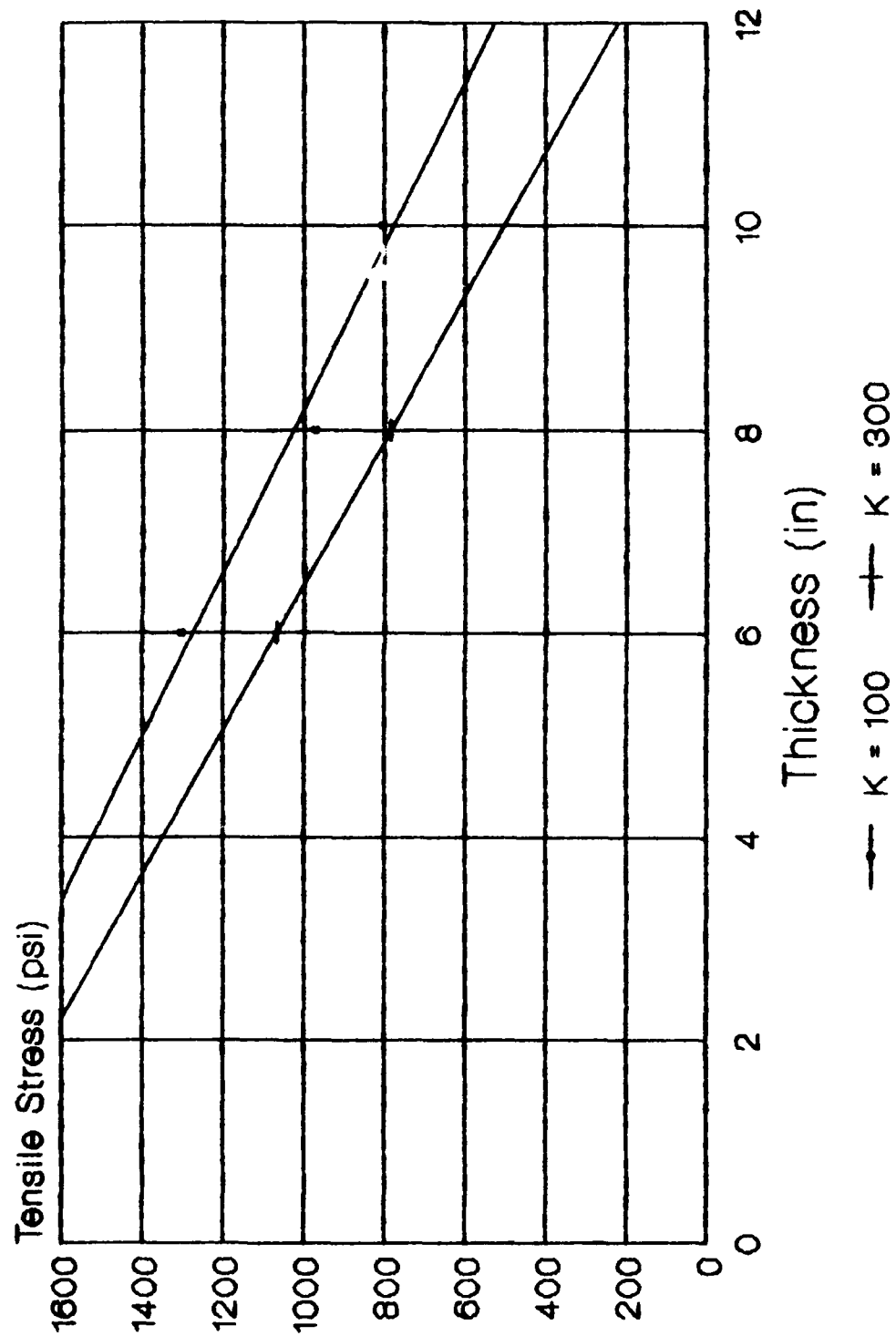


Figure 29 - chart of L-1011 data

Top Thickness vs Bottom Stress

Bottom Layer Thickness = 1 in.

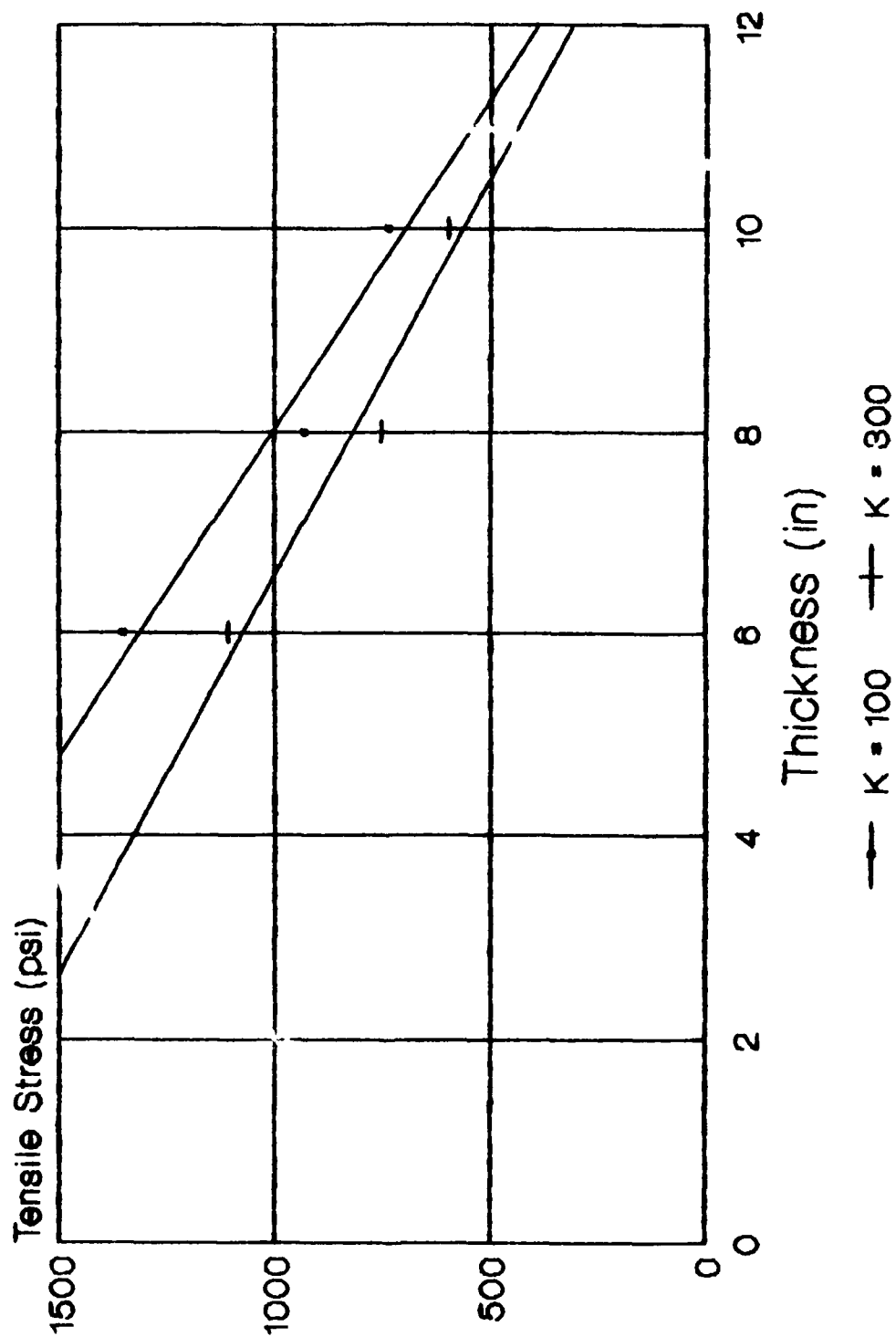
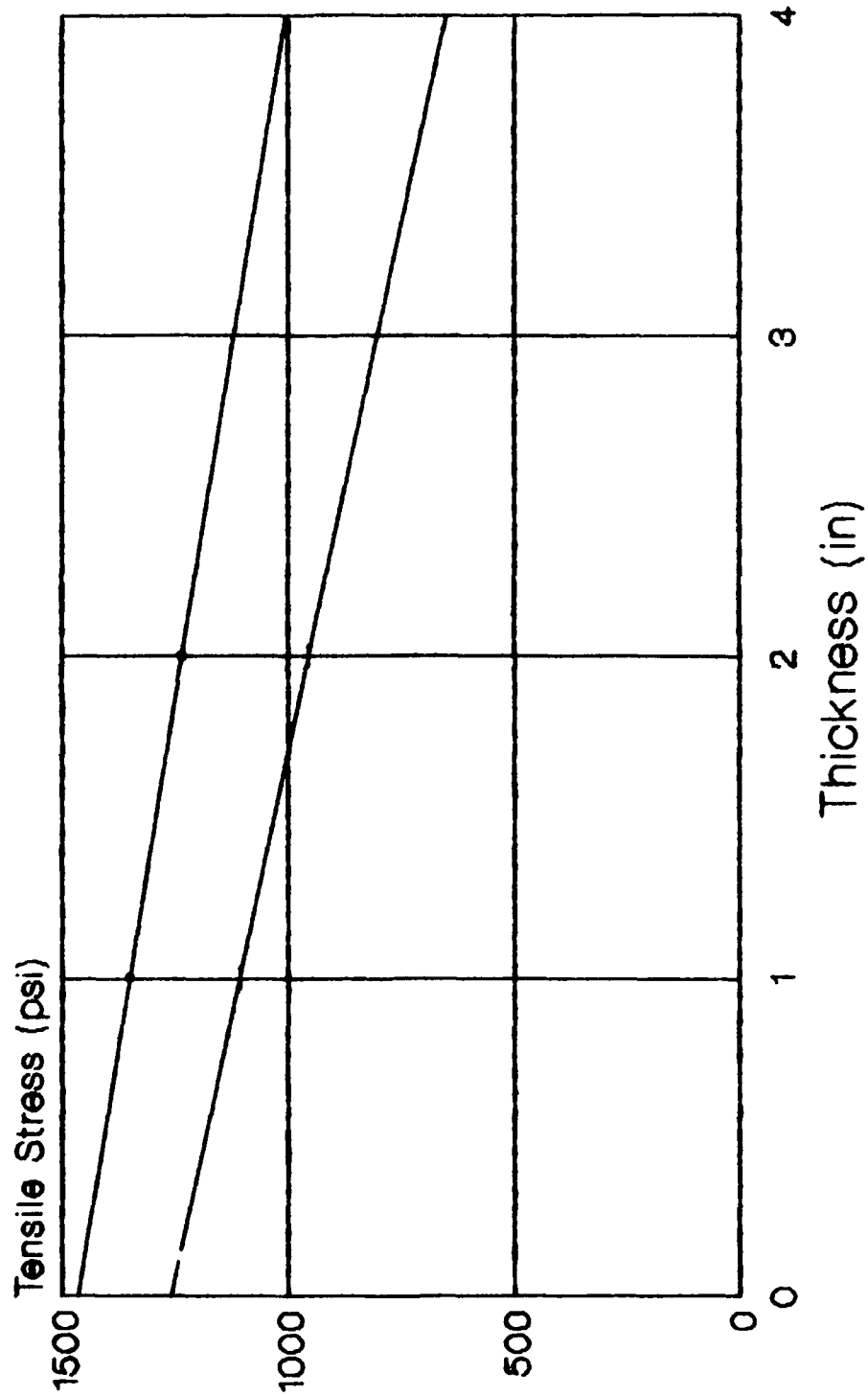


Figure 30 - chart of L-1011 data

Bottom Thickness vs Bottom Stress

Top Layer Thickness = 6 in.

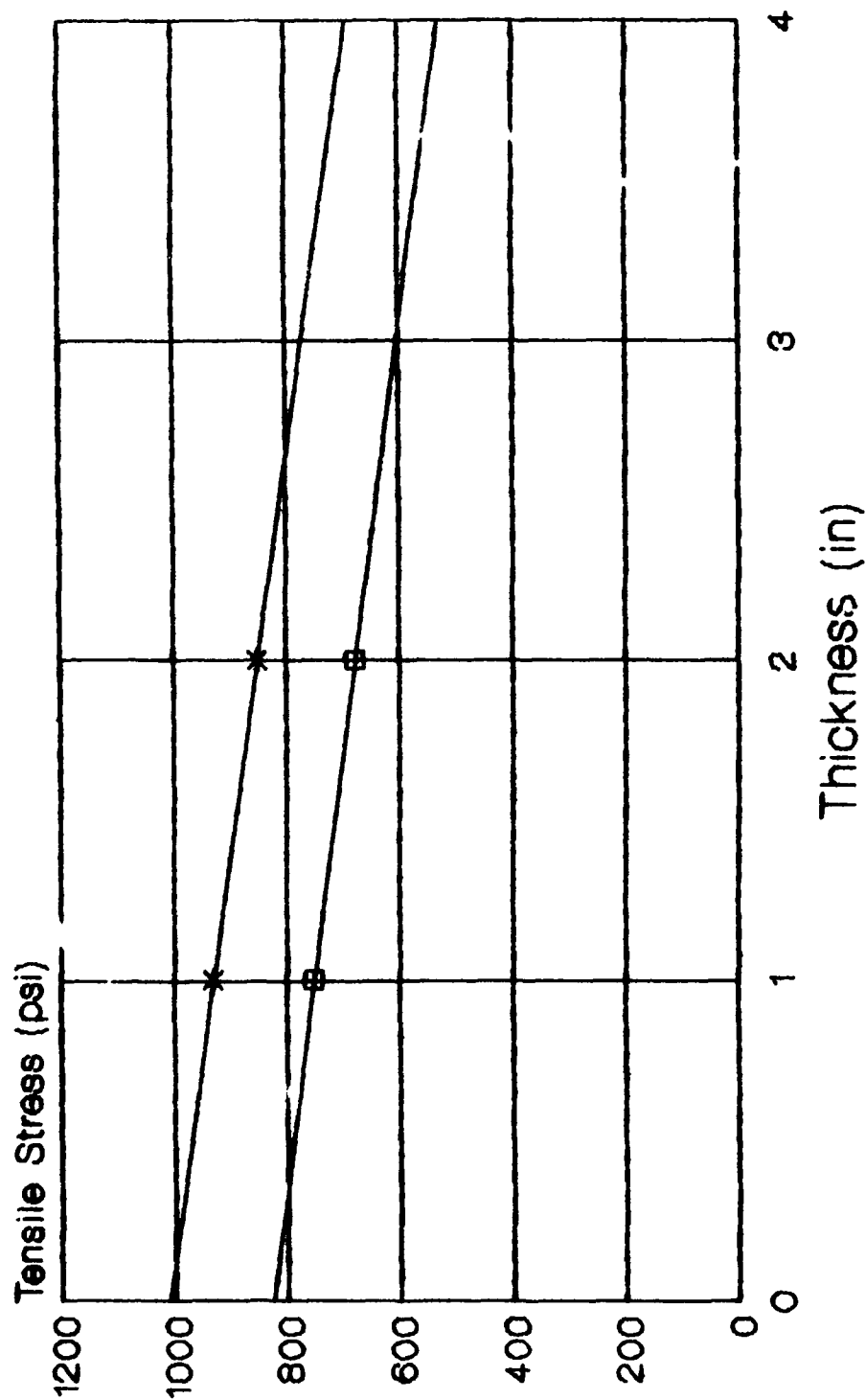


—•— K = 100 —+— K = 300

Figure 31 - chart of L-1011 data

Bottom Thickness vs Bottom Stress

Top Layer Thickness = 8 in.

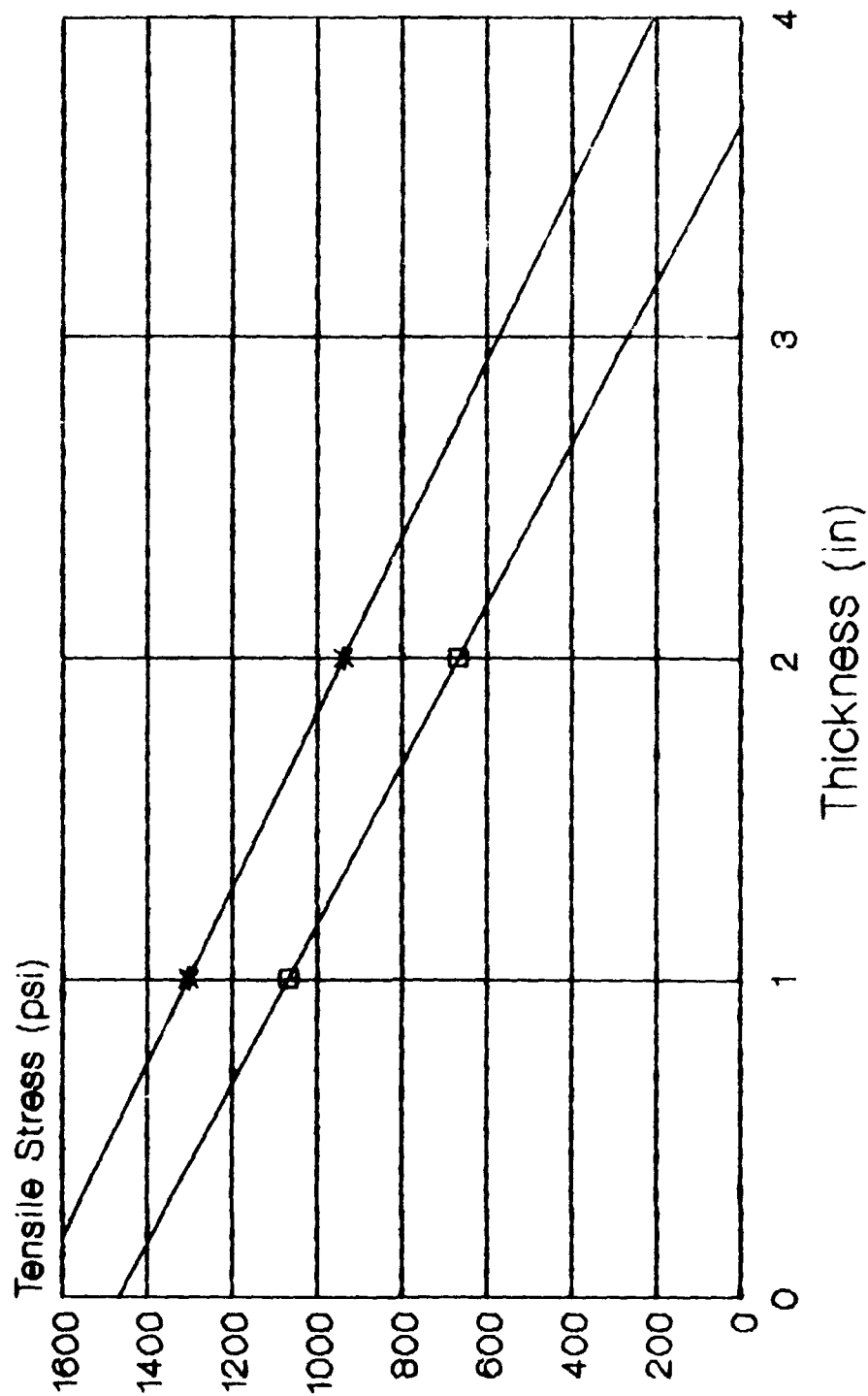


—*— K = 100 —□— K = 300

Figure 32 - chart of L-1011 data

Bottom Thickness vs Top Stress

Top Layer Thickness = 6 in.

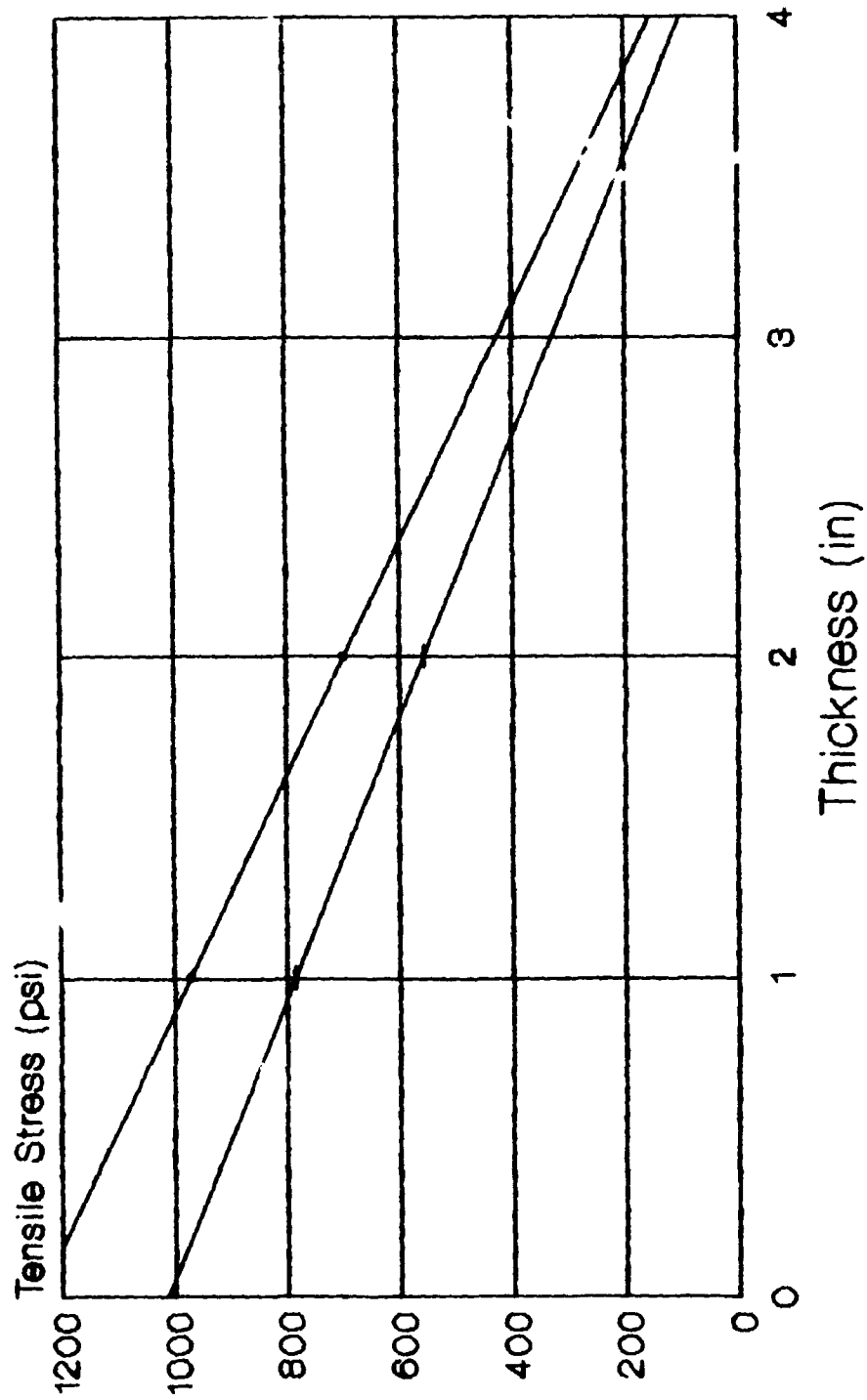


* K = 300 □ K = 100

Figure 33 - chart of L-1011 data

Bottom Thickness vs Top Stress

Top Layer Thickness = 8 in.



— K = 100 + K = 300

Figure 34 - chart of L-1011 data

Chapter 4 - Quality Control Methods

While constructing an airport runway of either PC or a combination of PC and PCC as discussed earlier, it is essential that careful attention be paid to quality control methods. In the case of PC, a chemical method of analysis will reveal the structure of the material used. These data will be compared to the standards for the PC and the results of this comparison will determine the quality of the material (See attached Infra red spectra of materials used in this study - pages 142-148). Other methods for quality control of PC include the fabrication of 3' by 6" cylinders and testing for compressive stress. Experience shows that 4 hours of curing should give sufficiently high (over 5000 psi) values depending on the mix design. Infrared spectra of various raw materials that have been used to fabricate laboratory samples are presented in this section. These raw materials are the ones that were used in the phase I study to develop mix designs and mechanical property characteristics. The following tables show the physical properties of the raw materials used including vapor pressure, vapor density, specific gravity, bulk density, solubility, volatility, flash point, and the manufacturer of these products. Table 9 contains this data for the various polymers and table 10 has similar information for the additives.

Table 9a
Physical Properties of Polymers - Epoxy and Polyester

	Epoxy	Polyester
Name	Epon 815	Roskyd 500a
Chemical Name	Modified 4'4' isopropylidenediphenol epichlorohydrin resin	unsaturated polyester
Color	Amber	Light yellow
Odor	-----	styrene odor
Vapor Pressure	1	less than 7.5
Vapor Density Air = 1	4.5	3.59
Specific Gravity	1.13	1.12
Bulk Density	9.41 lb/gal	9.3 lb/gal
Solubility in Water	Negligible	Insoluble
Percent Volatile	-----	25
Flash Point	164 F	98 F
Manufactured By	Shell Chemical Houston, TX	Mobay Chemical Pittsburgh, PA

Table 9b
Physical Properties of Polymers -MMA and Styrene

	MMA	Styrene
Name	Methyl Methacrylate	Styrene Monomer
Chemical Name	2-propenonic acid 2-methyl-methylester	styrene monomer
Color	clear	colorless
Odor	styrene odor	Sweet odor
Vapor Pressure	29	4.5
Vapor Density Air = 1	3.5	3.6
Specific Gravity	0.94	0.9034
Bulk Density	7.83 lb/gal	7.53 lb/gal
Solubility in Water	Moderate	0.032
Percent Volatile	100	
Flash Point	49 F	88 F
Manufactured By	Rohm & Haas Co Philadelphia, PA	Dow Chemical Co Midland, MI

Table 10a
Physical Properties of Additives - DETA and DMA

	DETA	DMA
Name	DETA	Dimethylaniline
Chemical Name	Dimethyltriamine	N,N Dimethyl aniline
Color	colorless	colorless
Odor	amine odor	amine odor
Vapor Pressure	less than 1	1
Vapor Density Air = 1	3.56	4.17
Specific Gravity	0.947	0.9563
Bulk Density	7.2 lb/gal	7.96 lb/gal
Solubility in Water	miscible	negligible
Percent Volatile	100	100
Flash Point	208 F	145 F
Manufactured By	Dow Chemical Co Midland, MI	Eastman Kodak Rochester, NY

Table 10b
Physical Properties of Additives - DMT and BZP

	DMT	BZP
Name	Dimethyl toluidine	Benzoil Peroxide
Chemical Name	N,N Dimethyl -p-toluidine	Peroxide
Color	yellow liquid	white crystal solid
Odor		odorless
Vapor Pressure	4.2	no data
Vapor Density Air = 1		greater than 1
Specific Gravity	0.937	1.33
Bulk Density	8.3	
Solubility in Water	insoluble	insoluble
Percent Volatile	100	Non-volatile
Flash Point	181 F	176 F
Manufactured By	Eastman Kodak Rochester, NY	Alfa Products Danvers MA.

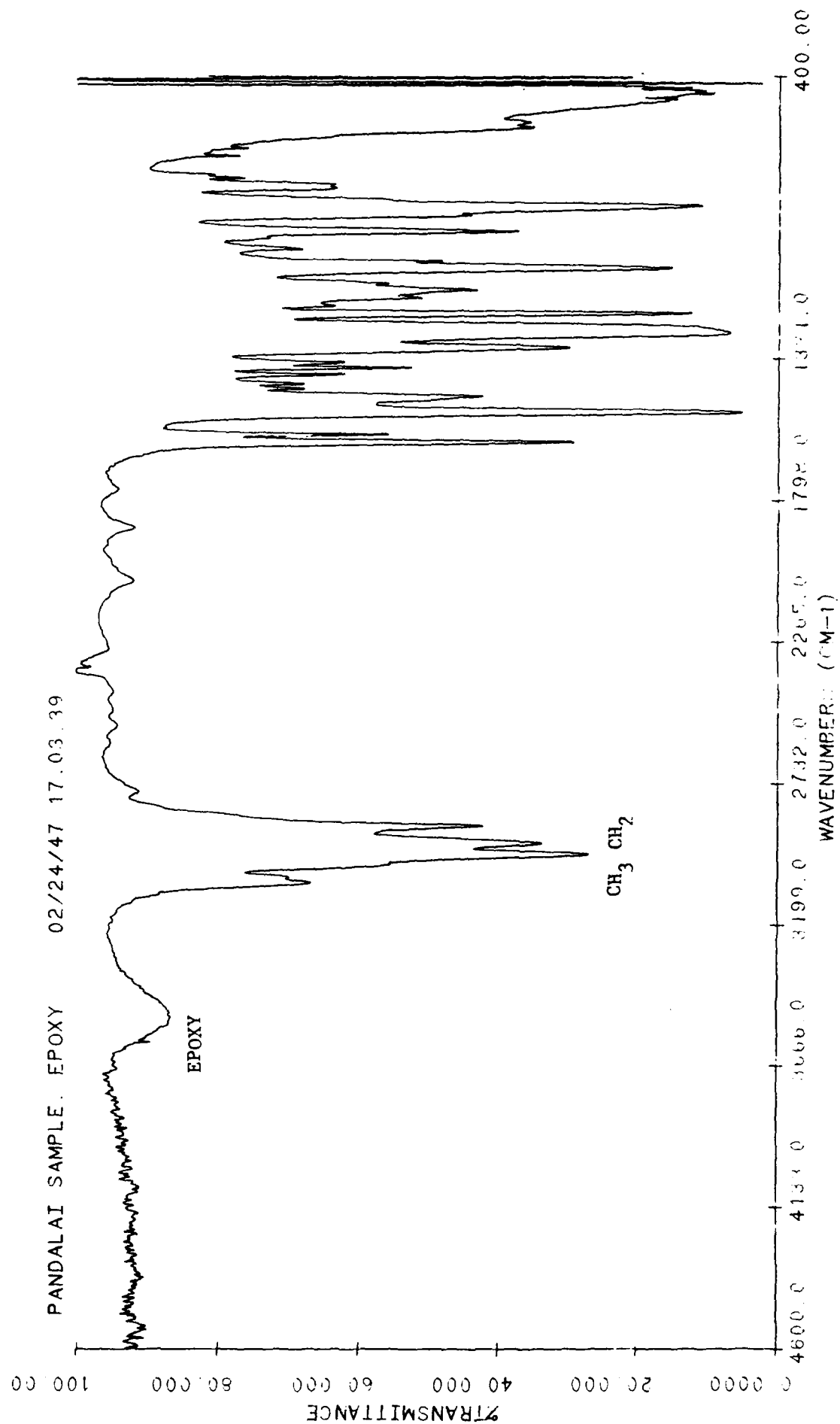


Figure 35 - Infra-red plots of Epoxy

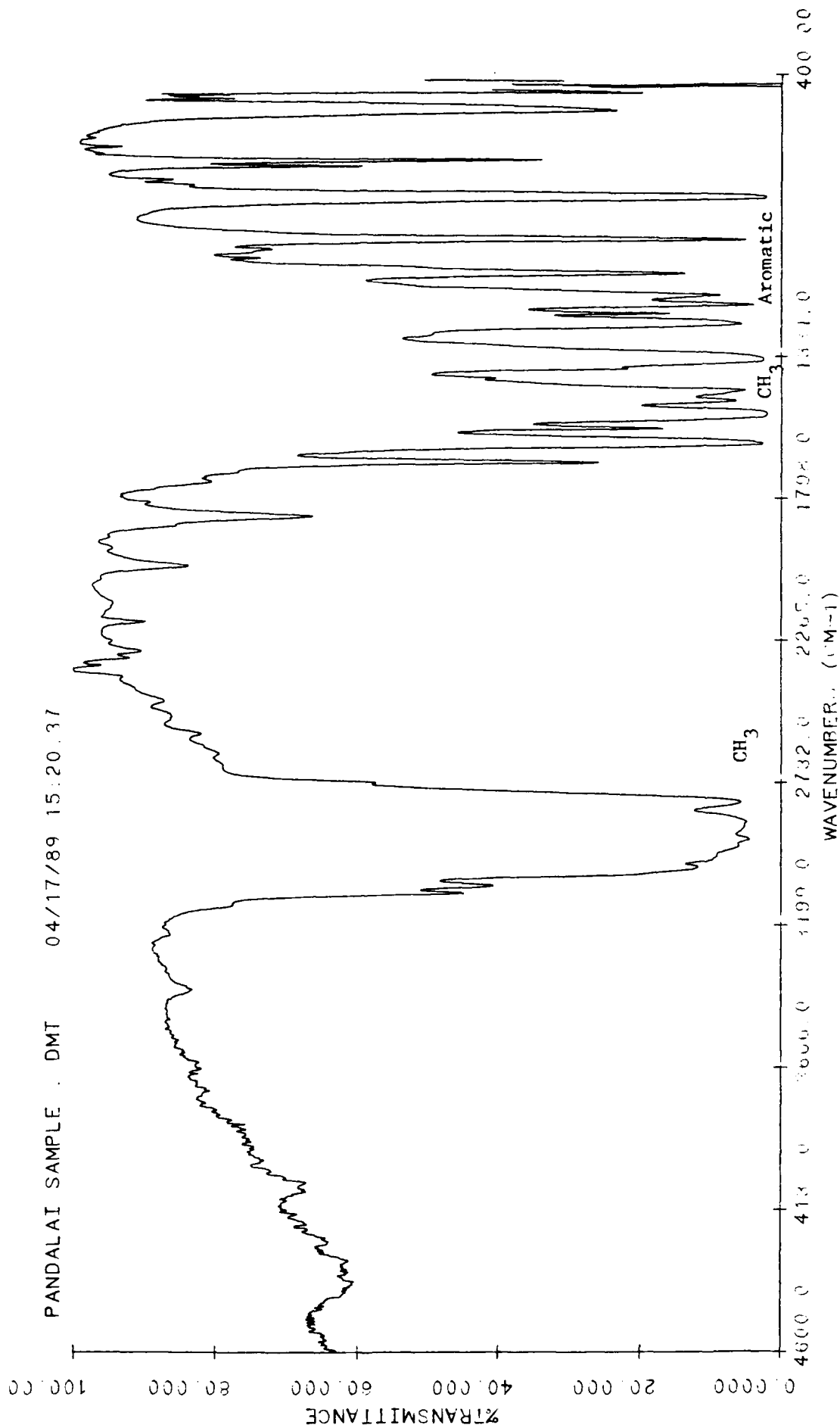


Figure 36 - Infra-red plot of DMT

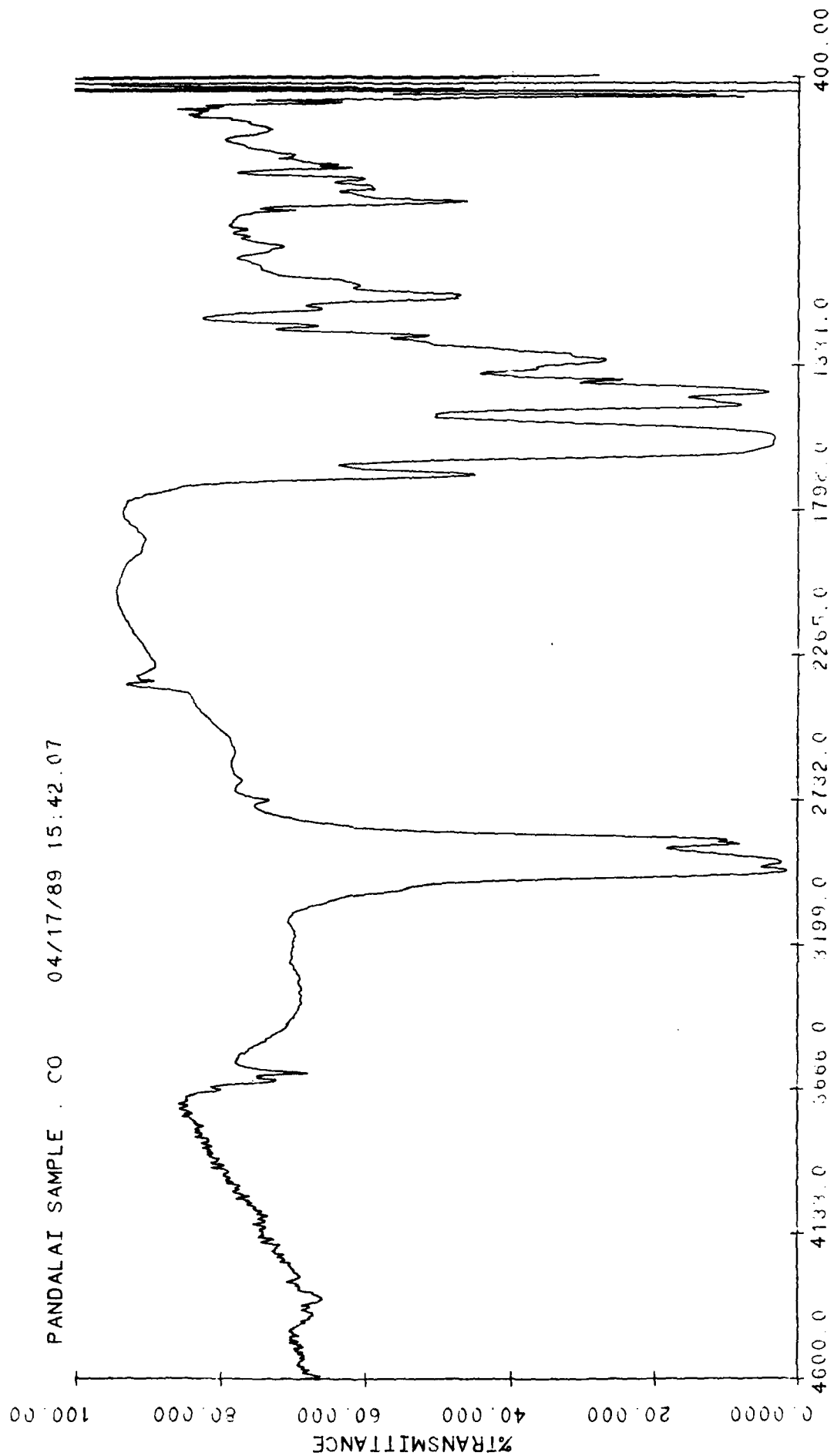


Figure 37 - Infra-red plot of CO

Methyl Methacrylate Ester

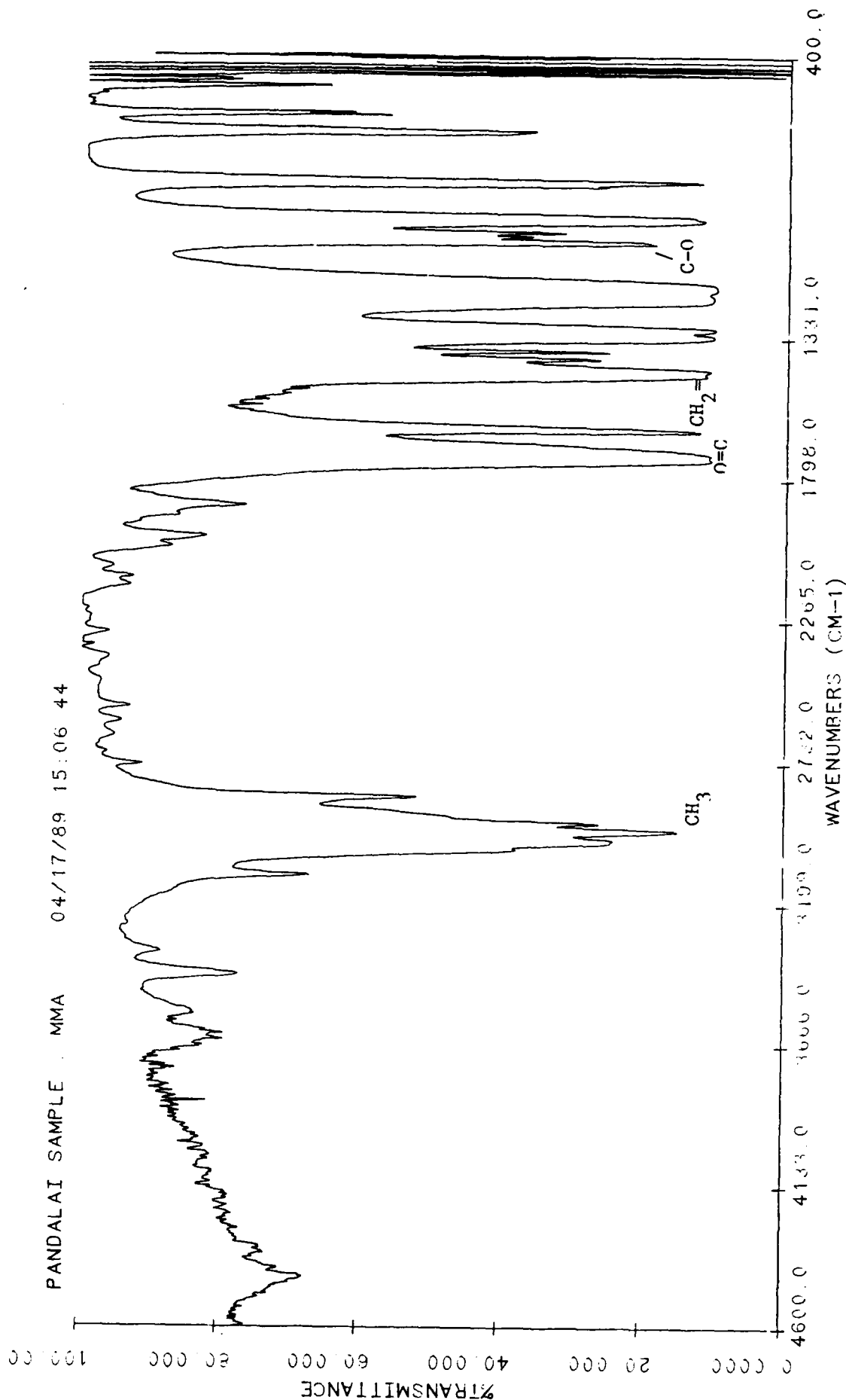
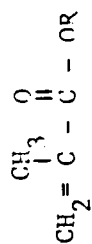


Figure 38 - Infra-red plot of MMA

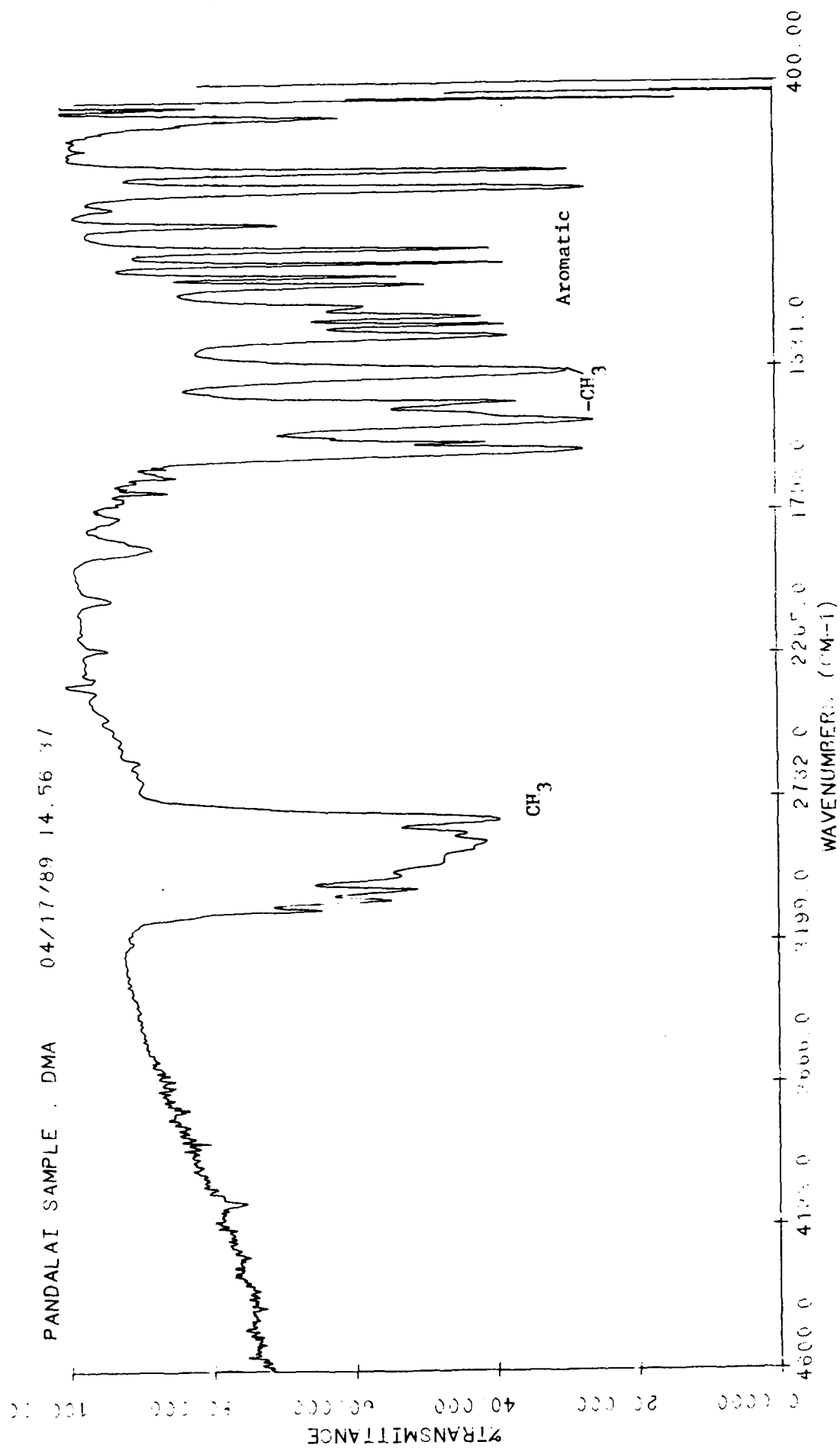


Figure 39 - Infra-red plot of DMA

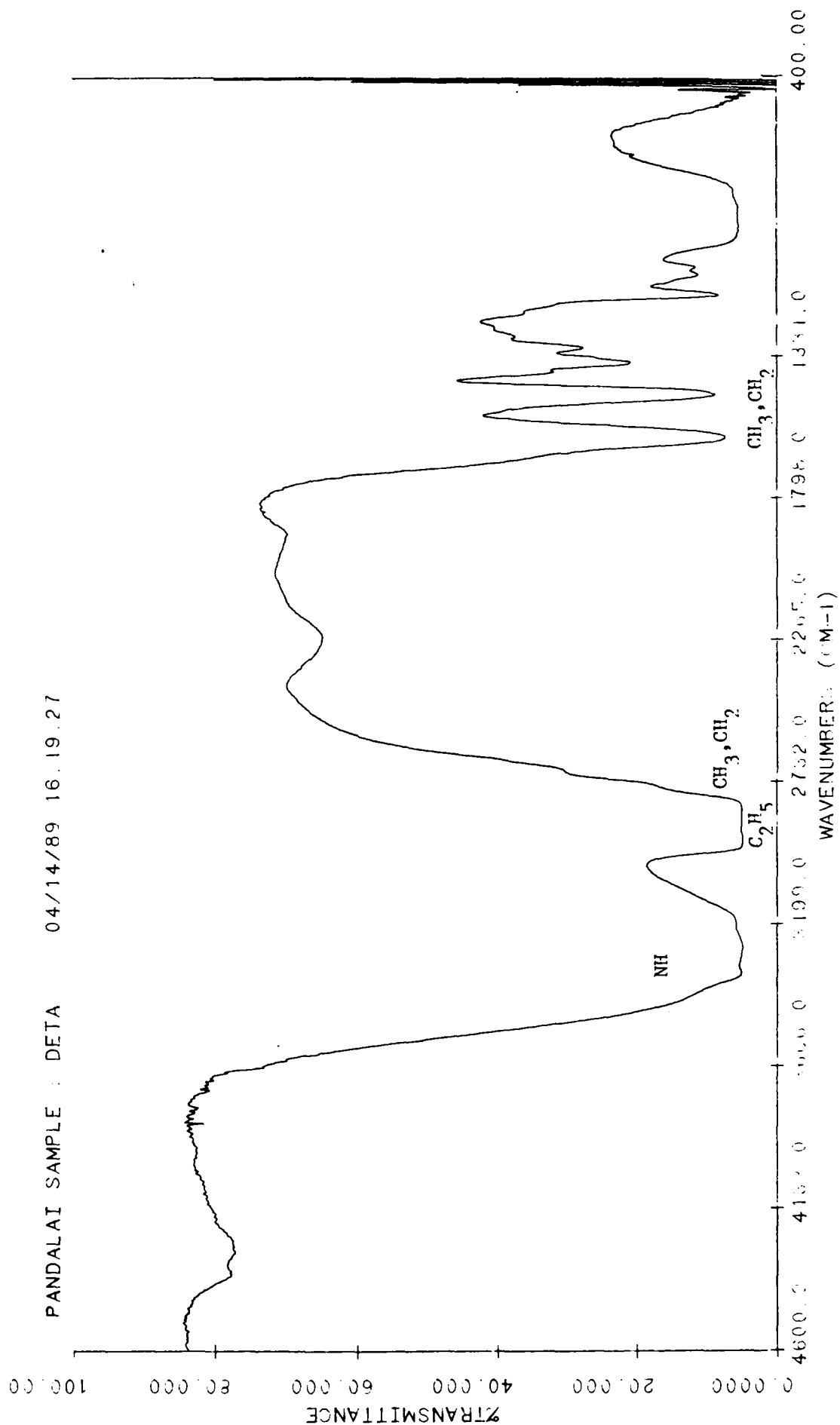


Figure 40 - Infra-red plot of DETA

Totally Impure Styrene



ALDRICH NEAT LIBRARY: STYRENE, 99+%, GOLD LABEL

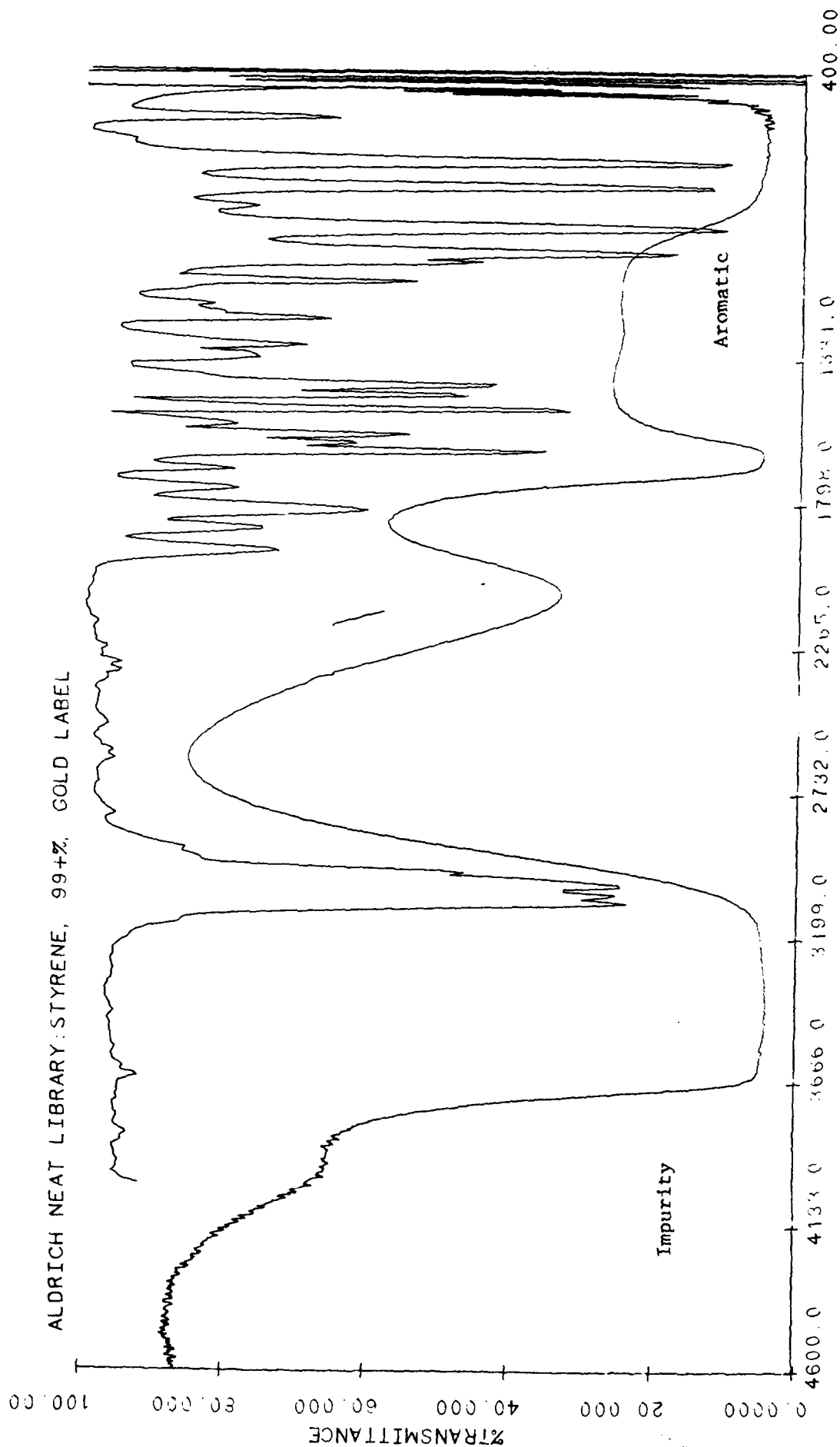


Figure 41 - Infra-red plot of Styrene

Chapter 5 - Construction Procedures

Before an actual runway is designed and constructed from polymer concrete, construction procedures must be clearly outlined and developed because the conditions governing the curing of polymer concrete differ radically from those for PCC. In the case of normal strength PCC, proportioning and mixing is done at the plant and not at the job site. However, due to the nature of polymer concrete, this is not possible. While proportioning and material transfer into separate compartments can be done at the plant, mixing will have to be done at the job site. This is due to the fact that a spontaneous chemical reaction takes place between the components of the PC during the curing process. The best procedure to follow would be to have pre-weighed ingredients shipped to the job site for mixing before lay down. Polymer concrete placement should be done before the curing reaction occurs.

Chapter 6 - Cost Analysis

When determining the viability of a new product, one of the most critical factors is cost. In any construction project, it is important to determine the life-cycle cost. The life-cycle cost depends on the raw material cost, labor cost, maintenance cost, and service life. An attempt is made in this chapter to analyze the cost of polymer concrete versus portland cement concrete, taking into account such factors as material and construction costs and service life costs. The life-cycle cost estimate is determined by adding all the cost elements. It is assumed that the major cost elements which differ between PC and PCC are the raw material costs and cost associated with service life.

6.1 - Estimating Costs for Polymer Concrete

The estimated material costs for polymer concrete are based on (1) the raw material costs for PC; (2) the cost of mixing the raw materials on site; and (3) comparing these costs for the material costs in PCC. Also, there will be a significant difference in the life-cycle and maintenance costs between PC and PCC. However, no data can be obtained to determine these differences until field tests are run.

Table 11
Cost for PCC Pavement at Different Thicknesses
 (Data obtained from Runway Rehabilitation Project done at the
 Pittsburgh International Airport)

Thickness (in)	Cost	
	\$/square yard	\$/cubic yard
10	46.35	166.86
12	56.65	169.95
15	55.65	133.56
18	61.80	123.60

If it is assumed that the cost of PCC is \$50/cubic yard, then the construction cost of PCC will be the amount in column 3 (\$/cubic yard) of table 11 minus the material cost (assumed to be \$50/cubic yard). This value, along with the percent material cost is given in table 12. Note that as the pavement thickness increases, the percent material cost increases.

Table 12
Cost Data for PCC

Pavement Cost (\$/cubic yard)	Construction Cost (\$/cubic yard)	% Material Cost
166.86	116.86	30
169.95	119.95	29
133.56	83.56	37
123.60	73.60	40

From these data, it can be seen that the material cost makes up approximately 34 percent of the total construction cost for PCC.

6.2 - Construction Cost Estimates

For a 16-inch portland cement concrete pavement, the estimated construction cost is \$45/Square Yard. It has been established that the raw material cost is 34 percent or \$15.30. If the PCC pavement is replaced by a PC pavement, the thickness required is about 7 inches. This can be seen to be true from figure 1 assuming a 90 percent stress ratio for PC. Assuming a raw material cost factor difference of 10 for PC pavement, the raw material cost for PC becomes $(15.3 \times 7 \times 10)/16$ or \$66.9. This brings the construction cost to \$96.6 per square yard for PC. In order to be economically viable the savings due to maintenance cost and increased service life should be more than 50 percent.

In the case of a composite pavement containing PC bottom layer and PCC top layer, a 16" thick pavement made entirely of PCC is equivalent to a composite pavement with a 2" PC underlay and 8" PCC overlay. The raw material cost for the composite would be equivalent to the raw material cost for a PCC pavement of 28" thickness. In other words, the cost factor in this case is 28/16 as far as raw materials are concerned. Based on this data, the following construction cost estimate can be made.

PCC pavement cost	100,000
PC pavement cost	\$126,250

The above calculation assumes that the quick curing of PC will enable PCC to be poured continuously on a big construction job and that no additional labor costs will be incurred even though 2 passes are necessary for the composite pavement construction. While the initial cost is 26.25 percent higher for composite pavements, the advantages appear to warrant additional work by way of field testing for the composite pavement configuration.

Chapter 7. Conclusions and Recommendations

Phase I work involved PC mix designs with 3 different polymer systems and laboratory determinations of mechanical properties. These properties were utilized in calculating the pavement thickness for various aircraft configurations. The Illi-slab finite element computer program developed at the University of Illinois was used to calculate composite pavement thickness for various underlay and overlay thicknesses. The thicknesses have been calculated for B-747, B-727, DC-10 and L-1011 aircraft and are presented in figures 3 through 34 and tables 5 through 8. Table 13 contains data comparing bending stress values when Young's modulus values were changed for the various aircraft.

Table 13

Aircraft	E2	K	S1	S2	h1	h2
B-747	3	100	1119	1071	8	1
B-747	6	100	888	1736	8	1
B-727	3	100	1235	1182	8	1
B-727	6	100	966	1889	8	1
DC-10	3	100	1100	1053	8	1
DC-10	6	100	874	1709	8	1
L-1011	3	100	971	930	8	1
L-1011	6	100	760	1487	8	1

Table 13 is presented to show the great improvement in bending stress values for the same PCC and PC composite layer thickness values when Young's modulus is changed from three million to six million. In order to obtain a value of six million for E2, the basic mix design must be altered. An extension of the present study to achieve a higher E2 value will be a very useful project because at a composite pavement thickness of one inch PC and

eight or even ten inches of PCC, the raw material cost is only 12 to 25 percent more than the 100 percent PCC pavement cost. This means that a PCC pavement which costs \$45.00/square yard would cost under \$50/square yard if the composite pavement configuration is selected. With many of the advantages of the composite pavement, the life cycle cost of the composite pavement might even be less than the PCC pavement. This, however, can only be verified by additional laboratory mix design work and field tests.

In summary, the present investigation has developed pavement design charts for four aircraft with the composite pavement design configuration. Quality control standards for the various ingredients have been presented along with mixing information and lay down procedures. It is important to mention that the mixed polymer concrete should be immediately poured. Other normal construction practices used when building a PCC pavement should be followed. The composite pavement configuration appears to be very competitive to PCC pavement and work must be continued to study in more detail, the field performance characteristics of PC. Increasing the modulus of elasticity for PC also appears to have definite advantages which also must be investigated.

REFERENCES

1. American Concrete Institute, Symposia on Polymer Concrete, SP-40 (1972 and 1973)
2. American Concrete Institute, Symposia on Polymer Concrete, SP-58 (1976)
3. American Concrete Institute, Symposia on Polymer Concrete, SP-69 (1981)
4. Overview of Current Research in Polymer Concrete: Materials and Future Needs, By John A. Manson.
5. J. M. Antonucci, Org. Coat. Plast. Chem; 42(1980) 198
6. "Filling the Cracks", Virginia Fairweather, Civil Engineering; Oct. 1986, pp38-41.
7. "Filling the Cracks", Virginia Fairweather, Civil Engineering; Oct. 1986, pp38-41.
8. "Filling the Cracks", Virginia Fairweather, Civil Engineering; Oct. 1986, pp38-41.
9. "Use of Concrete Polymer Materials in the Transportation Industry" by Jack J. Fontana and John Bartholomew. ACI publication, SP 69-2.
10. "One in Six U.S. Highway Bridges is Deficient", Engineering News Record, McGraw Hills Construction Weekly, March 10, 1977.
11. Kukacka, L.E. and Fontana, J., Polymer Concrete Patching Materials Users' Manual, FHWA-IP 77-11 Vol. I and BNL 22361, April 1977.
12. Kukacka, L.E. and Fontana, J., Polymer Concrete Patching Materials Users' Manual, FHWA-IP 77-11 Vol. 2, April 1977.
13. Fontana, Jack J., and Webster, Ronald, Thin Sand Filled Resin Overlays, BNL 24079, March 1978.
14. Jenkins, J.C., Beecroft, G.W., and Quinn, W.J., Polymer Concrete Overlay test Program Users' Manual Method A, FHWA-TS-78-218, December 1977.

15. Webster, R., Fontana, J., and Kukacka, L.E., Thin Polymer Concrete Overlays Interim Users' Manual Method B, FHWA-TS-78-225, February 1978.
16. Smoak, W.G., Polymer Impregnation of New Concrete Bridge Deck Surfaces Users' Manual, FHWA-IP 78-5, January 1978.
17. Kukacka, L.E., et al., The Use of Polymer Concrete for Bridge Deck repairs on the Major Deegen Expressway, FHWA-RD-75-513 and BNL 19672, January 1975.
18. Schrader, E.K., et.al., Polymer Impregnation Used in Concrete Repairs of Cavitation/Erosion Damage, ACI Publication SP 58-13. pp 225-247
19. Scanlon, Jr., J.M., Applications of Concrete Polymer Materials in Hydrotechnical Construction, ACI Publication SP 69-3, pp 45-54.
20. McDonald, James. E., and Liu, Tony C., Repair of Concrete Surfaces Subjected to Abrasion-Erosion damage, MP SL-79-15, U.S. Army Engineer Waterways Experiment Station, Vicksburg, MS. 1979.
21. Paturoyev, V.V., Technology of Polymer Concrete, Stroyizdat Press, USSR, 1977.
22. "Polymer Impregnation of Concrete at Dworshak Dam", U.S. Army Engineer Dist. Walla Walla, WA., April 1977
23. "Surface Impregnation of Spillway Floor, Shadow Mountain Dam", Water and Power Resources Specification # 70-C0038, Water and Power Resources Service, Denver Federal Center, Denver, CO.
24. Causey, F.E., "Vinyl Ester Polymer Concrete and Experimental Repair of Madera Canal Drop Structure," USBR, GR-7-77., July 1977.
25. "Cavitation Erosion Test of Polymer-Dry Sand Repair of Concrete, Libby Dam, Sluiceways and Stilling Basin,." North Pacific Division Materials Laboratory, Corps of Engineers, US Army, February 1977.
26. Ignonin, L.A., "Polymer Compositions in Hydraulic Engineering", Second International Congress on Polymers in Concrete, College of Engineering, the University of Texas at Austin, Austin, TX. pp 535-554.
27. Kovalenco, P.I., and Reznik, V.B., "Practice and Prospects for Polymer Concrete Utilization in Hydrotechnical Construction", Second International Congress on Polymers

in Concrete, College of Engineering, the University of Texas at Austin, Austin, TX. pp 555-566.

28. "Manual for Construction of Precast Protective Linings from Furan Polymer Concrete for Hydrotechnical structures", VTR-S-15-79, USSR Ministry of Reclamation and Water Management, Moscow, USSR, 1979.
29. Liu, Tony C., Maintenance and Preservation of Concrete Structures, Report 3, Abrasion/Erosion Resistance of Concrete, Vicksburg, MS., 1980
30. Perry, Robert E., "Polymer Concrete and Electric Power Industry", ACI Publication SP 69-4, pp 63-72.
31. Zeldin, et.al., "New, Novel Well-Cementing Polymer Concrete Composite", ACI Publication, SP 69-5, pp 73-92.
32. McNerney, Michael T., "Research in Progress: Rapid All-Weather Pavement Repair with Polymer Concrete", ACI Publication, SP 69-6, pp 93-105.
33. Fowler, et.al., "Techniques to Improve Strength of Polymer Concrete Made with Wet Aggregate", ACI Publication, SP 69-7, pp 107-122.
34. "Predictive Design Procedure: VESYS User Manual," by Kenis, W., FHWA-RD-77-154, Final Report, 1978.
35. Abdulshafi, A., Viscoelastic/Plastic Characterization, Rutting and Fatigue of Flexible Pavements, Ph.D., Dissertation, Ohio State University, 1983.
36. Majidzadeh, K. et al., "Implementation of a Pavement Design System, Volume 1," Final Report, Project EES 578, the Ohio State University Engineering Experiment Station, 1981.

APPENDIX A
FINITE ELEMENT ANALYSIS OF AIRPORT PAVEMENTS
INCORPORATING POLYMER CONCRETE

The analytical examination of the structural response of airport pavements incorporating a layer of Polymer Concrete (PC) presented in the main body of this Report was conducted using the ILLI-SLAB finite element (f.e.) computer program. The purpose of this Appendix is to document briefly the main features of ILLI-SLAB, particularly those involved in the analyses conducted.

ILLI-SLAB was first developed at the University of Illinois in the late 1970's for structural analysis of jointed, one- or two-layer concrete pavements with load transfer systems at the joints [Tabatabaie and Barenberg, 1980]. It was later expanded significantly to incorporate a variety of subgrade support characterization models, including the dense liquid (WINKLER), elastic solid (BOUSSINESQ), two-parameter (VLASOV) and stress dependent (RESILIENT) idealizations [Ioannides, et al., 1985]. More recently, the ability to accommodate a linear temperature variation through the thickness of the slab has also been added [Korovesis and Ioannides, 1987].

The original ILLI-SLAB model is based on the classical theory of a medium-thick plate on a Winkler foundation, and can evaluate the structural response of a concrete pavement system with joints and/or cracks. It employs the 4-noded, 12-dof plate bending (ACM or RPB12) element [Zienkiewicz, 1977]. The Winkler type subgrade is modeled as a uniform, distributed subgrade through an equivalent mass formulation [Dawe, 1965]. This is a more realistic representation than the four

concentrated spring elements used in similar f.e. codes, such as WESLIQID and FINITE. A work equivalent load vector [Zienkiewicz, 1977] is used in ILII-SLAB, as in FINITE.

Assumptions regarding the concrete slab, stabilized base, overlay, subgrade, dowel bar, keyway, and aggregate interlock can be briefly summarized as follows:

- (i) Small deformation theory of an elastic, homogeneous medium-thick plate is employed for the concrete slab, stabilized base and overlay. Such a plate is thick enough to carry transverse load by flexure, rather than in-plane force (as would be the case for a thin membrane), yet is not so thick that transverse shear deformation becomes important. In this theory, it is assumed that lines normal to the middle surface in the undeformed plate remain straight, unstretched and normal to the middle surface of the deformed plate; each lamina parallel to the middle surface is in a state of plane stress; and no axial or in-plane shear stress develops due to loading;
- (ii) The subgrade behaves as a Winkler foundation. As noted above, other subgrade idealizations are currently also available, but only the WINKLER option was used in this study;
- (iii) In case of a bonded stabilized base or overlay, full strain compatibility exists at the interface; or for the unbonded case, shear stresses at the interface are neglected;
- (iv) Dowel bars at joints are linearly elastic, and are located at the neutral axis of the slab;

- (v) When aggregate interlock or a keyway is used for load transfer, load is transferred from one slab to an adjacent slab by shear. However, with dowel bars some moment as well as shear may be transferred across the joints.

Various types of load transfer systems, such as dowel bars, aggregate interlock, keyways, or a combination of these can be considered at pavement joints. The model can also accommodate the effect of a stabilized base or an overlay, either with perfect bond or no bond. Thus, ILLI-SLAB provides several options, that can be used in analyzing the following problem types:

1. Jointed concrete pavements with load transfer systems;
2. Jointed reinforced concrete pavements with cracks having reinforcement steel;
3. Continuously reinforced concrete pavements;
4. Concrete shoulders with or without tie bars;
5. Pavements slabs with a stabilized base or overlay, assuming either perfect bond or no bond between the two layers;
6. Concrete slabs of varying thicknesses and moduli of elasticity, and subgrades with varying moduli of support.

The program inputs are:

- (a) Geometry of the slab, including type of base or overlay, load transfer system, subgrade, and slab dimensions;
- (b) Elastic properties of concrete, stabilized base or overlay, load transfer system, and subgrade;
- (c) Loading.

The outputs given by the program are:

- (a) Nodal stresses in the slab, and stabilized base or overlay;
- (b) Vertical reactions at the subgrade surface;
- (c) Nodal deflections and rotations;
- (d) Reactions on the dowel bars;
- (e) Shear stresses at the joint for aggregate interlock and keyed joint systems.

The model has been verified by comparison with the available theoretical solutions and the results from experimental studies [Tabatabaie and Barenberg, 1980; Ioannides, et al., 1985; Ioannides and Salsilli-Murua, 1989].

The analytical results presented in this Report were obtained using the two-layer model in ILLI-SLAB. This is a plate bending model, i.e. assumes that all layers above the subgrade behave like elastic plates. These layers are characterized by a Young's modulus, E_i , and a Poisson's ratio, μ_i . Implicit in this characterization is that these materials possess a tensile strength, as is the case with both conventional Portland Cement Concrete (PCC), as well as PC. It is also assumed that there is full contact between the subgrade and the layer immediately above it, but no shear is assumed to develop between them (i.e. smooth interface assumption).

In general, the interface between successive layers may be perfectly rough, or perfectly smooth, or somewhere in between. In the current version of ILLI-SLAB, the maximum number of layers above the subgrade is limited to two, but more layers could be accommodated by an extension and modification of the code. This did not become necessary at this stage of the investigation. Furthermore, ILLI-SLAB assumes

that interlayer friction is zero (unbonded, ICOMP=0) or full (bonded, ICOMP=1). Partial friction could be accommodated in ILLI-SLAB using an appropriate formulation. For all cases examined, full bond between the PCC and PC layers was assumed.

For the unbonded case, the combined stiffness of the two layers is simply taken as the algebraic sum of the two individual stiffnesses. Stresses are recovered by assuming two discontinuous linear distributions of stresses and strains through each layer, with two zero-stress points arising at the neutral axis location in each layer. In the bonded case, the concept of composite sections is used to transform the bottom layer to an equivalent layer whose modulus is equal to that of the top layer. An alternative interpretation is that this formulation reduces the system to an unbonded case, the two layers having their original stiffnesses, but their thicknesses being increased appropriately to account for the bonding restraint. Stresses are determined by assuming a single continuous linear distribution of strain through the combined full depth of the two layers. This gives rise to a single strain (and stress) free point, at the location of the effective neutral axis of the combined two-layer system. Due to the difference between the two layer moduli values, a discontinuity of the stress distributions arises at the layer interface.

It is evident from this exposition, that the ILLI-SLAB model is strictly applicable only to the case of stabilized bases and similar materials possessing a substantial stiffness and tensile strength. Granular materials which have no tensile strength, can only be accommodated in ILLI-SLAB by assigning to them E and μ values.

REFERENCES

1. Dawe, D.J. (1965), "A Finite Element Approach to Plate Vibration Problems," *Journal of Mechanical Engineering Science*, Vol. 7, No. 1.
2. Ioannides, A.M. and Salsilli-Murua, R.A. (1989), "Temperature Curling in Rigid Pavements: An Application of Dimensional Analysis," presented at the 68th Annual Meeting, Transportation Research Board, National Research Council, Washington, D.C., January.
3. Ioannides, A.M., Thompson, M.R., and Barenberg, E.J. (1985), "Finite Element Analysis of Slabs-On-Grade Using a Variety of Support Models," *Proceedings, Third International Conference on Concrete Pavement Design and Rehabilitation*, Purdue University, April 23-25.
4. Korovesis, G.T. and Ioannides, A.M. (1987), Discussion of "Effect of Concrete Overlay Debonding on Pavement Performance," by T. Van Dam, E. Blackmon, and M.Y. Shahin, *Transportation Research Record* 1136, Transportation Research Board, National Research Council, Washington, D.C.
5. Tabatabaie, A.M., and Barenberg, E.J. (1980), "Structural Analysis of Concrete Pavement Systems," *Transportation Engineering Journal*, ASCE, Vol. 106, No. TE5, September, Proc. Paper 15671.
6. Zienkiewicz, O.C. (1977), "The Finite Element Method," 3rd Edition, McGraw-Hill.

Note: To obtain a copy of the ILLI-SLAB code, write to:

Professor Ernest J. Barenberg
1213 Newmark Civil Engineering Laboratory
205 N. Mathews Ave.
Urbana, IL 61801